LOCATING MOBILE TELECOMMUNICATION FACILITIES IN EXTREME EVENTS EVACUATION

A Dissertation

by

NANNAN CHEN

Submitted to the Office of Graduate and Professional Studies of
Texas A&M University
in partial fulfillment of the requirements for the degree of

DOCTOR OF PHILOSOPHY

Chair of Committee,	Justin Yates
Committee Members,	Halit Uster
	Erick Moreno-Centeno
	Michael Bishop
	Ana Goulart
Head of Department,	Cesar O. Malave

December 2015

Major Subject: Industrial Engineering

ABSTRACT

Large regional evacuations caused by severe weather such as hurricane's and tsunami's are fraught with complexity, uncertainty and risk. During such events, evacuees have to make decisions on route planning and point-of-destination while emergency managers need to ensure that appropriate personnel and infrastructure are available and capable of facilitating the evacuation. In parallel, the widespread usage of social media and micro-blogs enabled by mobile technology is leading to more dynamic decision-making and real-time communication by evacuees.

This research uses deterministic and simulation techniques to model regional hurricane evacuation. A mixed integer formulation for telecommunication equipment location is used to identify gaps or strains in mobile service and to locate mobile telecommunications equipment to temporarily alleviate system stress. This problem unifies location allocation and routing characteristics with signal interference processing to maximize the number of served users through the evacuation. A Greedy Randomized Adaptive Search Procedure (GRASP) metaheuristic and a Lagrangian Relaxation-based heuristic are used to solve larger problem instances.

Agent-based simulation modeling is used to investigate the reliability, robustness and effectiveness of telecommunications equipment location given the inherent diversity and uncertainty of individual decision-making during evacuation. The agent-based simulation adopts Fuzzy Cognitive Maps to model individual evacuation decision-making that dynamically integrates external information (e.g., physical environment,

interpersonal communication) and internal data (e.g., historical empirical, demographic trends). This research shows how social communication among evacuees positively impacts travel patterns as well as overall evacuation time and the usage of mobile telecommunications equipment.

NOMENCLATURE

ABM	Agent-based Simulation Model
ABME	Agent-based Simulation Model for Extreme Event Evacuation
CDMA	Code Division Multiple Access
DEM	Digital Elevation Model
FCM	Fuzzy Cognitive Maps
GIS	Geographic Information Systems
GRASP	Greedy Randomized Adaptive Search Procedure
TELP	Telecommunications Equipment Location Problem

TABLE OF CONTENTS

Page

LIST OF FIGURES

Page

LIST OF TABLES

Page

CHAPTER I

INTRODUCTION

I.1. Introduction to Evacuation Problems

In the past ten years, Hurricanes Katrina, Ike, Rita, and Sandy have caused significant destruction among coastal cities and towns in the U.S. while simultaneously leading to countless loss of life (either from the storms themselves or from the challenging conditions that follow). Furthermore, additional extreme weather events have occurred outside of the U.S., such as the tsunamis in Indonesia and the Philippines, the earthquake in Haiti, and the tsunami (and subsequent nuclear catastrophe) in Japan. Large populations and areas of the world have begun to experience stronger, more inclement, more destructive, and more frequent severe weather.

A large population evacuation caused by natural disasters is intrinsically complicated and full of uncertainty and dynamic risks. Evacuees must make important decisions concerning both route-planning and their end destinations. At the same time, emergency managers are responsible for facilitating evacuations by ensuring the availability of necessary emergency personnel and infrastructure.

The ubiquity of mobile technology has led to dramatic shifts in the way people communicate with one another. Text messages, social media, and micro-blogs all enable (and favor) shorter content bursts with a higher frequency of messages than face-to-face or phone conversations. The connectivity of these devices to the Internet further extends their reach, enabling users of mobile technology to browse the web, download and

upload content, and obtain real-time information on a variety of topics from traffic and the stock market to weather and celebrity sightings.

During an extreme event evacuation, mobile technology has enabled a new decision making option for evacuees. The widespread use of social media and micro-blogs has engendered a steady stream of real-time communication that can be used by evacuees to make dynamic decisions.

In this research, we focus on the effect of mobile technology on regional evacuation and how the changing behavioral landscape of evacuations can be better captured through more realistic and representative modeling. Specifically, we note the importance of models that not only capture realistic individual behaviors (e.g., texting and social networking) but that simultaneously model the supportive physical infrastructure (e.g., cell phone towers and internet access) to ensure maximal connectivity and resilience of the communication systems that support and enable evacuee decision-making. Through our modeling, we illustrate the criticality of adaptation and flexibility within communication systems and show how integrated models, while complex, can be solved efficiently and effectively. The scope of this article is limited to hurricane evacuation, noting that the logic of the model can easily be applied to many extreme events where advance notice through forecasting is possible.

An optimization formulation for telecommunication equipment location problem with time component (TELP) is developed to locate mobile telecommunications equipment to temporarily relieve cellular network system stress. TELP is defined as the following: given potential microcell station locations, existing macrocell station

locations and users' travel patterns on a road network, locate number of p mobile microcell stations to maximize the total number of users served over multiple time periods.

An agent-based simulation model for extreme event evacuation (ABME) is proposed as well. ABME is used to investigate the information dispersion through simulated social networks regarding evacuation effectiveness. ABME can also be used as a tool to examine the availability or use of mobile telecommunication stations for regional evacuations, considering the diverse and uncertain behavior of individuals and the interactions between individuals.

I.2. Motivation of the Dissertation

For a regional evacuation, evacuation decisions such as where to go, how to get there, and where to stop along the way are largely left to the individual to plan themselves or to determine on-the-go during the evacuation itself. The inherent uncertainty of a natural event necessitates that evacuees remain adaptive to changing conditions and their decisions are largely affected by a combination of what they see and what they hear. Mobile technology and social networking have recently begun to dramatically influence these evacuation decisions.

Extensive study of historical evacuations has demonstrated that people rely on a variety of information (both visual and auditory) to determine when to evacuate and where to go. Friends, family, and peers are now better connected to one another through social networks that can be accessed via mobile technology. Given the known

importance of friends and family to evacuation decision-making, mobile technology can increase the frequency of family and friend contact while improving the quality of content (through links to blogs, streams, news sources, etc.). Additionally, the ability to connect through mobile technology decreases an individual's reliance on past hurricane evacuation experiences, a historically important factor in evacuation decision-making.

During Hurricane Sandy and other recent extreme events, the use of mobile technology to influence decision making has become more evident within the population for the dissemination and collection of information for planning and in real-time on site decision-making. A recent survey among residents of Monmouth County, NJ (one of the counties that was most affected by Hurricane Sandy) showed that 65% of households had access to at least one smartphone and 96% of all households had access to at least one smartphone or one cellphone during the hurricane. Social media usage (specifically Twitter and Instagram) increased 100%+ during the hurricane and respondents agreed that they used their mobile devices to obtain information and to communicate during the hurricane.

The preference to use and reliance of individuals on mobile technology during evacuations necessitates that connectivity remains established and consistent. While many research efforts have been focused on regional evacuation models, the vast majority are focused on pre-planning strategies and the influence of dynamic and uncertain behavior among evacuees. There is little to no emphasis on the corresponding problem of maintaining connectivity between evacuees. In this case, connectivity is critical to the creation of a more realistic model and is dictated by the changing

paradigms of evacuation decision-making. Models that do not account for infrastructure issues such as cell phone or 4G connectivity, call reliability, and infrastructure reliance, are operating under "best case circumstances" that may lead to significant underperformance during real-world event conditions in which cell towers go down or local network capacity is exceeded due to demand. Most evacuees travel on major roads and highways to maintain cellular and data service during an evacuation. This tendency leads to extreme demand and potential network outages.

Communications systems (e.g., radio, cellular) regularly fail during extreme weather events. The White House report, "The Federal Response to Hurricane Katrina: Lessons Learned" (2006), showed that 1,477 cell towers were incapacitated during Hurricane Katrina and nearly three million customers lost telephone service, preventing them from calling emergency centers, connecting with emergency services, or reaching out to families and friends.

However, there are low cost, easy set-up mobile telecommunications options available such as Cell on Wheels (COW) that are compatible with existing radio and cellular networks. Setting up these mobile devices at identified dynamic tele-service demand areas can help strengthen existing radio and cellular systems during large-scale, regional evacuations.

We motivate the need for the ABME model by noting the inability of existing evacuation, which are often based on discrete events or other network flow variations, to capture the behavior and uncertainty in interactions between individual vehicles during an evacuation. Specifically, these deterministic models rarely take human and social

behaviors into consideration when modeling emergency scenarios. Agent-based simulation models (ABM) are designed to model behavior at an individual level, which enables them to replicate more realistic individual behaviors and the resulting group dynamics that emerge. ABM is suitable for this research not only because it can model individual behavior such as route choice and travel speed, but also because it has the capability to simulate dynamic human decision-making based on multiple kinds of external information and individual inherent demographic characteristics such as gender and age.

I.3. Contributions of this Dissertation

A mathematical model is proposed to identify mobile telecommunication infrastructure location strategies to support demand-stressed systems during emergency events. This model considers temporally and spatially distributed users with a planning horizon composed of discrete, non-overlapping time intervals. The model captures signal interference constraints, which are a major restriction in determining the number of users each cellular channel can carry in contemporary Code Division Multiple Access (CDMA) systems. A routing sub-problem is also included in the model to improve the usage of mobile telecommunication equipment due to its portable character.

This TELP model can consider all of these realistic factors and provide solutions containing the decision variables of user assignment, installation locations of mobile facilities, and routes corresponding to shipping these facilities over time intervals. We focus specifically on the challenge of regional evacuation and use real-world data such

as road networks, demographics, DEM, and terrain to support our model. Heuristic approaches are introduced and compared to solve the time-dependent location-allocation problem for realistic instances.

This research has also resulted in the development of a spatial, behavioral evacuation ABM that uses novel fuzzy cognitive maps (FCMs) as the driver for establishing agent decision logic and that will integrate the physical environment, interpersonal communication, and historical empirical data when determining agent decisions. This is the first time that FCMs have been applied and implemented in the domain of travel behavior under the complicated scenario of evacuation due to extreme events. FCMs are suitable to represent more realistic behavior models compared with the traditional IF/THEN behavior rules used in ABM: with the help of FCMs, evacuees are able to make dynamic and adaptive decisions based on real-time and updated information.

By integrating the TELP model with ABM, we are able to explore the use of mobile telecommunication facilities and evacuees' behavior simultaneously. The usage of telecommunication facilities with widespread social communication is also revealed. This is the first time that the facility planning problem considering the power of social media is examined for emergency evacuation. Emphasizing the importance of social media use during facility planning can help emergency managers or commercial agencies improve facility use, enhance service quality, and reduce expenses.

In addition, integrating the TELP model with ABM can help TELP provide more accurate, real-time facility planning strategies. If better solutions are acquired from

TELP, more evacuees' tele-service demands can be satisfied in ABME, and the evacuees will have fewer restrictions to their telecommunication access, resulting in a better evacuation experience.

I.4. Organization of the Dissertation

This dissertation is organized as follows. In Chapter II, we review the relevant literature on telecommunication systems planning and ABM models for evacuations. In Chapter III, we present the mathematical model for TELP and the heuristic algorithms for solving TELP. In Chapter IV, an agent-based simulation model for evacuation in extreme events is introduced. In Chapter V, we show the application results for Boston and San Francisco. Lastly, Chapter VI will conclude this research and suggest directions for future research.

CHAPTER II

LITERATURE REVIEW

II.1. Telecommunication Infrastructure Location Problem

The optimal base station location problem was first addressed by the telecommunication research society. Statamatelos and Ephremides (1996) introduced the optimal placement strategies of fixed base-stations for indoor wireless networks. The goal was to maximize coverage area while minimizing co-channel interference considering spatial diversity. Calegari et al. (1997) provided a genetic approach for finding the best possible sites for base-stations while maintaining service for a given percentage of tele-traffic, with the goal of minimizing associated costs. For the Code Division Multiple Access (CDMA) system, Tcha et al. (2000) presented a base-station location model to minimize the cost of establishing base stations while controlling the blocking probability. To solve this model, they proposed two heuristics: the construction heuristic for choosing an initial feasible subset from all candidate sites, and an improvement heuristic to reduce set-up costs.

To this point, few solution techniques in operations research had been applied to address the base station location problem. Bose (2001) proposed a technique using dynamic programming to determine optimal base-station locations in an urban environment based on cell coverage. Lee and Kang (2000) offered a binary integer programming model to minimize cost while considering base-station capacity and user

received signal power. A Tabu Search heuristic was applied by Lee and Kang for solving base-station planning problem.

Akella et al. (2005) presented a mixed integer programming (MIP) model. The model was designed to maximize the total number of user demands for multiple time slots given base-station coverage radius and channel capacity and integrate the emergency notification problem. Two greedy heuristics and their extended versions were proposed to solve this MIP. To further improve solution quality, a Lagrangean heuristic was developed that built on the solution obtained by the greedy heuristics. Although the model considered multiple time slots, it assumed the demand nodes were fixed and did not change over time. The MIP formulation was based on the maximum coverage problem and only added one linear channel capacity constraint. These simplifications and assumptions for telecommunication systems can cause over-estimates when applied to real-world planning problems. However, the proposed heuristics and rich computation study provide good insights regarding the nature of the problems and potential solution techniques.

In a CDMA system, users are allowed to send information simultaneously over a single communication channel with a capacity (the number of simultaneous users) governed by a signal to interference ratio. Veeravalli and Sendonaris (1999) revealed a nonlinear relationship for the coverage of a cell as a function of the number of its users. This coverage-capacity relationship was provided under the assumption that user density is uniformly distributed. In reality, user demands are often not balanced. In other words, there are hotspots, or high-traffic density areas within small regions. The presence of

hotspots can result in smaller coverage areas. If a base-station serves a large number of users from high-traffic regions, it will block access to users in other regions, resulting in reduced coverage. Hence, in a CDMA system, coverage (i.e. the region where base stations can provide quality call service), capacity, and user distribution must be addressed concurrently. Therefore, base-station location models derived from coverage problems with simple capacity constraints are no longer suitable and realistic.

Amaldi et al. (2003a, 2003b, 2003c) proposed MIP models for the location and configuration of fixed base stations to maximize signal coverage and minimize installation costs considering signal quality requirements. In a study performed by Amaldi et al. (2003b), heuristic approaches of randomized greedy procedures and Tabu Search were proposed to obtain solutions. Their studies showed the trade-off between coverage and capacity in cellular systems. However, those models simplified intercell interference as a constant fraction and assumed that traffic distribution among cells is homogeneous.

Kishore et al. (2003) derived a non-linear inequality of signal interference representation that examined user capacity in a Macrocell-Microcell CDMA system. In this inequality, the geographic distribution of user traffic was considered and the interference between cells was captured as well.

In our TELP model, in addition to considering the traditional coverage problem, we adopted the inequality representation derived by Kishore et al. (2003) as the signal interference requirement, which is a must-have condition in cellular systems. Signal interference from both user and intercell sources were included. The user traffic is time-

dependent and its geographic distribution is considered. These two characters reflect real-world situations and are important to consider, especially for evacuation scenarios in which user demands change spatially at different time stages. The evacuees (users) always travel on evacuation routes that follow main roads; therefore, the user tele-service demand is not homogenously distributed throughout the entire target evacuation region. The routing constraints are integrated to utilize the mobile feature of telecommunication facilities, reuse these facilities, and satisfy more tele-service demands with a limited budget. The base-station location problem is an NP-hard problem as described in the literature mentioned above. To obtain good solutions with less computation effort, we propose two heuristic approaches: greedy randomized adaptive search procedure (GRASP) and Lagrangean heuristics. Although the general idea is similar to previous work at some level, the implementation is very different due to the specific problem properties.

II.2. Evacuation Simulation Models

Dynamic traffic simulation models investigate dynamic travel demand, dynamic trip distribution, and dynamic traffic assignments – all of which influence decision-making in evacuation participation, departure time choice, destination choice, and route choice. Pel et al. (2012) and Alsnih and Stopher (2004) reviewed dynamic traffic simulation models for evacuations and summarized macrosimulation and microsimulation models for evacuation problems and travel behavioral models in the literature. Many crowd evacuation simulation models attempt to incorporate more

realistic human behaviors that may result from psychological responses to emergency conditions. This can be accomplished by extending the dynamic traffic simulation models to more sophisticated agent frameworks.

Bonabeau (2002) discussed methods and techniques to simulate human systems in ABM. It is pointed out that modeling the diffusion of behaviors in social networks has been the most common application for ABMs. These models require more computational effort since sophisticated ABMs often incorporate neural networks or evolutionary algorithms to allow realistic learning and adaptation. A framework for using ABM to simulate human and social behaviors during emergency evacuations was introduced by Pan et al. (2007).

Many agent-based emergency evacuation simulation models have been developed regarding pedestrian behaviors. Christensen and Sasaki (2008) proposed a bottom-up Modeling of Mass Pedestrian flows – implications for the Effective Egress of individuals with disabilities to explore emergency evacuation with individual with disabilities in the population. Bo et al. (2009) developed an ABM for park emergency evacuations integrated with geographic information systems (GIS). Although geographic information about obstacles, stairs, and roads was imported into the model, the agent behavior was grid-cell-based. Tsai et al. (2011) presented an airport evacuation simulation model that included four key features: (1) different agent types (individual travelers, family agents, and authority agents); (2) emotional interactions; (3) informational interactions; and (4) behavioral interactions. Few ABMs had previously captured emotional and informational intersections. It is important to represent these two

aspects of human behavior, especially for emergency scenarios. However, the behavior rules in this ABM are based on a different cognitive category and all the agents who belong to the same cognitive category would behave the same. The emotional and informational interactions only occur between neighbors and family agents who are assumed to move together.

Compared to ABM applied to the pedestrian domain, fewer examples of existing literature can be found for evacuations of large geographic areas where traveling by vehicles is necessary. Zhang et al. (2009) presented an ABM for hurricane evacuation that considered two types of agents: normal and greedy. The normal agents always choose the shortest routes and the greedy agents choose the least congested route based on updated traffic information. The model assumed that the destinations were preselected and would not change during the evacuation. Their results indicated that greedy behavior makes the whole evacuation inefficient although it can sometimes reduce individual evacuation times by detouring and avoiding congested roads. The behavior rules used for this research are relatively simple: route changes only based on congestion level and speedup and slowdown behaviors only dependent on whether there are other vehicles blocking one's path.

Chen and Zhan (2004) investigated the effectiveness of simultaneous and staged evacuation strategies using agent-based simulations. They modeled traffic flows at the individual vehicle level and tested three different network structures. Dynamic routing procedures were adopted for route choice, that is, agents can change their routes dynamically based on real-time traffic conditions and they always choose the fastest

route. Agents' destinations result from the route choice, which means that agents have less flexibility to choose their evacuation location. While the agents travel on road segments, car-following and lane-changing models were applied for the dynamics of vehicular movement. The car-following model built into their simulation toolkit was based on Fritzsche (1994) and Olistam and Tapani (2004).

II.3. Social Media Use in Travel Behavior and Emergency Event

With respect to the effects of an individual's social network on travel behavior, Arentze and Timmermans (2008) proposed a theoretical framework to incorporate the dynamics of activity-travel choice and social networks in microsimulations of activity-travel patterns. A utility function in this research derived from social interaction is a function of dynamic social and information needs, and similarity between the relevant characteristics of the persons involved. Hackney and Marchal (2009) introduced a general spatial social interaction model based on the Multi-Agent Transportation Simulation Toolbox. Their model constructed social networks for a geographically distributed population of agents. This network was then used in a further step to modify travel demand. Han et al. (2011) addressed the formation and adaptation of location choice sets under the influence of social networks to investigate the dynamic traffic generation caused by collective activity-travel choice behavior. Handford and Roger (2012) extended the current state-of-the-art in driver route choice models and developed a route choice forces model, in which decisions are influenced by a set of forces. Two forces are incorporated: a driver's desire to travel the quickest route and a driver's desire

to travel with others. The authors evaluated their model against two existing route choice algorithms (shortest time and real-time re-routing) using three road networks.

The widespread use of social media plays a more and more important role in daily lives, which draws attention to social media usage during extreme events. Qualitative methods such as observation, interviews, questionnaires, and collection of on-line texts have been used to examine the importance of social communication. Eisenman et al. (2007) found that strong socially connected groups such as extended family, friends, and community groups mediated evacuation behavior through access to transportation, shelter, and the interpretation of official messages. The observations were based on Hurricane Katrina in 2005. Based on a study of the Southern California Wildfires, Sutton el al. (2008) pointed out that social media serves as backchannel communication and supports peer-to-peer communication during a natural disaster; Shklovski et al. (2008) provided evidence that information sharing can help communities stay connected despite geographical dispersal post-disaster. Hughes et al. (2008) described on-line behavior as socially convergent activity that parallels geographical onsite behavior after examining several disaster events. Sutton et al. (2011) showed that traditional news media, social media, and other pre-existing networks played different roles in the 2010 tsunami in Hawaii. They suggested that multiple channels should be used to ensure effective communication with the public.

A few ABMs have previously addressed the effect of social networks on emergency evacuations. Hasan and Ukkusuri (2011) proposed a threshold model of social contagion to characterize the social influence in the evacuation decision making

process. The condition of a cascade decides to evacuate was examined. Simulation models investigate the effects of community mixing patterns, the initial seed, and the strength of ties on the average cascade size. Widener et al. (2012) revisited the influence of social network effects on evacuation decisions due to the augmentation of information diffusion through the new social media. They examined how real-time interpersonal communication effects people's hurricane evacuation participation and decision-making. Three laboratorial social networks were examined regarding hurricane evacuation in Bay County, Florida. Both Han and Widener's works were examined using ABM.

Wang (2012, p.76 -- p.119) studied the influence of social media and broadcast on individual travel behavior for regional emergency evacuation using the proposed multi-agent simulation model. The simulation model imported the optimal routes/shelters resulted from the proposed optimization model as individual's guild line, and used a real-time IF/THEN decision-making logic for individual's route/shelter choice. The experiments showed both types of information sharing can shorten overall evacuation time and individual's travel time, and reduced average transportation cost. Compared to social media, information sharing on broadcast plays a more significant role.

The structure of social networks should also be examined when investigating the usage of social media. Mislove et al. (2007) presented a large-scale measurement study and analysis of the structure of four popular online social networks. The high-degree core structure property along with small-world phenomenon can allow information to diffuse extremely fast compared with other dissemination systems. Butts et al. (2012)

investigated whether geographical variability in population distribution would have an effect on social network structure and how this geographic heterogeneity would affect network structure. They found that local social network structure is highly dependent on local population distribution. This insight attracts attention because a variety of recent research projects have simulated social networks based upon population distribution and ignored the socio-geographic relationship.

Lindell et al. (2011) also showed how demographic variables such as age, gender, ethnicity, marital status, education, number of persons in the household, annual household income, and household ownership influence evacuation logistics using questionnaire data from Hurricane Lili. They examined these demographic variables in terms of departure timing, vehicle use, evacuation routes, travel distance, shelter type, evacuation duration, and evacuation cost. The report data showed that about 90% of the evacuation population took their own vehicles and single households generally took multiple cars. It was also shown that people tend to choose a familiar route based on their own past experience. Their results indicated that higher income families were particularly likely to rely on personal experience, while groups with little hurricane experience, the elderly, females, households with children, and inland residents were more likely to rely on recommendations from peers and media.

II.4. Fuzzy Cognitive Map Approach

Fuzzy Cognitive Maps (FCMs), introduced by Kosko (1986, 1992, 1994, 1997, 1998), are graph structures that represent causal relationship between concepts. The

fuzziness allows hazy degrees of causality and the graph structure (forward and backward chaining) allows knowledge to be developed by connecting concepts and different FCMs. Kosko also proposed a fuzzy causal algebra to govern causal propagation on FCMs. The vector-matrix operations allow FCMs to model dynamic systems and to capture the dynamic aspect of system behavior (Bertolini and Bevilacqua, 2010; Miao et al., 2010). Aguilar (2005) pointed out that FCMs are hybrid methods that lie in-between fuzzy systems and neural networks. Hence, FCMs possess the combined robust properties of fuzzy logic and neural networks. On the other hand, it is easier to use FCMs to represent knowledge and knowledge adaptive processes, and interference can be calculated using numeric algebra operations instead of IF/THEN rules.

Recently, FCMs have drawn a significant amount of research attention and have been applied to a variety of areas such as medicine, education, decision making and support, the environment, and social and political science. In the medical domain, Georgopoulos et al. (2003) and Papageorgiou et al. (2006, 2008) proposed an FCM approach for medical diagnosis and decision support in language impairment and radiotherapy, areas in which expert systems are usually applied. In the engineering domain, Stylios and Groumpos (2004) applied FCM to model complex industrial systems and supervisory control systems. Papageorgiou et al. (2006) implemented extended FCMs, which used nonlinear Hebbian rules to model industrial process control problems. They demonstrated that their proposed scheme outperformed other existing schemes and resulted in very good maximum power operation under different conditions, such as changing insulation and temperature.

Due to its properties and features, FCM can be a very good tool to model social and political situations and to support the decision-making process. Acampora et al. (2009) introduced the FCM approach to Ambient Intelligence (AmI) system design. AmI systems consider human beings who are placed in relatively small environments and surrounded by computing devices. The dynamic computational-ecosystem seeks to satisfy users' requirements and optimize environmental parameters such as comfort or energy reduction. FCM models the dynamic interactions between users and environmental sensors such as temperature and lightning. The theory of timed automata is integrated in the framework and FCM evolution (changes of FCM graph structure) is considered in this research. Carvalho (2010) discussed the structure, the semantics, and the possible use of FCMs as tools to model and simulate complex social, economic, and political systems, while also clarifying some issues that have been recurrent in published FCM papers.

Researchers have realized that the FCM approach is suitable for modeling human behavior and simulating complex social systems, and the FCM framework has been proposed at a very high level. However, very little implementation work has been done to simulate relatively large groups of users in social systems. Up to this point, we have not found FCM-related literature on human driving behavior and no FCM framework has been proposed for emergency evacuations in which human beings interact with a quickly-changing environment and knowledge development is necessary. Due to the widespread use of social media, our FCMs also include information sharing on social networks.

CHAPTER III

TELECOMMUNICATION EQUIPMENT LOCATION PROBLEM WITH TIME COMPONENT MODEL

In this chapter, we present the telecommunication equipment location problem with time component model (TELP) for evacuation processes to satisfy the telecommunication service demand. We focus on the impact of mobile technology in regional evacuation and how the changing evacuation behavior can be better captured through more realistic and representative modeling. Specifically, we note the importance of models that not only capture realistic individual behavior (e.g., voice calling, social networking, etc.) but which simultaneously model the supportive physical infrastructure (e.g., cell phone towers, internet access) to ensure maximal connectivity and resilience of the communication systems that support and enable evacuee decision-making. Through our modeling, we illustrate the criticality of adaptation and flexibility within a communication system and show how integrated models, while complex, can be solved efficiently and effectively. In particular, by solving our model, emergency managers can obtain decision support concerning the number and configuration of mobile telecommunication equipment; where and when to install mobile equipment and corresponding routes. We limit the scope of this model to evacuation, noting that the logic of the model can be easily applied to other extreme events that require population movement through a large geographic region with some advance notice through forecasting.

Due to the complexity of our mathematical model, only small instances can be solved by directly using optimization solver. Hence, we develop efficient heuristic methods to solve relatively large problems. Later on this model is integrated in the ABM model for offering real-time updated solutions to maintain robust communication systems.

III.1. Problem Setting

While more and more people use their mobile cell phone devices to communicate with each other through voice calls, text messages, and social media, instead of face-to-face conversation, the importance of the telecommunication infrastructure has become self-evident. There is significant risk that the existing telecommunication infrastructure is not sufficient to provide service during extreme events like a hurricane or earthquake. In an extreme event, the existing cell towers may suffer destruction. Additionally, users' service requests will increase significantly due to the large amount of information following these events. Specifically, for the evacuation problem, users need to know the traffic conditions on the evacuation routes and the shelter information as they select destinations. We realize the availability of mobile cell station can assist to relieve the communication stress. A mobile cell station consists of a cellular antenna tower and electronic radio transceiver equipment on a truck or trailer. Now the questions are: where and when to install the equipment; if there is a limited number of facilities, what are the best routes to ship from one location to another so that we can serve as many users as possible during the evacuation process.

The telecommunication infrastructure that we are dealing with in this research is made up of two components: Macro-Stations and Micro-Stations. A Macro-Station (macrocell) is a traditional, high-power, high-cost cellular base station which provides a coverage radius up to 10km. A Micro-Station (microcell) is a smaller, low-cost unit which transmits at lower power levels and its coverage radius is less than 1km (Coombs and Steels, 1999). We consider the existing fixed cellular base station as Macro-Station and the mobile cell site on truck as Micro-Station. Since a Micro-Station is designed to be part of a cellular network, it can be deployed inside and outside of Macro-Station coverage. Figure 3-1 shows an example of a Macro-Station with overlay Micro-Stations. In this problem, we assume the locations of effective Macro-Stations are known.

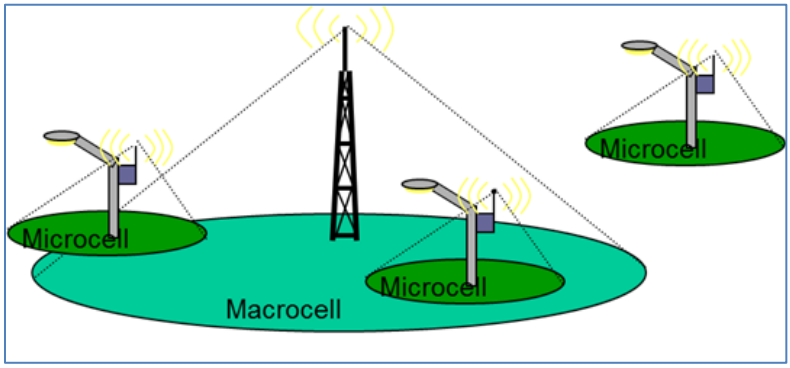

Figure 3-1 Example of a Macro-Station with overlay Micro-Stations

One characteristic of this problem is that all users will travel on the established road network. Hence, their locations will be restricted to the geographic area of the roads. For an evacuation, users' travel routes are predictable because they have fixed destinations already in mind. As evacuation time increases, users travel on the roads and their physical locations in general will be closer to their destinations. These two

characteristics indicate two points: 1. it will be beneficial to set up the Micro-Stations along the road network for better the user coverage; 2. moving Micro-stations during an evacuation can allow emergency managers to utilize the limited mobile Micro-Stations as much as possible. Therefore we limit the candidate Micro-Station locations along the road networks used during the evacuation. Micro-Stations can be shipped among these candidate locations during the multiple time periods.

Our formal mathematical problem is defined as follow: locate P mobile Micro-Stations to maximize the total number of users served over multiple time periods, given candidate Micro-Station locations, existing fixed Macro-Stations locations and users' anticipated travel patterns on a road network.

III.2. TELP Model

In the model that follows, we assume the configuration of all Macro-Stations are the same, that is the coverage radius, transmission power and pole capacity are all set at the same level. Specifically, the pole capacity refers to the maximum number of users a cellular station can support if there is no noise and other station interference (Gilhousen et al., 1991). The cellular station coverage is defined as the maximum distance that a given user of interest can be from the station with reliable received signal (Veeravalli and Sendonaris, 1999). The special relationship between coverage and capacity is captured in this model as well. To simplify our problem, we assume the station interference only happen between pair-wise stations.

Similarly, we assume the configuration for all Micro-Stations are the same. We also assume that Micro-Stations cannot operate while travelling. In other words Micro-Stations can only provide service while they are installed at candidate Micro-Station locations. We consider the installation and break-down time of Micro-Stations take a predefined period of time and it's included in the travel time from one candidate location to another. We limit the usage of each candidate Micro-Station location for one Micro-Station at a time.

We define the following notation:

Model Parameters

$\mathcal{I}$ set of users who need to connect to tele station, $i \in \mathcal{I}$

$\mathcal{M}$ set of existing Macro-Stations, $m \in \mathcal{M}$

$\mathcal{J}$ set of candidate Micro-Station locations, $j \in \mathcal{J}$

$\mathcal{T}$ set of time periods, $t \in \mathcal{T}$

K_M single-cell pole capacity of Macro-Station

K_J single-cell pole capacity of Micro-Station

d_{imt} distance from user i to Macro-Station m at time t

d_{ijt} distance from user i to candidate Micro-Station location j at time t

R_M Macro-Station coverage radius

R_J Micro-Station coverage radius

P total number of Micro-Station can be used

$\tau_{jj'}$ Shipping time from candidate Micro-Station j to j'

Decision Variables

x_{ijt} 1 if user i is assigned to Micro-Station located at j at time t

z_{imt} 1 if user i is assigned to Macro-Station m at time t

y_{jt} 1 if Micro-Station located at j operating at time t

$v_{jtj't'}$ 1 if Micro-Station is shipped from location j at time t to location j' at time t'

Objective

$$\boldsymbol{Max} \sum_{t\in \mathrm{T}} \sum_{i\in \mathrm{I}} \sum_{j\in \mathrm{J}} x_{ijt} + \sum_{t\in \mathrm{T}} \sum_{i\in \mathrm{I}} \sum_{m\in \mathrm{M}} z_{imt} \quad (3.1)$$

Constraints

$$\sum_{j\in \mathrm{J}} x_{ijt} + \sum_{m\in \mathrm{M}} z_{imt} \leq 1 \qquad \forall\, i \in \mathcal{I}, \forall\, t \in \mathcal{T} \quad (3.2)$$

$$x_{ijt} \leq y_{jt} \qquad \forall\, i \in \mathcal{I}, \forall\, j \in \mathcal{J}, \forall\, t \in \mathcal{T} \quad (3.3)$$

$$\sum_{i\in \mathrm{I}} x_{ijt} < K_J \qquad \forall\, j \in \mathcal{J}, \forall\, t \in \mathcal{T} \quad (3.4)$$

$$\sum_{i\in \mathrm{I}} z_{imt} < K_M \qquad \forall\, m \in \mathcal{M}, \forall\, t \in \mathcal{T} \quad (3.5)$$

$$\sum_{j\in \mathrm{J}} y_{jt} \leq P \qquad \forall\, t \in \mathcal{T} \quad (3.6)$$

$$x_{ijt}\, d_{ijt} \leq R_J \qquad \forall\, i \in \mathcal{I}, \forall\, j \in \mathcal{J}, \forall\, t \in \mathcal{T} \quad (3.7)$$

$$z_{imt}\, d_{imt} \leq R_M \qquad \forall\, i \in \mathcal{I}, \forall\, m \in \mathcal{M}, \forall\, t \in \mathcal{T} \quad (3.8)$$

$$(K_J - \sum_{i\in \mathrm{I}} x_{ijt})\,(K_M - \sum_{i\in \mathrm{I}} z_{imt}) \geq \sum_{i\in \mathrm{I}} x_{ijt}\, a_{ijmt} \sum_{i\in \mathrm{I}} z_{imt}\, b_{ijmt}$$

$$\forall\, j \in \mathcal{J}, \forall\, m \in \mathcal{M}, \forall\, t \in \mathcal{T} \quad (3.9)$$

$$(K_M - \sum_{i\in \mathrm{I}} z_{imt})\,(K_M - \sum_{i\in \mathrm{I}} z_{im't}) \geq \sum_{i\in \mathrm{I}} z_{imt}\, b_{im'mt} \sum_{i\in \mathrm{I}} z_{imt}\, b_{imm't}$$

$$\forall\, m, m' \in \mathcal{M}, m \neq m', \forall\, t \in \mathcal{T} \quad (3.10)$$

$$(K_J - \sum_{i\in \mathrm{I}} x_{ijt})\,(K_J - \sum_{i\in \mathrm{I}} x_{ij't}) \geq \sum_{i\in \mathrm{I}} x_{ijt}\, a_{ijj't} \sum_{i\in \mathrm{I}} x_{ij't}\, a_{ij'jt}$$

$$\forall\, j, j' \in J, j \neq j', \forall\, t \in \mathcal{T} \qquad (3.11)$$

$$y_{jt} \leq \sum_{t' \in \mathrm{T}} \sum_{j' \in \mathrm{J}} v_{j't'jt} \leq 1 \qquad \forall\, j \in J, \forall\, t \in \mathcal{T} \qquad (3.12)$$

$$\sum_{t' \in \mathrm{T}} \sum_{j' \in \mathrm{J}} v_{j't'jt} = \sum_{t' \in \mathrm{T}} \sum_{j' \in \mathrm{J}} v_{jtj't'} \qquad \forall\, j \in J, \forall\, t \in \mathcal{T} \qquad (3.13)$$

$$(1 - \sum_{t' \in \mathrm{T}} \sum_{j' \in \mathrm{J}} v_{jtj't'}) \geq y_{jt} \qquad \forall\, j, j' \in J, j \neq j', \forall\, t \in \mathcal{T} \qquad (3.14)$$

$$v_{jtj't'}(1 - (t' - t - \tau jj')) = 0 \qquad \forall\, t, t' \in \mathcal{T}, t < t', \forall\, j, j' \in J \qquad (3.15)$$

$$x_{ijt}, z_{imt}, y_{jt} \in B \qquad \forall\, i \in I, \forall\, j \in J, \forall\, m \in \mathcal{M}, \forall\, t \in \mathcal{T} \qquad (3.16)$$

$$v_{jtj't'} \in B \qquad \forall\, j, j' \in J, \forall\, t, t' \in \mathcal{T}, t < t' \qquad (3.17)$$

The objective (3.1) is to serve as many users as possible through evacuation periods. Constraints (3.2) - (3.8) are location-allocation constraints. Constraints (3.2) limit each user covered by at most one tele station. Constraints (3.3) ensure that if a user is covered by a Micro-Station located at *j* there must be a Micro-Station operating at location j. Constraints (3.4) - (3.5) make sure user assignments do not exceed the base station pole capacity. Constraints (3.6) indicate the total number of P Micro-Station available for installation each time period. Constraints (3.7) and (3.8) ensure the user's distance from the tele station is less than or equal to the effective radius of the corresponding tele station.

Constraints (3.9) – (3.11) are the interference constraints. In CDMA radio network, capacity and coverage of tele station have to be considered simultaneously and both are restricted by the signal quality constraints. Signal quality is restricted by signal interference within the tele station and from other stations. The interference considered

here is from voice users. a_{ijmt} = $[h_m(d_{imt}/d_{m0})^{-\alpha}]/[h_j(d_{ijt}/d_{j0})^{-\alpha}]$ and $b_{ijmt} = [h_j(d_{ijt}/d_{j0})^{-\alpha}]/[h_m(d_{imt}/d_{m0})^{-\alpha}]$, these two terms become constant once a user's location is known. h is a constant that depends on wavelength, antenna heights, antenna gains, etc. Use h_m and h_j to represent this constant value for Macro-Station and Micro-Station respectively. d is the distance from user to station, d_0 is the close-in reference distance. Use d_{m0} and d_{j0} to represent the close-in reference distance for Macro-Station and Micro-Station respectively. χ is a zero-mean normal random variable with standard deviation σ_M and σ_J for Macro-Station and Micro-Station respectively. α is path loss exponents. (3.9) – (3.11) shows the relationship between base station capacity and signal interference.

Constraints (3.12) - (3.15) are the routing constraints. Specifically, constraints (3.12) ensure Micro-Station j can only be turned on when it is at location j at time t. Constraints (3.13) are flow balance constraints. Constraints (3.14) indicate Micro-Station can be shipped from location j at time t if it's not operating. Constraints (3.15) are the shipment availability constraints.

III.3. Computational Setup

In the following numerical studies, we conduct computational experiments on a computer with an Intel Core2 Quad 3.0 GHz processor, and 8GB RAM. The algorithms are implemented in Python 2.5 and Concert Technology when CPLEX (ILOG CPLEX

12.1) was used. Although the latest Python version is 3.4, we have to use Python 2.5 in order to use the Python API for CPLEX 12.1.

III.4. Preliminary Result Using CPLEX Only

III.4.1 Linearization Model

To solve the TELP model directly in CPLEX, we convert nonlinear constraints (3.9) – (3.11) to linear constraints. The linearization technique which transforms the integer quadratic program into an equivalent zero-one binary linear program is presented here. Consider constraints (3.9) as an example.

$(K_J - \sum_{i\in I} x_{ijt})\,(K_M - \sum_{i\in I} z_{imt}) \geq \sum_{i\in I} x_{ijt}\, a_{ijmt} \sum_{i\in I} z_{imt}\, b_{ijmt}$

$$\forall\, j \in J, \forall\, m \in \mathcal{M}, \forall\, t \in \mathcal{T} \qquad (3.9)$$

Moving all quadratic forms to one side gives us:

$$K_J * K_M - K_M * \sum_{i\in I} x_{ijt} - K_J * \sum_{i'\in I} z_{i'mt} > \sum_{i\in I} x_{ijt} a_{ijmt} \sum_{i'\in I} z_{i'mt} b_{i'jmt} - \sum_{i\in I} x_{ijt} \sum_{i'\in I} z_{i'mt}$$

$$= \sum_{i\in I} \sum_{i'\in I} x_{ijt} z_{i'mt} (a_{ijmt} b_{i'jmt} - 1), \forall j \in J, \forall m \in M, \forall t \in T$$

Following the idea of the standard 0-1 linearization (Fortet, 1960), we substitute the binary quadratic terms by adding a set of new variables and a family of inequalities. We replace $x_{ijt}\, z_{imt}$ by set of $T_{iji'mt}$ binary variables. Add the following inequalities:

$$T_{iji'mt} \leq x_{ijt} \qquad \forall\, i \in \mathcal{I}, \forall\, i' \in \mathcal{I}, \forall\, m \in \mathcal{M}, \forall\, j \in \mathcal{J}, \forall\, t \in \mathcal{T} \qquad (3.18)$$

$$T_{iji'mt} \leq z_{i'mt} \qquad \forall\, i \in \mathcal{I}, \forall\, i' \in \mathcal{I}, \forall\, m \in \mathcal{M}, \forall\, j \in \mathcal{J}, \forall\, t \in \mathcal{T} \qquad (3.19)$$

$$T_{iji'mt} \geq x_{ijt} + z_{i'mt} - 1 \qquad \forall\, i \in \mathcal{I}, \forall\, i' \in \mathcal{I}, \forall\, m \in \mathcal{M}, \forall\, j \in \mathcal{J}, \forall\, t \in \mathcal{T} \qquad (3.20)$$

Inequalities (3.18) and (3.19) guarantee that $T_{iji\prime mt}$ will be zero if either x_{ijt} or $z_{i\prime mt}$ are zero. Inequality (3.20) will make sure that $T_{iji\prime mt}$ will equal to 1 if both x_{ijt} and $z_{i\prime mt}$ are set to 1.

Using Fortet's linearization approach, we transform our nonlinear problem to binary linear program. As mentioned in many articles (Sherali et al., 1986; Billionnet et al., 2008), the main drawback of this approach is that it increases problem size significantly. It becomes less and less practical as we increase the number of users and Micro-Station candidate locations.

We can improve this general linearization method by adding more valid inequalities based on the assignment properties: each individual is served by at most one base station. Therefore, our problem is very sparse, meaning that many of the decision variables are populated by zero values. We replace inequalities (3.18) and (3.19) by (3.21) and (3.22) which leads to an integer linear program of significantly smaller size.

$$\sum_{m\in \mathrm{M}} \sum_{j\in \mathrm{J}} T_{iji\prime mt} \leq \sum_{j\in \mathrm{J}} x_{ijt} \qquad \forall\, i \in \mathcal{I}, \forall\, i' \in \mathcal{I}, i \neq i', \forall\, t \in \mathcal{T} \tag{3.21}$$

$$\sum_{m\in \mathrm{M}} \sum_{j\in \mathrm{J}} T_{iji\prime mt} \leq \sum_{m\in \mathrm{M}} z_{i\prime mt} \qquad \forall\, i \in \mathcal{I}, \forall\, i' \in \mathcal{I}, i \neq i', \forall\, t \in \mathcal{T} \tag{3.22}$$

III.4.2 Computational Results for Linearized TELP Model

To see the performance of the CPLEX optimization solver on our model and better understand the impact of different parameters, we generated 9 small problem sets. For each problem, we fixed the value of K_M and K_J at 5 and 3 respectively, and set $\mathcal{T}$ at 4. Each problem set included 3 instances which have different user movement patterns:

single direction (SD), small degree of randomness (SR), complete randomness (CR). Other parameter settings are summarized in Table 3-1.

Table 3-1: Parameter values for the data sets

Set	$\|\mathcal{M}\|$	$\|J\|$	P	$\|\mathcal{I}\|$
1	1	4	2	5
2				6
3				7
4	2	8	4	10
5				12
6				14
7	4	16	8	20
8				24
9				28

We tested all the instances in CPLEX12.1 with default settings. The computational results can be found in Table 3-2. We found that even small problems are hard to solve to optimality. For these hard instances, we use "Gap 3% RT", i.e., the running time when the gap between the given solution and optimal solution reach 3%. For instances which the solver cannot give good solutions after 3 hours, we use "Opt. Gap" to show the gap between current solution and optimal solution. The running time is in seconds.

Here are observations from testing 9 problem sets: 1. the linearized TELP model is very hard to solve to optimality. The largest instances we tested were 28 users with 4 Macro-Stations and 16 candidate Micro-Station locations. After running 3 hours, we

could only obtain 90% optimal solution gap. It seems impossible to solve this model within reasonable time for real-world problem since the number of constraints and decision variables increases exponentially as the problem size increases. 2. The user movement pattern is an important factor that effects how difficult it is to solve in terms of running time and solution quality. From Table 3-2, we can see user movement followings a single direction usually leads to a longer running time or a bigger Opt Gap. During a real evacuation, instead of randomness, user movement patterns will follow evacuation routes. Therefore, it is not realistic to solve real-world problem by simply using CPLEX.

Table 3-2: Computational results of linearization TELP model

Set	Instance	Opt. RT	Gap3%RT	Opt. Gap	Obj. Val.
1	SD	3.45			19
	SR	0.695			20
	CR	0.764			20
2	SD	3.54			20
	SR	1.097			20
	CR	0.655			24
3	SD	5.1			21
	SR	1.365			21
	CR	1.263			28
4	SD		397.63		36
	SR	1322			37
	CR		2.995		39
5	SD		3282.7		38
	SR	2156			39
	CR		21.06		47
6	SD			5.13%	39
	SR	4587			42
	CR		155.57		55
7	SD	21617		8.11%	74
	SR			3.90%	77
	CR	209.5			80
8	SD			31.51%	73
	SR			88.24%	51
	CR		13170		94
9	SD			100%	56
	SR			87.72%	57
	CR			89.83%	59

III.4.3 Solution Illustration

To better understand the features of optimal solutions and develop efficient algorithms, we illustrate solution characteristics in this section. Here we use problem set 4 SD instance which has 1Macro-Station, 4 candidate Micro-Station locations (CML), 2 Micro-Stations and 5 users with a single direction movement pattern. The coordinates of CML and the shipping time between any two locations can be found in Table 3-3 and Table 3-4 respectively.

Table 3-3: Coordinates of candidate micro-station locations

StationID	X Coordinate	Y Coordinate
Macro-Station (M)	2000	2000
Micro-Station1 (j1)	1000	3000
Micro-Station2 (j2)	1000	1000
Micro-Station3 (j3)	4000	1000
Micro-Station4 (j4)	4000	3000

Table 3-4: Shipping time from CML j to j'

	j1	j2	j3	j4
j1	0	1	2	1
j2	1	0	1	2
j3	2	1	0	1
j4	1	2	1	0

Figure 3-2 shows the assignment of users to cellular stations at each time period. Red dash lines indicate the assignment of Micro-Station users to the corresponding Micro-Stations. And the green dash lines indicate the assignment of Macro-Station users.

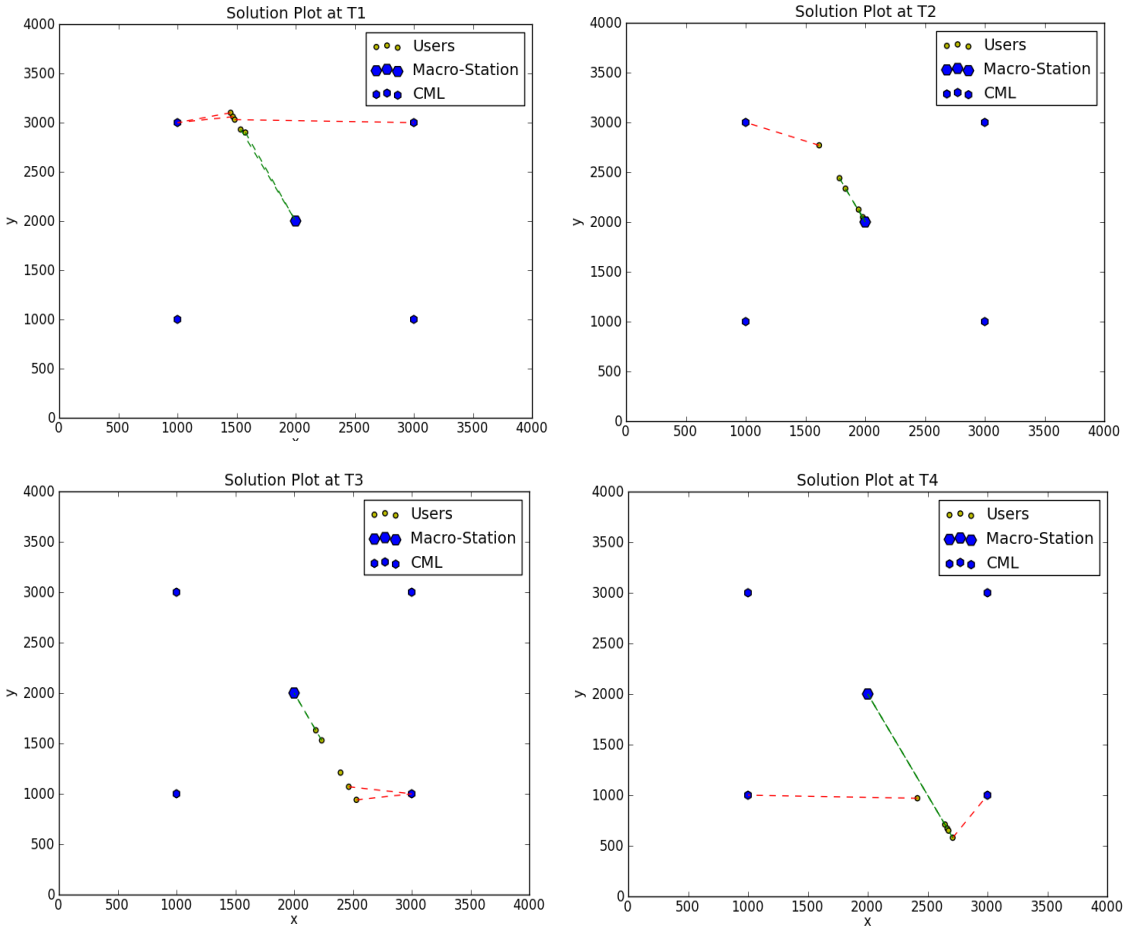

Figure 3-2: Assignment of users to cellular stations

We use a space-time network to demonstrate installation and routing solutions. Figure 3-3 shows the location solution where Micro-Stations should be installed and routing strategy detailing how Micro-Stations can be shipped from one candidate location to another between time periods. All Micro-Stations initially leave the pseudo node S0 and arrive at the pseudo node S1 at the end. No shipping cost between any candidate locations and pseudo nodes. At time period 1, Micro-Station1 and Micro-Station2 are located at j1 and j4 respectively. Micro-Station1 remains at j1 at time period

2 while Micro-Station2 travels from j4 to j3. At time period 3, Micro-Station2 arrives at j3 and Micro-Station1 travels from j1 to j2. Both Micro-Stations operate at time period 4 at location j2 and location j3 respectively. Note that a better installment solution which gives a higher objective value is to install a Micro-Station at j2 at time period 3. However, due to routing constraints, Micro-Station1 cannot arrive at j2 at time period 3 which may cause unfulfilled user demand. Routing constraints actually reduced the feasible candidate location set. This solution feature can be utilized when we develop our heuristic solution in the next section.

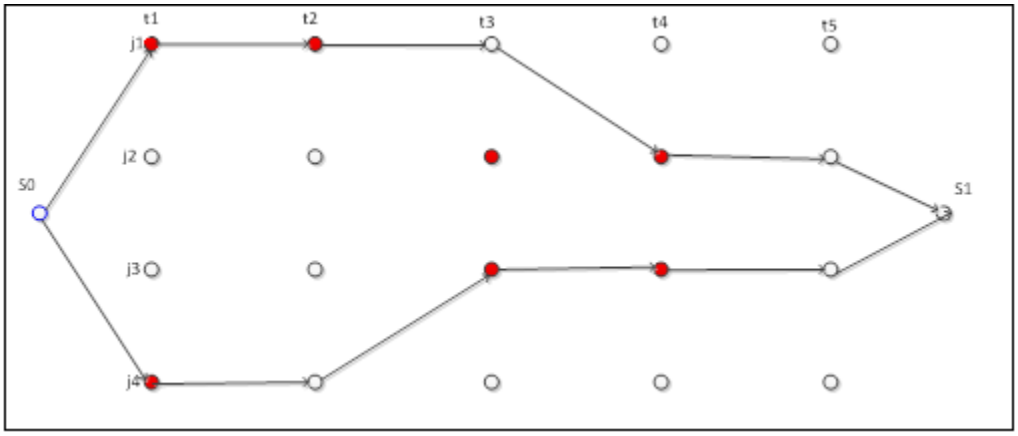

Figure 3-3: Micro-Station installation and routing solution

III.5. Heuristics

Although linearization technique helps in problem simplification and enable us to use CPLEX to solve TELP model, it is not efficient in terms of runtime and memory required when we apply our model to relatively large-scale instances for extreme event evacuation. Therefore, it is necessary for us to develop heuristic solution approaches which take advantage of the well-understood explicit model formulation and solution

characteristics we found in last section. In this section, we present a greedy randomized adaptive search procedure (GRASP) metaheuristic and Lagrangian relaxation heuristic and the implementation of these two heuristics.

III.5.1 Metaheuristic -- GRASP

Recall that routing constraints limit the Micro-Station locations. Instead of considering the best installation and assignment strategy at the first stage and checking if routing constraints are satisfied at the second stage, this heuristic approach generates feasible routes and decides Micro-Station installation locations at the same time.

GRASP is a multi-start procedure where each iteration consists of two major parts: 1. Construction of a greedy randomized feasible solution; 2. Local search: find a locally optimal solution, starting from the constructed solution. The pseudocode of GRASP approach is found in Algorithm 1.

Algorithm 1 *Procedure* GRASP

```
1   BestSolutionFound = ∅; F (BestSolutionFound) = −∞;
2   for i = 1… MaxIter:
3       x = HybridGreedyRandomizedConstruction (Random Seed);
4       x' = LocalSearch (x);
5       If F (x') > F (BestSolutionFound):
6           BestSolutionFound = x';
7       End if;
8   End for;
9   Return BestSolutionFound
```

Procedure HybridGreedyRandomizedConstruction

SolutionFound = ∅;

While solution is not complete:

    Generate reachable candidate Micro-Station locations as set Sp;

    List all possible Micro-Station installation strategies based on Sp as set K;

    For each k ∈ K:

        CPLEX solve assignment problem

        While interference constraints is violated:

            Change corresponding x_{ij} or z_{im} status

            CPLEX solve updated assignment problem

        End while;

        f (k) = $\boldsymbol{Max}\ \sum_{i\in \mathrm{I}}\sum_{j\in \mathrm{J}} x_{ij} + \sum_{i\in \mathrm{I}}\sum_{m\in \mathrm{M}} z_{im}$

    End for

    U = max {f (k): k ∈ K}

    L = min {f (k): k ∈ K}

    Build the Restricted Candidate List (RCL):

        RCL = {k ∈ K: f (k) ≥ L+ α (U-L)};

    Select element s from RCL at random;

    SolutionFound = SolutionFound ∪{s};

End while;

Return SolutionFound

We demonstrate the greedy randomized solution construction procedure in Figure 3-4. This solution construction procedure builds up a sub-solution at each time period and produces the complete solution at the end of last time period. By breaking down multiple time periods into single time period, we can simplify the sub-problem.

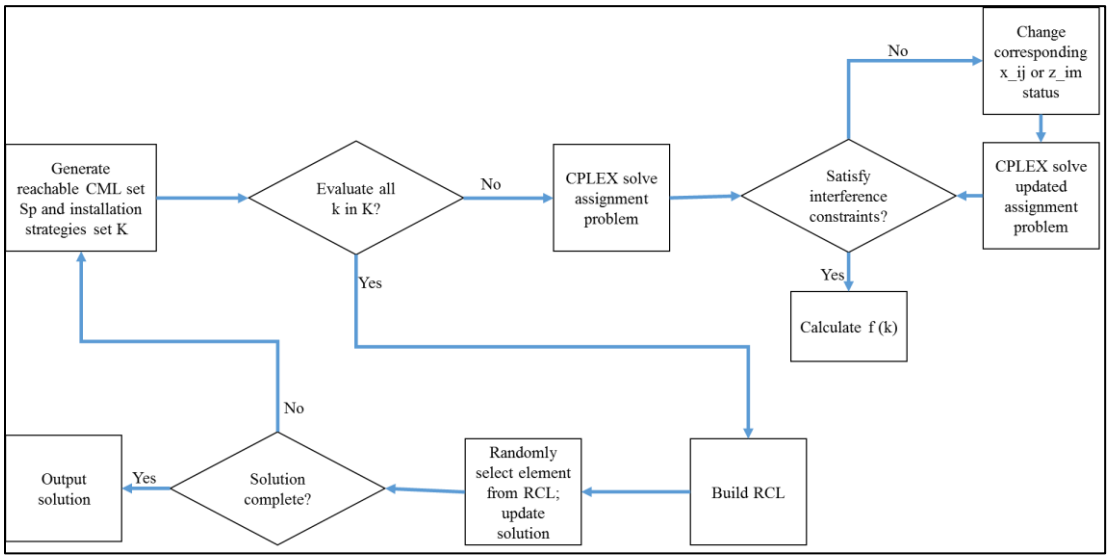

Figure 3-4: Flow chart of GRASP solution construction

At each time period Ti, we generate a set of reachable candidate Micro-Station locations J'. Based on the information from previous time periods such as the Micro-Station's location, whether it's operating or not and shipping time, we can get a set of feasible locations where a Micro-Station can be shipped to at time period Ti. These locations are referred to as the reachable candidate Micro-Station locations. At the first time period, we consider all CML as J'. Obviously, J' is a subset of CML and by creating such a set of locations we can reduce the model parameter $|J|$ and ensure the routes are feasible. Furthermore, at each time period Ti we generate a set of all possible

Micro-Station installation strategies called K. For P given Micro-Station facilities, K = {0, 1, 2… P}. It is necessary to examine all elements in K, because it may not be beneficial to operate all available Micro-Stations at each time period.

After completing the previous steps, what remains is a relatively simple assignment problem. The objective function and constraints are given as following:

$$\boldsymbol{Max} \sum_{i\in \mathrm{I}} \sum_{j\in \mathrm{J}} x_{ij} + \sum_{i\in \mathrm{I}} \sum_{m\in \mathrm{M}} z_{im} \tag{3.23}$$

s.t.

$$\sum_{j\in \mathrm{J}} x_{ij} + \sum_{m\in \mathrm{M}} z_{im} \leq 1 \qquad \forall\, i \in \mathcal{I} \tag{3.24}$$

$$x_{ij} \leq y_j \qquad \forall\, i \in \mathcal{I}, \forall\, j \in \mathcal{J}' \tag{3.25}$$

$$\sum_{i\in \mathrm{I}} x_{ij} < K_J \qquad \forall\, j \in \mathcal{J}' \tag{3.26}$$

$$\sum_{i\in \mathrm{I}} z_{im} < K_M \qquad \forall\, m \in \mathcal{M} \tag{3.27}$$

$$\sum_{j\in \mathrm{J}} y_j = P \tag{3.28}$$

$$x_{ij}\, d_{ij} \leq R_J \qquad \forall\, i \in \mathcal{I}, \forall\, j \in \mathcal{J}' \tag{3.29}$$

$$z_{im}\, d_{im} \leq R_M \qquad \forall\, i \in \mathcal{I}, \forall\, m \in \mathcal{M} \tag{3.30}$$

Note that constraints (3.26) – (3.20) are very easy constraints and we use CPLEX to solve this assignment problem for each k ∈ K. The last set of constraints we need to consider is interference constraints which can effect decision variables x_{ij} and z_{im} and objective value. Here we exhaust all pairs of cellular stations which have interference impact and check if all constraints are satisfied. If the current assignment violates any interference constraint, we delete the assignment causing violation and set the corresponding x_{ij} or z_{im} equal to 0. We then add corresponding x_{ij} = 0 or z_{im} = 0 as

new constraints and resolve the updated assignment problem until all the interference constraints are valid. Then we calculate the objective value of the assignment problem namely f (k).

After examining all k ∈ K, we have a list of feasible solutions and objective values for single time period Ti. Let the largest and smallest f (k) be U and L respectively and build the Restricted Candidate List (RCL): RCL = {k ∈ K: f (k) ≥ L+ α (U-L)}. Randomly pick an element s from RCL and update SolutionFound to SolutionFound ∪{s}. Repeat process (step 3-17) until the end of the last time period which terminates the solution construction phase.

RCL is actually where the greedy randomization takes place. Instead of always take the local best solution, RCL gives the opportunity to take a look at the solution that may be good but not the best. Parameter α controls the tradeoff between greediness and randomness, where α = 0 is purely greedy and α = 1 is purely random. We use α = 0.5 for testing our problems. For an individual time period the best solution is to operate all available Micro-Stations. However, it may be beneficial for whole time horizon to stop operating selected Micro-Stations at some point in time and ship them to another locations that can fulfill larger demand at a later time.

To start local search, we need to first define the "neighborhood" for our problem. Consider the constructed solution as the initial solution and construct adjacent solutions that have the same routing strategy but different installation solutions. Basically, adjacent solutions have different y_{jt} values but maintain the same route solution as the initial solution. Notice that we may miss better installation strategies when we randomly

pick an element from RCL. If these installation strategies also satisfy the current routing solution, then we can improve our initial solution. For any adjacent solution we limit the number of different y_{jt} from the initial solution to 1. The collection of adjacent solutions is defined as the neighborhood. Local search is to find the best solution in the neighborhood and replace the current solution if there is a better solution.

III.5.2 Lagrangian Relaxation-based Heuristic

The second heuristic we apply to the TELP model is a Lagrangian relaxation with local search technique. Fig.3-5 is flowchart for a Lagrangian relaxation heuristic approach. The Lagrangian relaxation formulation LR (λ) of TELP is given as follows.

$$\boldsymbol{Max}\ \sum_{t\in \mathrm{T}}\sum_{i\in \mathrm{I}}\sum_{j\in \mathrm{J}} x_{ijt} + \sum_{t\in \mathrm{T}}\sum_{i\in \mathrm{I}}\sum_{m\in \mathrm{M}} z_{imt} + \sum_{t\in \mathrm{T}}\sum_{i\in \mathrm{I}}\sum_{j\in \mathrm{J}} \lambda^0_{ijt}(y_{jt} - x_{ijt}) + \sum_{t\in \mathrm{T}} \lambda^1_t(P - \sum_{j\in J} y_{jt}) + \sum_{t\in T}\sum_{j\in J} \lambda^2_{jt}\left(\sum_{j'\in J}\sum_{t'\in T} v_{j't'jt} - y_{jt}\right) + \sum_{t\in T}\sum_{j\in J} \lambda^3_{jt}\left(1 - j'\in Jt'\in Tvj't'jt + t\in Tj\in J\lambda jt4j'\in Jt'\in Tvj't'jt - j'\in Jt'\in Tvjtj't' + t\in Tj\in J\lambda jt51 - j'\in Jt'\in Tv jtj't' - yjt + j\in Jt\in T{:}t<t'j'\in Jt'\in T\lambda jtj't'6vjtj't'(1-(t'-t-\tau jj'))\right)$$

(3.31)

s.t.

$$\sum_{j\in \mathrm{J}} x_{ijt} + \sum_{m\in \mathrm{M}} z_{imt} \le 1 \qquad \forall\, i \in I,\ \forall\, t \in \mathcal{T} \qquad (3.32)$$

$$\sum_{i\in \mathrm{I}} x_{ijt} < K_J \qquad \forall\, j \in J,\ \forall\, t \in \mathcal{T} \qquad (3.33)$$

$$\sum_{i\in \mathrm{I}} z_{imt} < K_M \qquad \forall\, m \in \mathcal{M},\ \forall\, t \in \mathcal{T} \qquad (3.34)$$

$$x_{ijt}\, d_{ijt} \le R_J \qquad \forall\, i \in I,\ \forall\, j \in J,\ \forall\, t \in \mathcal{T} \qquad (3.35)$$

$$z_{imt}\, d_{imt} \le R_M \qquad \forall\, i \in I,\ \forall\, m \in \mathcal{M},\ \forall\, t \in \mathcal{T} \qquad (3.36)$$

$$x_{ijt}, z_{imt}, y_{jt} \in B \qquad \forall\, i \in \mathcal{I}, \forall\, j \in \mathcal{J}, \forall\, m \in \mathcal{M}, \forall\, t \in \mathcal{T} \tag{3.37}$$

$$v_{jtj't'} \in B \qquad \forall\, j, j' \in \mathcal{J}, \forall\, t, t' \in \mathcal{T}, t < t' \tag{3.38}$$

$$\text{All } \lambda \geq 0 \tag{3.39}$$

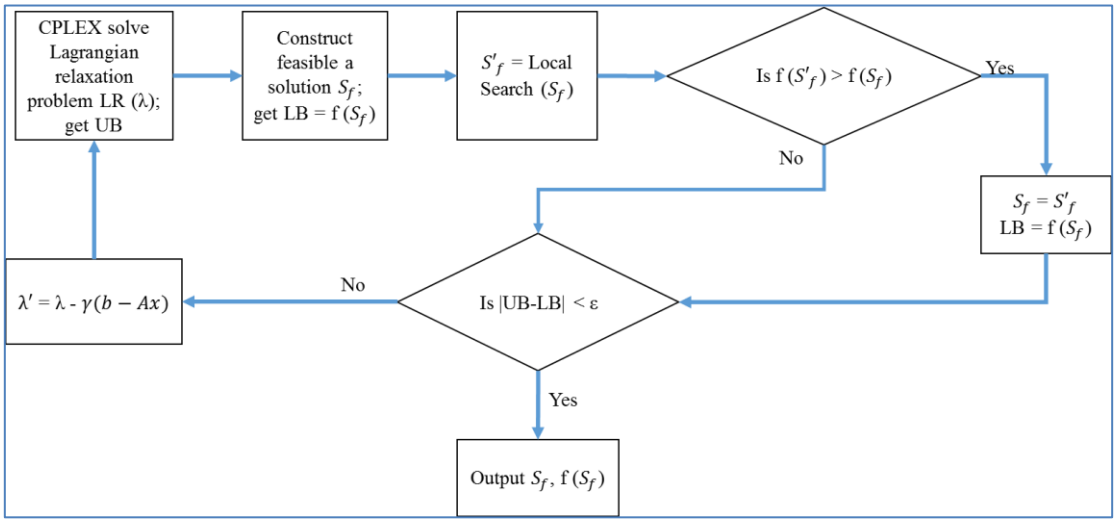

Figure 3-5: Flow chart of Lagrangian relaxation heuristic

First, we use CPLEX to solve LR (λ) and get the Upper Bound. To construct feasible solution S_f of original problem from LR (λ), we need:

(1) y_{jt}: We have (1-$\sum_{t\in \mathrm{T}}\sum_{i\in \mathrm{I}}\sum_{j\in \mathrm{J}}\lambda^0_{ijt}$)$x_{ijt}$ in the objective of LR (λ). For each $t \in \mathcal{T}$, find P largest coefficient of x_{ijt} from term (1-$\sum_{i\in \mathrm{I}}\sum_{j\in \mathrm{J}}\lambda^0_{ijt}$)$x_{ijt}$ and let these x_{ijt} and the corresponding y_{jt} equal to 1.

(2) Feasible $v_{jtj't'}$: Construct a directed spatial temporal graph G, and each vertex V_j^t in G corresponding to a location j and time t. Add pseudo node s and t as source node and sink node. Add edges between V_j^t and V_j^{t+1} for t >0, t +1 ≤ T. For

vertices whose y_{jt} equal 0, add edges between V_j^t and $V_{j'}^{t'}$ if transportation time between j and j' equals $(t' - t - 1)$. Add edges from s to V_j^1 and V_j^T to t. For incoming edges of vertices whose y_{jt} equal 1, assign unit weight on these edges and assign 0 weight to the other edges. In this DAG graph we can find the longest path from s to t to get a route for each mobile cell station. In particular, after obtain a longest path from s to t, remove the vertices and edges comprised in the path and construct another longest path from the new graph until we obtain P routes.

(3) Adjust y_{jt} and x_{ijt} : If vertices whose y_{jt} equal to 1are not covered by any of the P routes, then make y_{jt} equal to 0 and adjust corresponding x_{ijt}

(4) Check the interference constraints: For each cell station (mobile station or fixed station), sort the user distance to the station in decreasing order. If the interference constraints are not satisfied, then remove the furthest user until interference constraints are satisfied.

The lower bound of the problem can be calculated once we find the feasible solution. Then we use the local search starting from the feasible solution constructed above. The local search algorithm we apply here followed the same idea as the GRASP metaheuristic. Again, in the adjacent solution we change y_{jt} for those such that status changing does not impact on routing constraints i.e., keep variable $v_{jtj't'}$ the same. Find the best solution S'_f in neighborhood. Check if we can get a better lower bound and update the lower bound and the best feasible solution as necessary. If the gap between

the upper bound and lower bound is smaller than threshold ε, then we output the best feasible solution and corresponding objective value. If the current best feasible solution is far away from the upper bound, we update each set of lagrangian multiplier λ by using following equations.

$$\lambda_{ijt}^{0\,\prime} = \lambda_{ijt}^{0} - \gamma(y_{jt} - x_{ijt})$$

$$\lambda_{t}^{1\prime} = \lambda_{t}^{1} - \gamma(P - \textstyle\sum_{j\in J} y_{jt})$$

$$\lambda_{jt}^{2\,\prime} = \lambda_{jt}^{2} - \gamma(\textstyle\sum_{j'\in J}\sum_{t'\in T} v_{j't'jt} - y_{jt})$$

$$\lambda_{jt}^{3\,\prime} = \lambda_{jt}^{3} - \gamma(1 - \textstyle\sum_{j'\in J}\sum_{t'\in T} v_{j't'jt})$$

$$\lambda_{jt}^{4\,\prime} = \lambda_{jt}^{4} - \gamma(\textstyle\sum_{j'\in J}\sum_{t'\in T} v_{j't'jt} - \sum_{j'\in J}\sum_{t'\in T} v_{jtj't'})$$

$$\lambda_{jt}^{5\,\prime} = \lambda_{jt}^{5} - \gamma(1 - \textstyle\sum_{j'\in J}\sum_{t'\in T} v_{jtj't'} - y_{jt})$$

$$\lambda_{jtj't'}^{6} v_{jtj't'}{}' = \lambda_{jtj't'}^{6} v_{jtj't'} - \gamma(1 - (t' - t - \tau jj'))$$

$$where\ \gamma = u * \frac{UB-LB}{SQ}$$

$$SQ =$$

$$\textstyle\sum_{t\in \mathrm{T}}\sum_{i\in \mathrm{I}}\sum_{j\in \mathrm{J}}(y_{jt} - x_{ijt})^2 + \sum_{t\in \mathrm{T}}(P - \sum_{j\in J} y_{jt})^2 +$$

$$\textstyle\sum_{t\in T}\sum_{j\in J}\left(\sum_{j'\in J}\sum_{t'\in T} v_{j't'jt} - y_{jt}\right)^2 + \sum_{t\in T}\sum_{j\in J}\left(1 - \sum_{j'\in J}\sum_{t'\in T} v_{j't'jt}\right)^2 +$$

$$\textstyle\sum_{t\in T}\sum_{j\in J}\left(\sum_{j'\in J}\sum_{t'\in T} v_{j't'jt} - \sum_{j'\in J}\sum_{t'\in T} v_{jtj't'}\right)^2 + \sum_{t\in T}\sum_{j\in J}\left(1 -\right.$$

$$\left.\textstyle\sum_{j'\in J}\sum_{t'\in T} v_{jtj't'} - y_{jt}\right)^2 + \sum_{j\in J}\sum_{t\in T:t<t'}\sum_{j'\in J}\sum_{t'\in T}(1 - (t' - t - \tau jj'))^2$$

u is the parameter that decides how big is the step from λ to λ’

III.5.3 Computational Results

The computational results of implementing GRASP metaheuristic and Lagrangian relaxation heuristic are presented in this section. To test and compare the heuristic approaches to the linearized model solved in CPLEX, we use the same parameter settings as shown in Table 3-1.

Table 3-5: Computational results of GRASP and Lagrangian relaxation

		GRASP				Lagrangian Relaxation	
Set	Instance	Avg. RT	Std. RT	RT reach best sol.	Obj. Val.	RT	Obj. Val.
1	SD	6.599	2.153	0.314	18	1.49	16
	SR	9.415	1.073	0.448	16	0.1247	14
	CR	6.545	1.867	0.311	20	0.4785	16
2	SD	7.961	0.946	0.571	18	2.39	17
	SR	10.18	1.488	0.484	16	0.2826	12
	CR	8.406	1.481	1.705	24	2.5427	17
3	SD	14.014	1.067	1.005	19	10.23316	18
	SR	12.162	2.269	0.966	16	0.351	13
	CR	12.095	3.165	2.951	24	18.1158	21
4	SD	38.881	4.566	5.218	34	7.0785	23
	SR	64.571	22.328	9.296	32	0.2714	23
	CR	54.385	16.254	14.369	40	3.1918	24
5	SD	53.375	8.371	4.181	34	11.34	29
	SR	95.797	28.272	29.73	33	0.83235	34
	CR	87.952	28.126	28.923	43	16.5217	31
6	SD	206.917	79.284	48.804	37	103.2878	31
	SR	231.874	130.215	75.554	34	19.725	30
	CR	146.446	37.763	47.16	48	34.9366	32
7	SD	605.172	237.45	164.156	71	15.432	45
	SR	560.961	198.421	148.826	64	1.0623	45
	CR	490.819	143.953	124.536	79	12.5131	43
8	SD	657.433	178.577	251.61	70	124	52
	SR	564.867	207.951	176.791	63	6.79	50
	CR	503.566	105.239	162.166	86	93.189	67
9	SD	480.46	131.595	204,786	73	566.2434	57
	SR	793.292	243.976	277.329	60	38.54191	58
	CR	704.317	227.95	246.224	94	274.3103	60

Note that GRASP is multi-start algorithm, we run 10 replications for each instance. Stopping criteria we used here is if no better solution is found for 20 iterations then we consider the current solution to be the best solution. To measure the running time for GRASP, we use the average running time, standard deviation of running time and the running time when the best solution is first found.

Figure 3-6 and Figure 3-7 show the running time and objective value comparison of the linearized model, GRASP heuristic and Lagrangian relaxation heuristic for SD, SR and CR instances respectively. For the smallest problem set 1-3 (1 Macro-Station, 5-7 users), all three approaches can give solutions within 20 seconds. Using CPLEX to solve the linearized model can give us the optimal solution quickly. When we increase the problem size to 2 Macro-Stations and 10-14 users, the linearized model starts to slow down and took at least 1 hour to solve for some test instances. By contrast, the two heuristic approaches can solve these instances within 200 seconds and most instances are solved within 100 seconds. Compared to GRASP, the Lagrangian relaxation heuristic is faster which can finish solving within 30 seconds for many instances from problem sets 4-6. However, GRASP provides better solutions than Lagrangian relaxation for almost all instances. Solution quality from GRASP can compete with the linearized model for many instances. The best solutions for the largest test instances are indeed from GRASP although it took longer running time compared to Lagrangian relaxation.

Solutions from Lagrangian relaxation are slightly better than the linearized model for larger problems, and it only takes a little computational effort. For all instances from

problem 9, Lagrangian relaxation can solve for a better solution in 10 minutes than the linearized model can solve for in 3 hours.

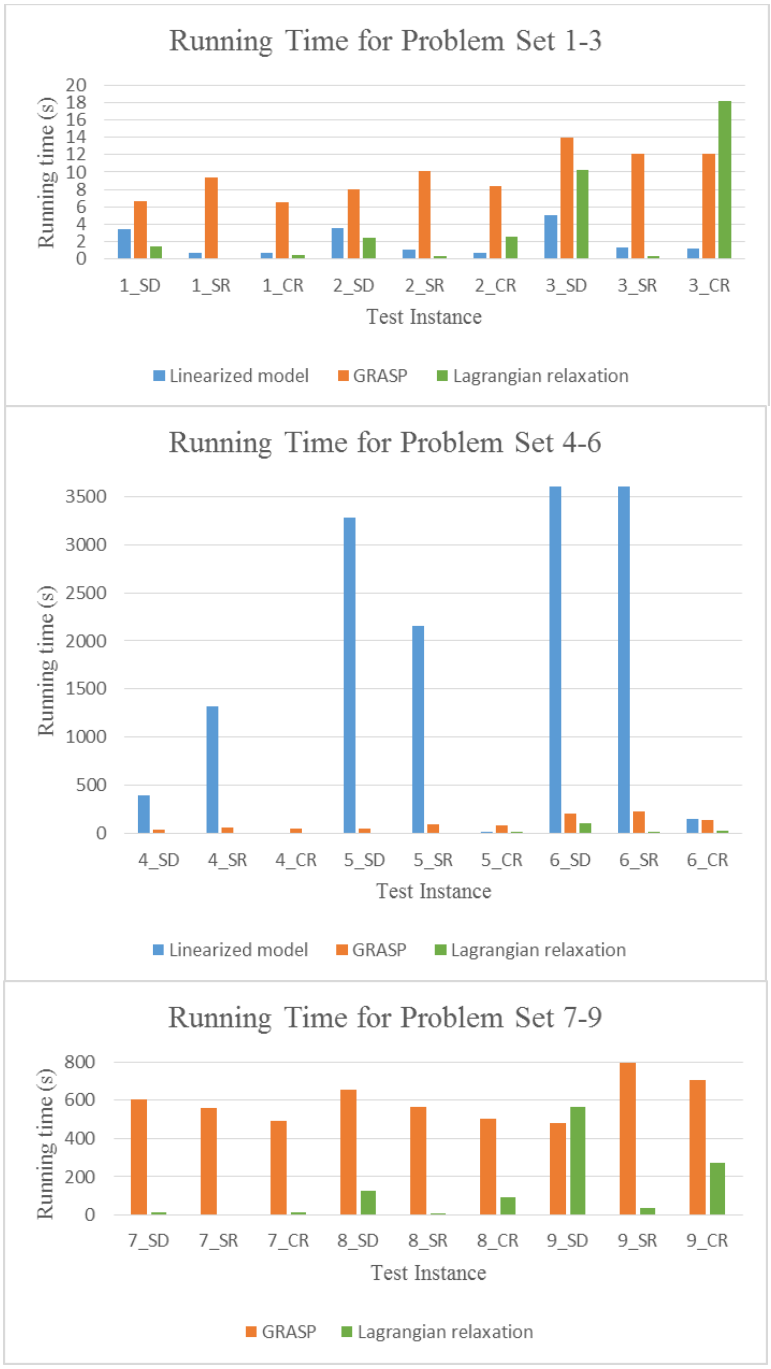

Figure 3-6: Running time comparison for three approaches

Figure 3-7: Objective value comparison for three approaches

III.6. Summary and Conclusion

In this chapter, we introduce telecommunication equipment location problem and provide the mathematical model TELP. This model considers where to locate mobile Micro-Stations and best routes to ship them based on existing cellular network to better serve cell-phone users for the extreme event evacuation process. Because of the nonlinear interference constraints, we cannot solve TELP simply using optimization solver. To obtain a linearization model, we have to add more variables and constraints by apply the linearization technique. Then we test the linearization model with small size problems. We found even for the small size problems, it is very hard to find optimal solutions. After study solution characters, we develop two heuristic approaches: GRASP metaheuristic and Lagrangian relaxation heuristic. Both heuristic approaches can solve test problems quickly compared to solve the linearization model. GRASP can yield very competitive solutions but need to have more computational effort. Lagrangian relaxation heuristic, by contrast, can obtain solutions very quickly but sacrifice the solution quality.

CHAPTER IV

AGENT-BASED EVACUATION PROCESS SIMULATION USING FUZZY COGNITIVE MAPS AS BEHAVIOR MODELS

This chapter presents an agent-based evacuation process simulation model for implementing the novel fuzzy cognitive maps (FCMs) as agent behavior models. Each component of the simulation and its relation with other components are described in detail. These components include the physical environment, general property of agents, agent information sharing and collection, and agent behavior models. Agent behavior models consist of genetic and FCM-supported types. Genetic behavior models simulate subconscious behaviors, such as lane change, whereas FCM-supported behavior models simulate more complicated behaviors involving analytical reasoning and a time-adaptive procedure. In this simulation, each agent has its own FCMs, which are used to make decisions on speeding up, slowing down, route changes, destination changes, and resulting corresponding behaviors.

IV.1. Agent-based Model Methodology

An agent-based simulation model (ABM) has been developed to explore individual travel behavior and collective group behavior during an extreme event evacuation process, considering human and social behaviors. Using ABM as a tool can help us understand better how social networking and the availability/use of mobile telecommunication stations impact regional evacuations, considering the uncertainty of

individuals and the interaction among individuals. Specifically, with this ABM, we are able to explore how social media use can improve evacuation efficiency and to investigate how mobile telecommunication infrastructure planning impacts evacuation efficiency.

The utility function approach is commonly used in ABM (see Chen and Zhan, 2004; Han et al., 2007; Widener et al., 2012). It is a linear or nonlinear function of concerned factors, and the calculated value compared to the defined threshold would decide an agent's behavior. However, instead of using the utility function to simulate decision-making, we use FCMs to mimic the causal decision-making process. The FCMs define the causal relationships among concepts, and they enable agents to evaluate temporal environment information and the fuzzy activation level for each concept. Agents will choose several possible actions after dynamically integrating external information and the evolution process. Compared to the utility function approach, FCMs can represent sophisticated relationships among different concepts, handle temporal information dynamically, and allow an adaptive learning process. Most importantly, FCMs provide realistic decision-making processes for this evacuation model, especially when the agents represent humans who operate vehicles. The adoption of FCMs distinguishes this ABM model from its peers and enables the integration of a variety of information; it also handles incomplete, unreliable, conflicting information and models the decision-making evolution.

First, the ABM environment in which agents can operate is defined. In this simulation model, it is assumed that agents travel via vehicles. Hence, the road network

defines the physical domain of all agent activities. The digital elevation model (DEM) is integrated as the physical environment so that agents can have third-dimensional geographic knowledge to assist their decision-making. Besides the physical environment, the information system is introduced and enabled by the telecommunication system. The information system allows agents to share and receive information; the collective information can encourage or inhibit agent decision-making.

The information system environment enabled by the telecommunication system exists only when the agent has cellular service. This environment is essential in utilizing social media, especially for emergency evacuation. The use of social networks without considering cellular support is insufficient. By introducing this virtual environment, agents can access and analyze information from other geographic regions, which actually extends agents' "vision."

Different from the discrete event simulation model, the ABM decomposes a complicated system into a number of basic artificial agents. In this model, each agent represents a small group of evacuees who travel together using one vehicle. The agents are so-called "artificial agents" because they have their own "brain" to decide how to interact with the surrounding environment and other agents. Section IV.3 presents a detailed description of agent properties.

The agent's "brain" defines a series of behavior rules that guide the agent in taking specific actions at specific times. In this model, these behavior rules include the genetic and FCM-supported behavior models. The genetic behavior model supports agents taking actions on lane changing and sending out traffic information while

traveling on road segments. The FCM-supported behavior model can analyze the causal relationship between related factors and previous historical data to support more complicated decision-making, such as route change and destination change.

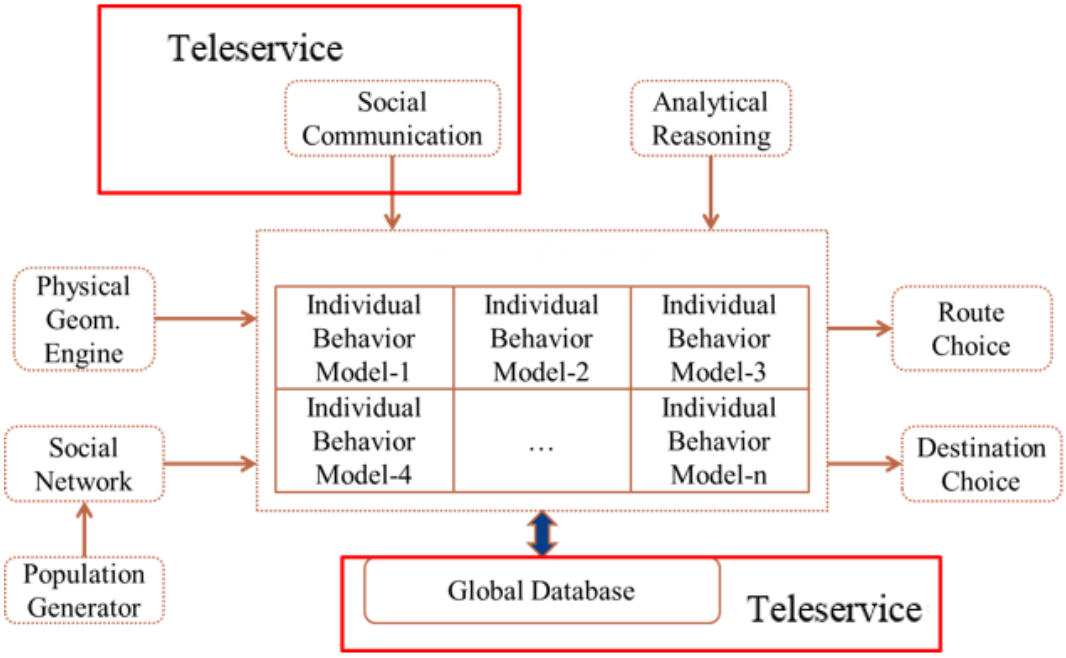

Figure 4-1: Framework of ABME

Figure 4-1 shows the framework of the ABM model. In its execution, a diverse population is randomly generated and distributed artificially within the region to be evacuated. The social networks are constructed among the generated population, considering both random networks and networks that have real-world, social network characteristics. A physical geometry engine (GeoMASON) imports geographic information system (GIS) data, the base station locations (obtained from the TELP model in Chapter III), and the United States Geological Survey (USGS) DEMs

(generated from satellite images) to the simulation model. Each agent will have its own behavior models. After integrating external information (e.g., the physical data, social communication, and broadcast information) and inherent data, individuals make adaptive dynamic decisions on the route and destination choices resulting from their own decision-making models.

In this simulation model, information passes among the agents through general broadcast information and the agents' social connections (i.e., agents send information to their "friends" as specified by their social network). It is assumed that every agent can receive the broadcast information whenever the agent is served by a teleservice. Again, only when the agent has teleservice can it successfully send or receive information via a social network.

IV.2. The Environment

IV.2.1 Physical Environment

Since the scope of this research includes the evacuees who travel in their vehicles, agent movement is restricted to the road network of the target region. The road network consists of a set of network intersections (nodes) and a set of road segments (arcs). It is assumed that each road segment is a bidirectional road, with multiple lanes for each direction. Intersections (forming a subset) are pre-chosen as evacuation origins where all agents are randomly placed in the initial step. Next, intersections comprising a different subset are identified as evacuation destinations representing the shelters where agents travel to after leaving their origins. There are no common nodes between the

origin and destination subsets. Additionally, there must be at least one path from the agent's origin to its destination node. It is assumed that the capacity of each destination shelter is limited to an assigned number.

For each agent, an evacuation route is computed once its destination node is selected. Instead of restricting the agents' travel to the shortest route, they are allowed to change their routes at intersections. In other words, agents can choose from the available multiple routes, based on their external information analysis. To generate more realistic alternative routes, the k-shortest paths were computed from each intersection to each destination node. The k-shortest paths comprise a sequence from the shortest path to the kth-shortest path between a pair of nodes. These paths are pre-loaded into the system before the simulation starts. It is assumed that each agent has full knowledge of these k-shortest paths and that all paths are loopless. Yen's (1971) k-shortest path algorithm was adopted for implementation in this model because (among other reasons) the time complexity $O(kn(m + nlogn))$ has remained unbeaten for so many years.

Considering that the geospatial information on the third dimension (the z-coordinate) may influence an individual's behavior, the DEM of the target region is imported. Specifically, different slopes of road segments can result in different vision ranges for agents, and the vision range can further influence agents' travel speed.

IV.2.2 Virtual Environment

Besides the physical environment, the information environment is the other important environment with which the agents interact. This virtual environment offers two types of information sharing: global broadcast and social media. The global

broadcast maintains the updated shelter capacity information. Every agent can access the global broadcast information as long as it has telecommunication service. Information sharing on social media only happens among agents with social connections. A simulated social network is constructed to represent the social connectivity among the agents. Again, information sharing on a social network can only be allowed when agents have access to telecommunication.

Scale-free networks are constructed as simulated social networks. The degree distribution of a scale-free network follows a power law distribution: the probability of a node having k connections to other nodes is $k^{-\gamma}$ for large values of k, where γ is a parameter $2 < \gamma < 3$. Since social networks are claimed to be scale-free, some phenomena, such as "small world," are expected to be observed from the constructed scale-free networks. In comparison, random networks are also constructed as another set of simulated social networks. The simulated social network is stored in the system and kept the same during the entire simulation. An adjacency matrix is used to represent social connectivity. Although Butts et al. (2012) point out that the geographic heterogeneity would influence the social network structure, it is assumed that there is no geographic correlation on the simulated social networks. This assumption is made to have observations under a more general social network structure.

Finally, the locations of cell stations are considered part of the environment, which determines whether or not an agent can be served. We export the output from the TELP model to determine when and where the mobile telecommunication facilities would be located during the evacuation process. The parameters associated with cell stations, such

as service range and pole capacity, are consistent with the parameters in the deterministic TELP model. Section IV.5 gives the implementation details of how the TELP model and ABM work together. Table 4-1 lists the parameters and variables associated with the above discussion.

Table 4-1: Environment parameters and variables

Environment Parameters	
O	A set of origin nodes
D	A set of destination nodes
R_{pq}^{k}	Kth shortest path from intersection node p to destination node q
vR_l	Vision range for an agent at location l
A^{SN}	Adjacency matrix of social connectivity
a_{ij}^{SN}	1 when agent i has social connection to agent j
L_M	Locations of Macro-Stations
Environment Variables	
L_m	Locations of Micro-Stations
GI^D	Global broadcast destination capacity information
SI^R	Congested road segment information shared on social media
SI^D	Destination information shared on social media

IV.2.3 Environment Variables

For every simulation iteration, the model updates the locations of mobile micro-stations and the destination capability information. Social media shares the information about destinations and congested road segments. At each iteration, if an agent's travel speed is lower than a threshold, then the agent is considered in traffic, and it will inform its social connections about the congestion of the road segment. The model maintains all congested road segment information shared among all agents, using variable SI^R. Since the congested road information is time sensitive, our model keeps this information,

lasting for t iterations; after that, this information is discarded unless the same road segment is still in traffic. Variable SI^D represents the updated destination information sharing on social media, such as the current and alternative destinations for each agent.

IV.3. Agents

IV.3.1 Agent Parameters

Each agent possesses several genetic properties that can be identified from other agents but always remain the same during the simulation. These genetic properties can be considered "agent parameters." The "top speed" is one of the genetic properties, which defines the highest speed the agent can reach. The agents' top speed values can vary from one another since each individual has its own comfortable driving speed. Another genetic property is "acceleration/deceleration." Similar to the top speed, each agent has its unique acceleration/deceleration rate. On one hand, the diversity of the travel speed can reflect the variation in individual driving behavior in the real world; on the other hand, it can provide a more interesting, collective travel pattern other than uniform travel behavior. Agent genetic properties can be expanded to different vehicle types, demographic trends, socioeconomic classes, and so on.

IV.3.2 Travel on Road Segments

Besides agent parameters, Table 4-2 also lists all the agent variables in our simulation model. At each simulation iteration, we track each agent's location and speed. In the initial step, agents are located at their assigned origins. As the simulation starts, we use the FCM-speedUp model to adjust the speed of agent i from 0 to the proper

speed. The FCM-speedUp model is one of the FCMs that is used for agent acceleration while agents travel on the road segments. On the other hand, the FCM-slowDown model is used for agent deceleration when agents reach congested road segments. The two models are explained in detail in Section IV.4.3 when we present all the FCM models. As an agent travels on the road segment, it needs the distance and speed information about the agent in front to adjust its own speed or decide whether or not it needs to change lanes. Besides the information about the agent in front, the elevation of the agents can impact their physical vision range and further affect agent speed.

Table 4-6: Agent parameters and variables

Agent Parameters	
v_i^u	Top speed of agent i
a_i^+	Acceleration of agent i
a_i^-	Deceleration of agent i
Agent Variables	
l_i	Location of agent i
v_i	Speed of agent i
h_i	Elevation of agent i
d_i^F	Distance from agent i to the front agent
v_i^F	Speed of the front agent from agent i
D_i^I	Current destination for agent i
D_i^{II}	Alternative destination for agent i
R_i^0	The current route for agent i $\{A_1^0, A_2^0, \dots, A_r^0, \dots A_n^0\}_i$
R_i^1	The alternative route with same destination for agent i $\{A_1^1, A_2^1, \dots, A_r^1, \dots A_n^1\}_i$
R_i^2	The route with alternative destination for agent i $\{A_1^2, A_2^2, \dots, A_r^2, \dots A_n^2\}_i$
T_i^0	The travel time on R_i^0 for agent i
T_i^1	The travel time on R_i^1 for agent i
T_i^2	The travel time on R_i^2 for agent i
e_i^0	The level of familiarity of R_i^0 for agent i
e_i^1	The level of familiarity of R_i^1 for agent i
e_i^2	The level of familiarity of R_i^2 for agent i
SI_i^R	Information about congested road segments from agent i's social connections
SI_i^D	Information about destination shelters from agent i's social connections
TS_i	Whether an agent i has tele-service or not
S_i^+	Whether an agent i speed up or not
S_i^-	Whether an agent i slow down or not
LC_i	Whether an agent i change lane or not
RC_i	Whether an agent i makes route change decision or not
DC_i	Whether an agent i makes destination change decision or not

IV.3.3 At Road Intersections

When an agent reaches a road intersection, it can choose from the following options: (1) stay on the current route, (2) continue toward the current destination but take an alternative route, and (3) change to an alternative destination and its corresponding route. To have these options available, we maintain three routes for each agent: R_i^0 is the current route for agent i, R_i^1 is the alternative route with the same destination, and R_i^2 is the route with an alternative destination for agent i. At the initial iteration, the shortest path from the agent's origin to the current destination is chosen as R_i^0. R_i^1 is the second shortest path from the agent's origin to the current destination. R_i^2 is the shortest path from the agent's origin to the alternative destination. These three routes are updated whenever agent i arrives at a road intersection. Although we use the shortest distance to select these three routes, different methods, such as the least travel time or the level of familiarity, can be applied to route selection.

The agents use the FCM-routeDest model (described in Section IV.4.4) to decide which route to take among the above three routes. The travel time and the level of familiarity associated with each route are the factors to be considered in this model. For agent i, T_i^0, T_i^1, T_i^2 and e_i^0, e_i^1, e_i^2 are used to represent the travel time for and level of familiarity with route R_i^0, R_i^1, R_i^2, respectively. The travel time is calculated, based on the length of the route and the average speed of the agents who travel on each road segment of the route. For example, $T_i^0 = \sum_{A_r^0 \in R_i^0} \frac{Length\ of\ A_r^0}{average\ speed\ of\ A_r^0}$, where A_r^0 is the road segment of route R_i^0 for agent i, and R_i^0 consists of a number of road segments

$\{A_1^0, A_2^0, \dots, A_r^0, \dots A_n^0\}_i$. For each agent, the level of familiarity with each route is set as a constant with the range [0, 1]. Whenever any of the three routes is updated, the level of familiarity corresponding to that route is also updated.

For each agent, among all available destination nodes, the one taking the least travel time from the agent's location is selected as the current destination, and the one taking the second least travel time is considered the alternative destination. The agent's current and alternative destinations are updated at road intersections. Whenever the number of agents at a destination shelter exceeds its capacity, that destination node is removed from the set of available destination nodes. Moreover, other agents cannot choose the overfilled destination as their current or alternative destination.

IV.3.4 Sharing/Collecting Information

Besides the travel time and route familiarity, agents also need information from the global broadcast and social media to help them make decisions on route and destination changes. If agent i is in traffic and has telecommunication service, it will send the congested road information about its current road segment to its social connections. Then all agents who connect to agent i can receive this information once they have telecommunication service. This information sharing can help the socially connected agents obtain better knowledge about congested roads so that they can try to avoid these roads when they make route or destination decisions. SI_i^R represents the congested road information that agent i collects from its social network. Here we assume that the information sharing on the simulated social networks is symmetrical, that is, an agent can both send information to and receive information from its connected agents.

For an extreme event evacuation scenario, a group of socially connected agents tends to evacuate to the same destination shelter. Otherwise, the agents need to know the locations of other connected agents. While each agent travels to its destination, it will also send out its current destination information to the social network. The destination information received from agent i's social connections, SI_i^D, can influence the destination decision of agent i.

To enable the road and destination information sharing, agents need to have telecommunication service. Variable TS_i is used to indicate whether or not agent i has teleservice, and TS_i is updated at every simulation iteration.

IV.3.5 Other Agent Variables Associated with Behaviors

While agent i travels on the road segments, it can have the following behaviors: speed up, slow down, and change lanes. Variable S_i^+ indicates whether agent i speeds up or not, S_i^- represents whether it slows down or not, and LC_i signifies whether it changes lanes or not. Route and destination changes happen when agents reach road intersections. Variables RC_i and DC_i represent agent i's route change and destination change decisions, respectively. These five variables are updated at every simulation iteration.

IV.3.6 Framework for an Agent

Figure 4-2 shows the framework for an agent and how agent parameters and variables connect. At each simulation iteration, agents collect the information from their

surrounding environment and from social media and global broadcast. Based on this information and their own property data, agents apply decision-making models under different scenarios to make decisions on whether they need to speed up, slow down, change lanes, change routes, or change destinations.

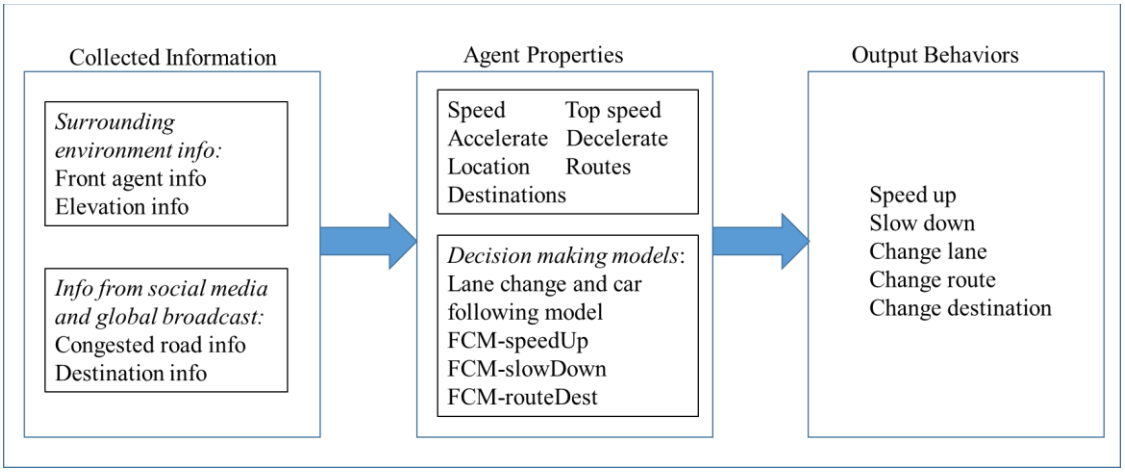

Figure 4-2: Framework of an agent

IV.4. Decision-making Models

IV.4.1 Following-car Model and Lane-change Model

We first present the following-car model (Fritzsche, 1994; Olstam and Tapani, 2004) that is adopted in our agent decision-making models of lane change, speedup, and slowdown. In Olstam and Tapani's following-car model, the risky distance (AR), desired distance (AD), speed of the leading vehicle (v_l), and speed of the following vehicle (v_f) are the parameters that decide whether the following vehicle needs to slow down, speed

up, or keep the current speed. The distance within which collision will happen is the AR, whereas AD expresses the distance that drivers try to maintain from the vehicle in front.

The three cases in this following-car model are “closing,” “free driving,” and “following.” In the “closing” case, the speed of the following vehicle exceeds that of the leading vehicle at a certain threshold, and the distance between the two vehicles is less than AD but greater than AR. To avoid collision, the following vehicle should slow down till it has the same speed as that of the leading vehicle. In the “free driving” case, the distance between the two vehicles is greater than AD, or the speed of the leading vehicle is faster than that of the following vehicle. In this case, the following vehicle can speed up till it attains its desired speed. In the “following” case, the distance between the two vehicles is less than AD and greater than AR, and the value of $|v_l - v_f|$ is less than a threshold with a small number. The “following” case can also happen in the scenario where the distance between two vehicles is greater than AD, but the following vehicle’s speed is faster than that of the leading vehicle. The following vehicle should keep its current speed in the “following” case.

The lane-change behavior is considered subconscious, which means that an agent will automatically change lanes when the required conditions are satisfied. Two lane-change conditions are used in this simulation model: (1) there are multiple lanes on the road segment where the agent travels, and (2) no other agent travels in the same direction within the desired distance. Once these two conditions are met, the agent will move to the same position on the next lane.

IV.4.2 Formal Definition of FCM

We focus on Glykas' (2010) definition of FCMs as fuzzy graph structures consisting of concept nodes C and signed weighted directed edges I representing the causal relationship between the concepts. Each node C_i represents a concept, of which there are two types: factor-concept nodes (inputs) and decision-concept nodes, which are used in decision-making. Each edge I_{ij} represents the influence of concept C_i on concept C_j. A positive value of I_{ij} corresponds to an excitation of concept C_j caused by C_i, whereas a negative value corresponds to an inhibition relationship. If the value of I_{ij} is 0, this means that there is no influence between C_i and C_j. For concept C_i, activation level a_i is also associated with it, and $a_i(t)$ is its activation level at time t. The activation level of factor-concept nodes is computed from the environment by using the fuzzification function. The fuzzification function maps a real number from the environment to a number with the range [0, 1]. The activation level of decision-concept nodes can be used to determine whether a corresponding action is taken. Finally, the recursive relation defines the relation between $a_i(t)$ and $a_i(t+1)$ for each concept. The recursive relation actually describes the dynamics of the map.

To build FCMs, we can follow the procedure below:

(1) Identify relative concepts and classify factor concepts and decision concepts.

(2) Construct causal relationship links between concepts and assign signed weights to links.

(3) Define a recursive relation for the activation level of each concept between time *t* and time (*t* + 1).

(4) Iterate the FCM over time, and update the activation level for each concept.

(5) The activations of decision-concept nodes yield the corresponding decision-making.

IV.4.3 FCM-speedUp and FCM-slowDown

This section explains the FCM-speedUp and FCM-slowDown decision-making models. In these two FCMs, the following-car model is integrated with other factors to determine whether the agent should speed up, slow down, or maintain the current speed while it travels on road segments. Besides the information associated with the vehicle in front, the geographic environment can also impact an agent's travel speed. When an agent is climbing to a higher region, its vision range decreases, which can inhibit the action of speeding up. On the other hand, the lane-change behavior can encourage the action of speeding up. Figure 4-3 illustrates the FCM-speedUp.

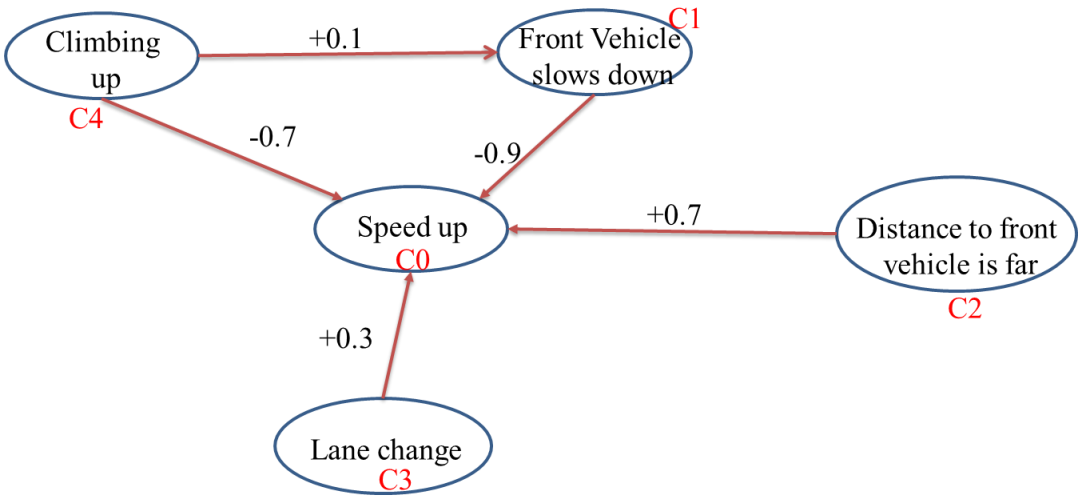

Figure 4-3: FCM-speedUp

In the FCM-speedUp, the concepts of "climbing up," "the vehicle in front slows down," "the distance from the vehicle in front is far," and "lane change" are the four factor-concept nodes, while the concept of "speedup" is the decision-concept node. There are five influence edges: the slowdown of the vehicle in front inhibits speedup, the far distance from the vehicle in front stimulates speedup, a lane change encourages speedup, and climbing up causes the vehicle in front to slow down and inhibit speedup at the same time. Figure 4-3 shows the weights of influence edges.

Activations of "the vehicle in front slows down" and "the distance from the vehicle in front is far" are computed by the fuzzification functions of the real value of speed and distance. Figures 4-4 and 4-5 display these two fuzzification functions. When the speed difference value ($v_f - v_l$) is less than 5 mph, the activation of "the vehicle in front slows down" is set at 0.3; when the speed difference value ($v_f - v_l$) is greater than 5 mph, the activation of "the vehicle in front slows down" is set at 0.8.

The activation of "the distance from the vehicle in front is far" is calculated by comparing the real distance to the distance concepts defined by the following-car model. If the distance between two cars is less than AR, then the activation value is set at 0. If the distance is greater than AD, then the activation value is set at 0.9. The safe distance defines the smallest headway where positive acceleration is accepted. Hence, the safe distance is larger than AR and smaller than AD. For the distance between the safe distance and AD, the activation of "the distance from the vehicle in front is far" is set at 0.2.

The activation of “climbing up” is set at 1 if the slope of the travel direction is greater than six degrees within AD. The activation of “lane change” is equal to 1 if the action of changing lanes is based on the lane-change model.

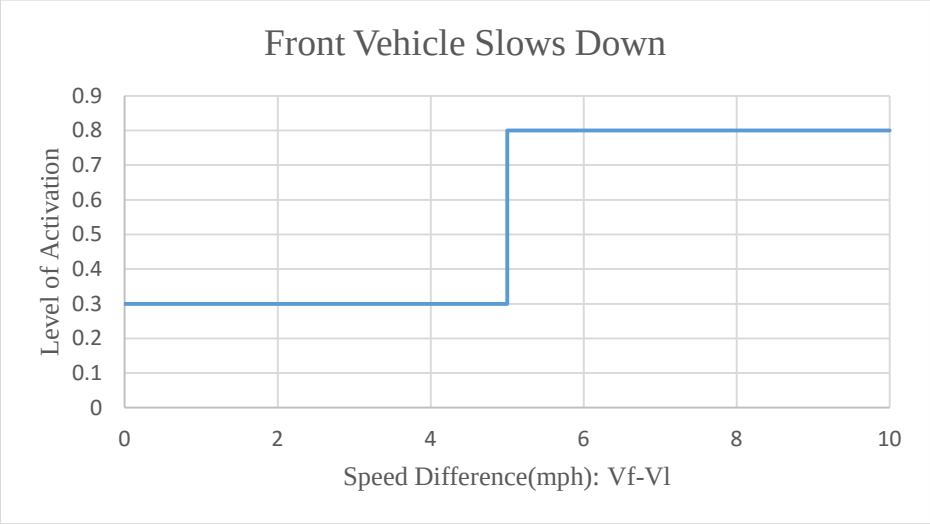

Figure 4-4: Fuzzification function for concept of “vehicle in front slows down”

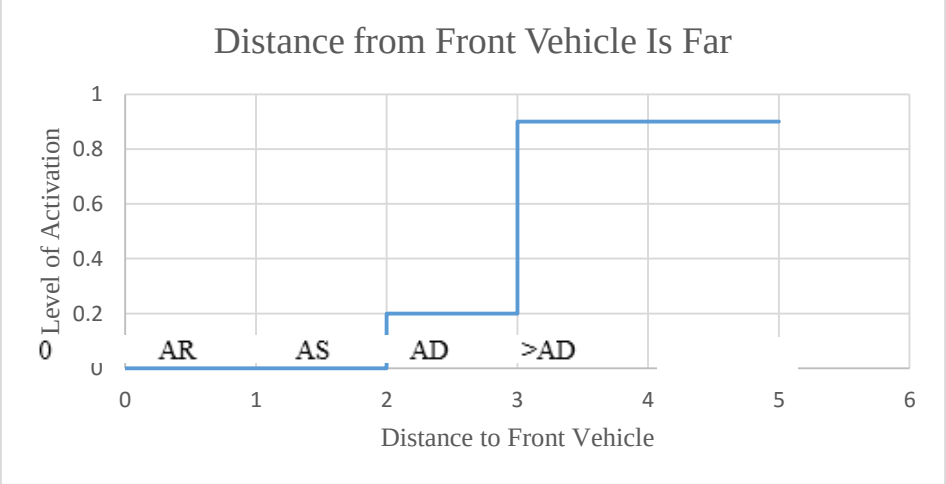

Figure 4-5: Fuzzification function for concept of “distance from vehicle in front is far”

The recursive relation for FCM-speedUp is defined as follows: $a_i(t+1) = a_i(t) + \sum_{1 \le j \le 5} I_{ji} * a_j(t)$. Figure 4-6 illustrates how this FCM yields the "speedup" decision for each agent. First, the activation for each concept c_i is calculated; $a_i(t)$ equals 0 when the agent is at a road intersection. Then the recursive relation is used to update the activations from the previous simulation iteration to the current iteration. If the activation of the "speedup" concept (C0) is greater than a threshold, then the agent will take the "speedup" action according to its acceleration. If not, then the current activations are carried to the next iteration, and the agent keeps its current speed.

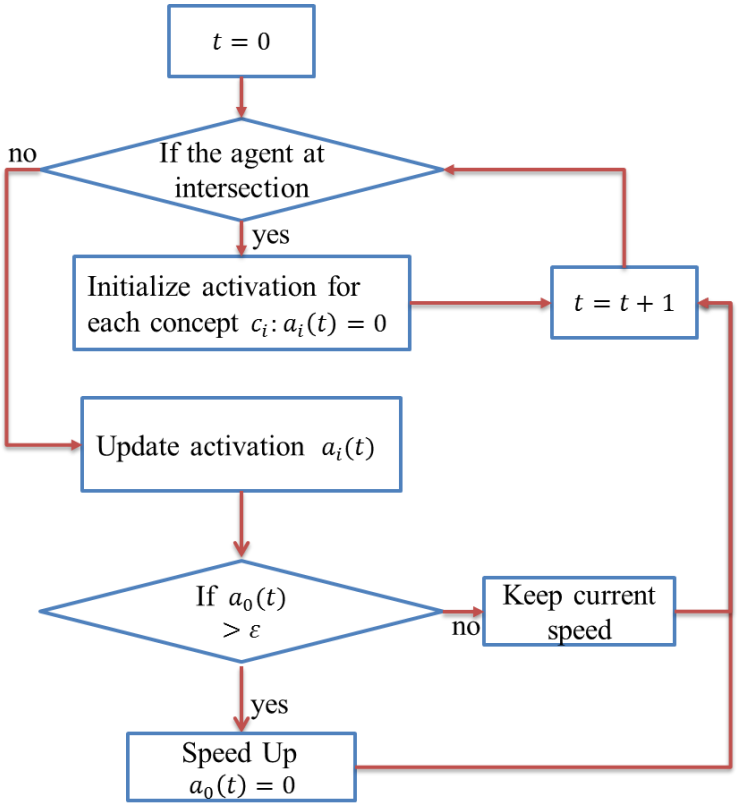

Figure 4-6: FCM-speedUp decision-making illustration

Following the same idea, FCM-slowDown is developed in a similar way, as shown in Figure 4-7. In FCM-slowDown, the concept nodes of "climbing up," "the vehicle in front slows down," and "short distance from the vehicle in front" stimulate "slowdown," whereas "lane change" inhibits "slowdown." The activations of factor-concept nodes are computed in the same way as in FCM-speedUp, except for the concept of "short distance from the vehicle in front." Figure 4-8 shows the fuzzification function for calculating "short distance from the vehicle in front." The same recursive relation is defined for FCM-slowDown as in FCM-speedUp.

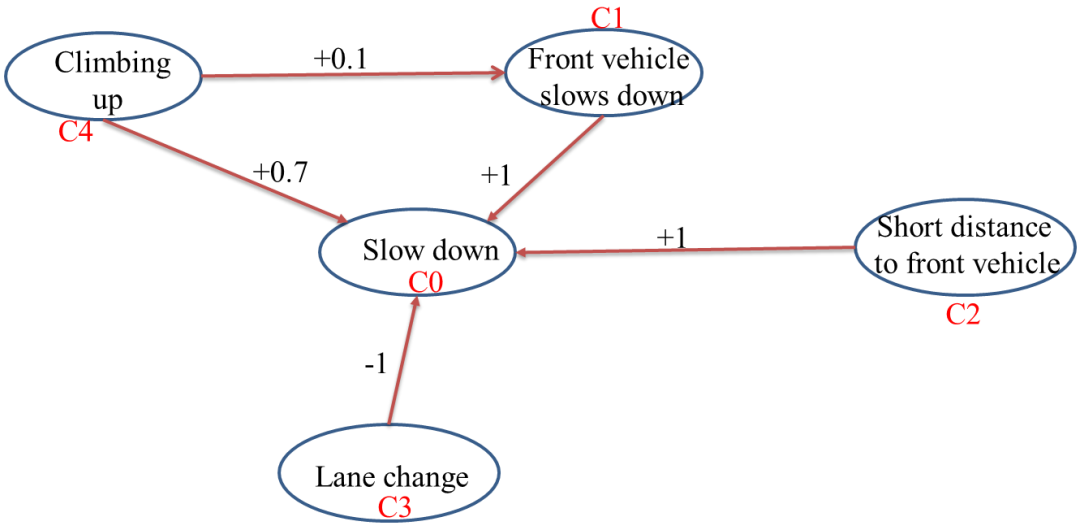

Figure 4-7: FCM-slowDown

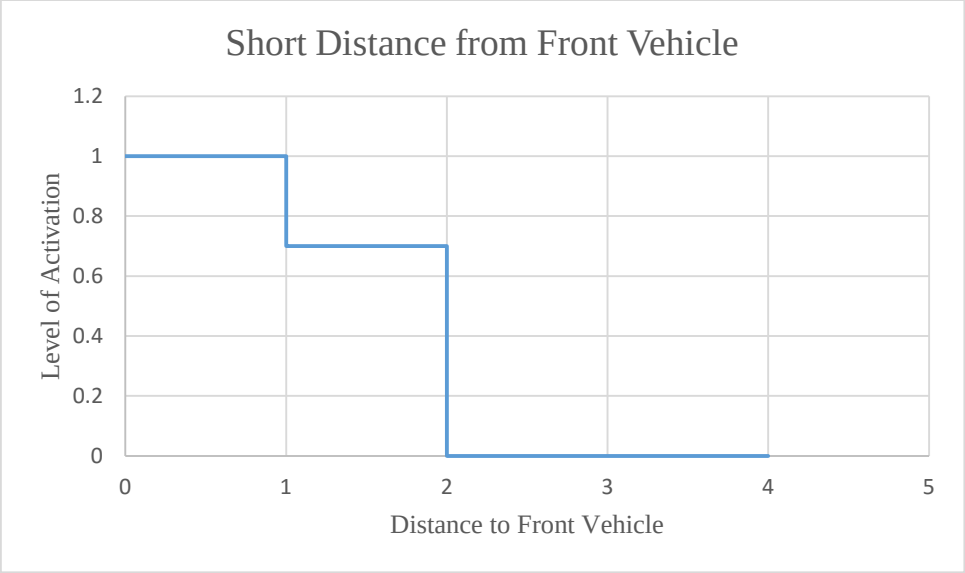

Figure 4-8: Fuzzification function for concept of "short distance from vehicle in front"

IV.4.4 FCM-routeDest

We have introduced the agent behavior models of FCM-speedUp and FCM-slowDown, which are operated when agents travel on road segments. This section presents the behavior models of decision-making on route and destination choices. When the agent reaches a road intersection, the actions of changing the route and destination may occur, based on the output of the FCM-routeDest model.

Figure 4-9 illustrates the FCM corresponding to the route and destination decision-making. In this FCM-routeDest model, "change route" and "change destination" are the two decision-concept nodes. The factor-concept nodes of "familiar

with alternative route" and "gridlock on upcoming road segments" can excite "change route." "Longer travel time on alternative route (R_i^1)" and "gridlock on current road segment" make the route change take more time; therefore, these two factor concepts inhibit "change route." For "change destination," "familiar with alternative route (R_i^2)" and "social connections go to the alternative destination" encourage destination change. Once the current destination overflows, the agent has to change to its alternative destination. Hence, the influence edge of "current destination overflows" on "change destination" has a large, positive weight. Moreover, "longer travel time on alternative route (R_i^2)" discourages destination change.

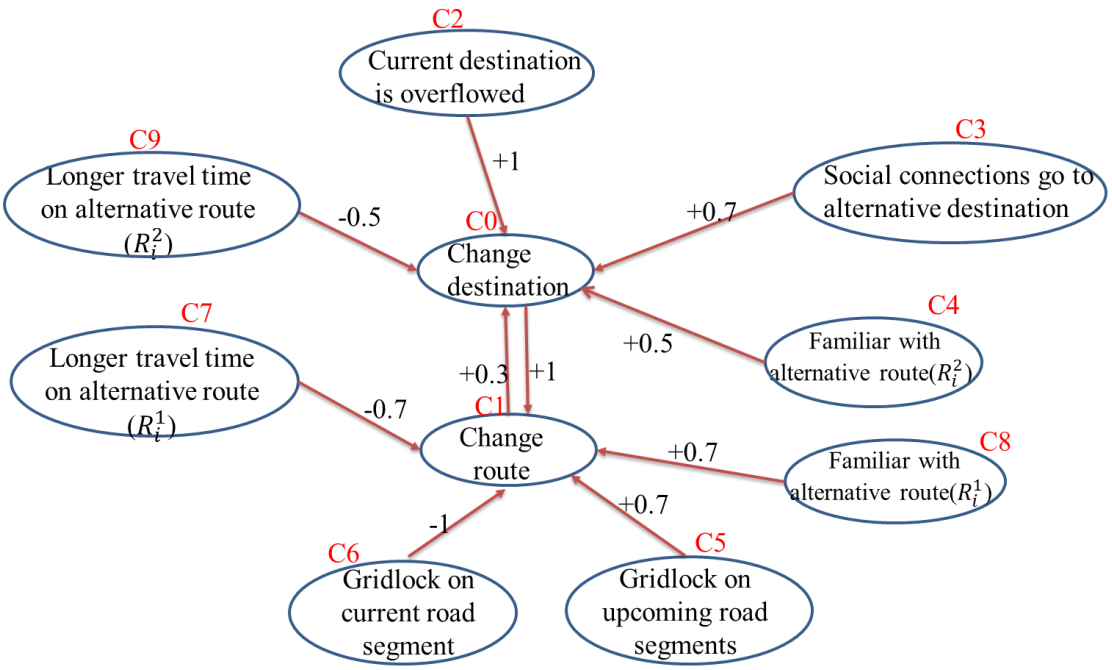

Figure 4-9: FCM-routeDest

Besides the factor-concept nodes discussed above, note that “change destination” can result in “change route.” “Change route” may also motivate “change destination.” Therefore, two influence edges with positive weights are constructed for the two decision-concept nodes.

This FCM-routeDest model reveals the advantages of using the FCM as a decision-making model. The complexity of the decision-making process and the dynamics and simultaneous impacts of multiple factors are able to be represented. It will be very difficult to express all these factors and corresponding relationships by using the utility function. Even if all the factors considered in this FCM can be written in multiple utility functions, the dynamics and simultaneous characteristics are hardly shown.

In our ABM model, each agent executes the same FCM-speedUp, FCM-slowDown, and FCM-routeDest. Here, we assume that each agent considers the same factors and has the same causal relationship for the concepts. We also assume that the weights on the influence edges are the same for all agents. These assumptions can be improved and further extended to multiple FCMs for each decision-making, according to different agent behavior groups.

Table 4-7: Activations of concepts in FCM-routeDest

Activations for concepts C_0 -- C_9 in FCM-routeDest at time t	
$a_0(t)$	$0.5 * a_0(t-1) + \sum_{0 \le j \le 9} I_{j0} * a_j(t-1)$
$a_1(t)$	$0.5 * a_1(t-1) + \sum_{0 \le j \le 9} I_{j1} * a_j(t-1)$
$a_2(t)$	1 if current destination is overflowed
$a_3(t)$	$\frac{\#\ of\ social\ connections\ who\ go\ to\ the\ alternative\ destination}{\#\ of\ social\ connections}$
$a_4(t)$	e_i^2: The level of familiarity of R_i^2 for agent i
$a_5(t)$	$p_5 * \frac{\#\ of\ road\ segments\ in\ SI_i^R\ that\ are\ upcoming\ in\ current\ route}{\#\ of\ social\ connections}$
$a_6(t)$	1 if speed is less than 10 mph
$a_7(t)$	$\frac{T_i^1 - T_i^0}{T_i^0}$
$a_8(t)$	e_i^1: The level of familiarity of R_i^1 for agent i
$a_9(t)$	$\frac{T_i^2 - T_i^0}{T_i^0}$

Table 4-3 presents the fuzzification functions used for calculating the activations of the concepts in FCM-routeDest. The activation of "social connections go to the alternative destination" (C_3) for agent i is computed as follows: the number of social connections going to the same alternative destination as that of agent i divided by the total number of social connections. The knowledge of agent i about "gridlock on upcoming road segments" (C_5) is based on the road information shared on the social network. SI_i^R represents all the information about congested road segments that agent i can collect from its social connections. The number of congested road segments contained in agent i's current route divided by the total number of agent i's social connections determines the activation of C_5. p_5 in $a_5(t)$ is the parameter used to amplify the ratio that is determined by the road network size and the social network size. Note that the knowledge about C_3 and C_5 is from social media supported by

telecommunication; if agent i has no teleservice at time t, then the activations $a_3(t)$ and $a_5(t)$ are equal to 0.

The activation of "longer travel time on alternative route (R_i^1)" is computed by comparing the travel time on alternative route R_i^1, which is T_i^1, to the travel time on the current route, which is T_i^0. Thus, $\frac{T_i^1 - T_i^0}{T_i^0}$ is used as the fuzzification function for $a_7(t)$. Similarly, $\frac{T_i^2 - T_i^0}{T_i^0}$ is used for $a_9(t)$. The activations of the rest of the factor concepts, "current destination overflows," "familiar with alternative route," and "gridlock on current road segment," can be calculated easily from agent variables and environment variables.

The activations of the decision concepts "change route" and "change destination" ($a_0(t)$ and $a_1(t)$) are determined by the activations of factor concepts (C_2--C_9) and the information from previous iterations. The recursive relation for these two decision concepts is defined as follows: $a_0(t+1) = 0.5 * a_0(t-1) + \sum_{0 \le j \le 9} I_{j0} * a_j(t-1)$ and $a_1(t+1) = 0.5 * a_1(t-1) + \sum_{0 \le j \le 9} I_{j1} * a_j(t-1)$.

The flowchart in Figure 4-10 illustrates the decision-making process about route and destination changes. For each agent, the activations of all concepts in FCM-routeDest are initialized at the road intersection. Then the activations of factor-concept nodes are updated by fuzzification functions, and the activations of decision-concept nodes are updated by recursive relations. If $a_0(t)$ exceeds threshold ε, then the "change destination" decision is made, and $a_0(t)$ remains ε. The reasons why $a_0(t)$ is set at ε after the "change destination" decision is made are as follows: (1) The "change

destination" decision still impacts the route change decision. (2) Once the decision is made, $a_0(t)$ can be considered a constant, and it does not change any more. The same logic is applied to the "route change" decision-making. Note that the actions of route and destination changes are taken at the next intersection although the decision-making happens on the road segments.

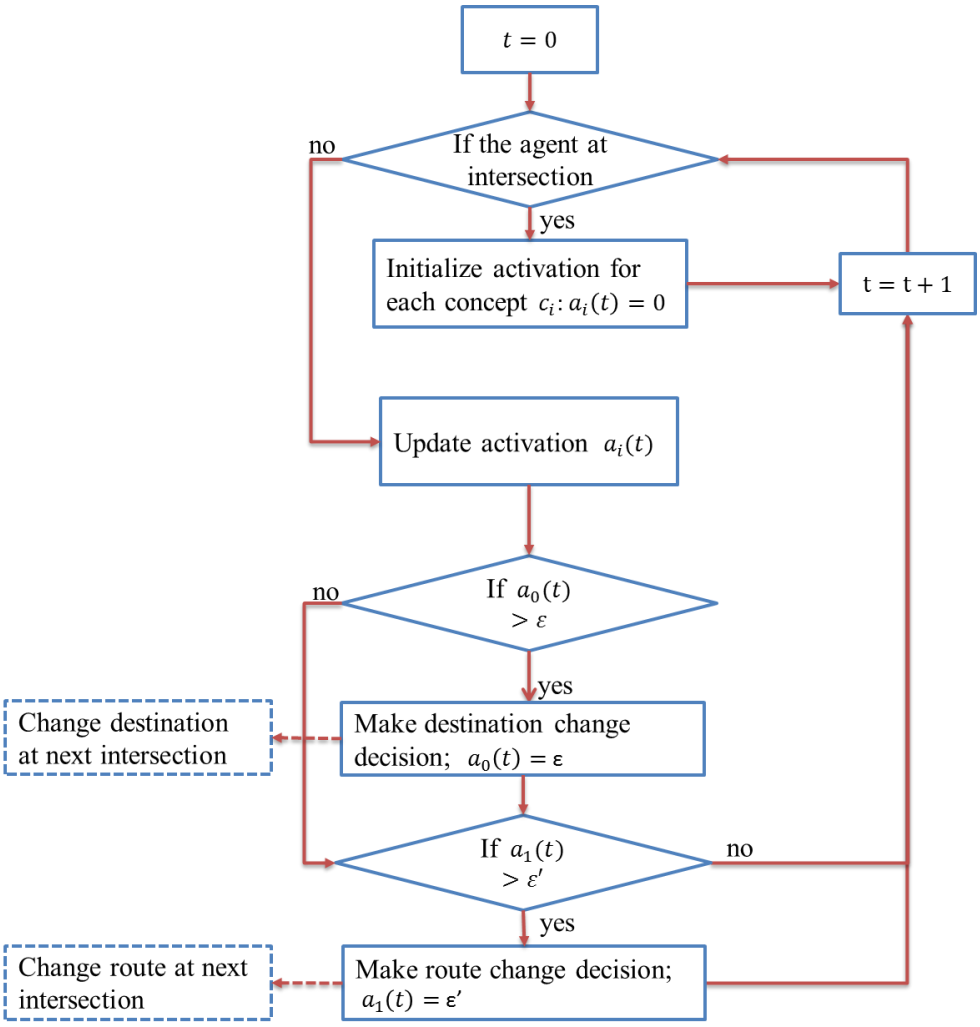

Figure 4-10: FCM-routeDest decision-making illustration

IV.5. How ABME and TELP Work Together

IV.5.1 The Logic

In general, we use ABME to generate predicted agent locations which are then used as input for TELP. TELP generates an optimal Micro-cell station location/installation solution over a finite time horizon based on the ABME predicted locations. The generated TELP locations are then used as input to the ABME model, which is run to identify agent locations for the TELP time horizon (note that this step is actually finding the 'exact' agent locations which replace the predicted locations previously obtained). At the end of the current time horizon, a new set of predicted locations for the next time horizon is identified and the entire process iterates again. The process stops when all agents have successfully reached a destination (i.e., evacuation is complete). This idea is shown in Figure 4-11 and is more formally presented as follows:

For any n time slots T_X to T_{X+n}:

⑴ Export agent's location, route and travel speed from ABME respectively with base station installation for T_X

⑵ Predict agent locations based on ⑴ for T_{X+1} to T_{X+n}

⑶ Using agent locations from ⑴ and ⑵ as input, solve TELP and obtain micro-cell station installation solution for T_{X+1} to T_{X+n}

⑷ Import solution ⑶ to ABME and continue running ABME from T_{X+1} to T_{X+n}

⑸ Iterate ⑴ -- ⑷ until all agents reach destination then stop

Note: at step (1), if x = 0 then pre-run ABME without micro-cell station, else T_X uses current micro-cell stations.

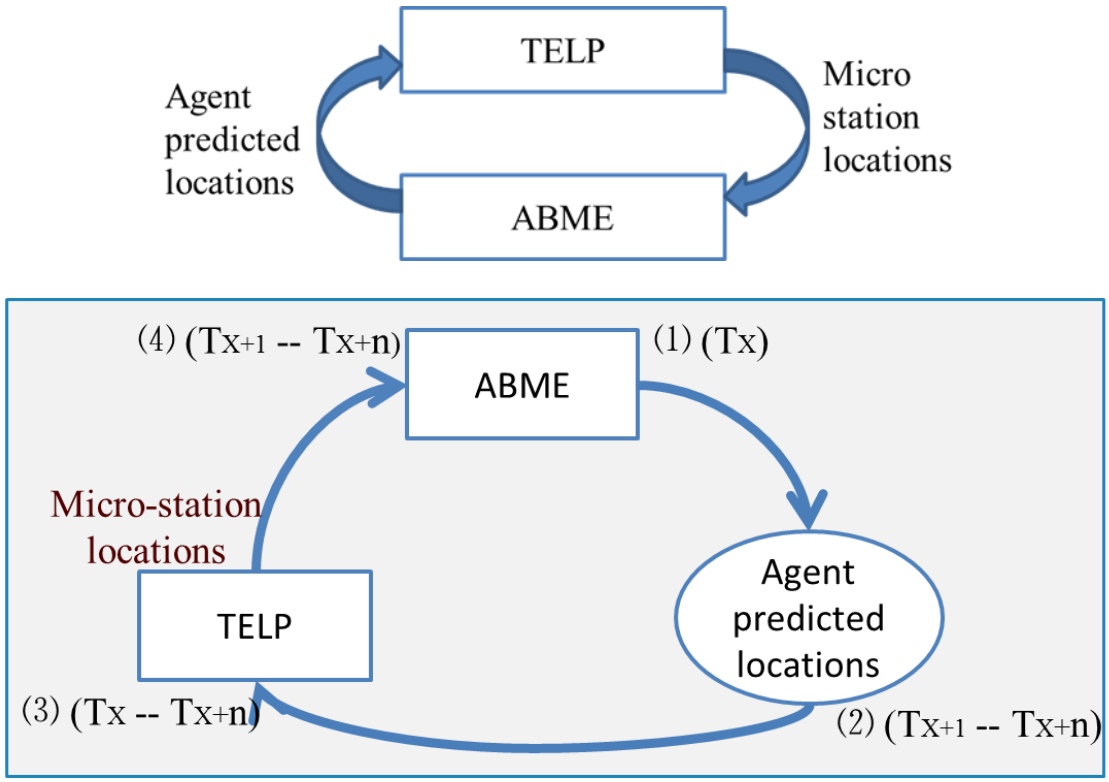

Figure 4-11: The logic of how TELP integrated in ABME

Novelty in this approach to evacuation modeling stems directly from the integrated TELP and ABME methodology. Instead of utilizing standard techniques where TELP solves for the entire evacuation time horizon and then ABME evaluates the outcomes/solutions, the integrated methodology here gives constant feedback to both TELP and ABME while saving significant computational time through reduced problem

complexity for TELP. In practice, the use of predicted agent locations is done at such a small time scale (roughly 8 time units or 320 simulation iterations) that little accuracy in agent positioning is lost. The methodology is also flexible enough to be adapted for sub-iterations to further address any positional accuracy concerns (i.e., TELP and ABME could iterate multiple times within each small time scale before moving forward). We note that if the time scale equals the evacuation horizon, then implementation of this methodology equates to the traditional single-form, non-integrated use typically observed in current literature.

IV.5.2 An Illustrated Example

A small example is presented here to demonstrate how the Agent-Based Model Environment (ABME) model works together with the output from Telecommunications Evacuation Location Problem (TELP) model.

IV.5.2.1 Problem setting

In this example, we use a road network presented in Figure 4-12. This network is composed of 5 bidirectional arcs and it defines the space where agents can interact with each other and interact with the physical environment. Each arc (road segment) has two lanes for moving traffic in each direction, representing a total of four lanes for each arc. Each arc has a 1200 meter length. A DEM (Digital Elevation Model) is produced and imported under the road network (shading in the figures indicates elevation with lighter areas being lower. This is important both for transportation and for establishing appropriate cell tower functionality). To simplify the problem, we only consider one

origin and one destination in this example. The locations of this one O-D pair are shown in Figure 3-1 as well.

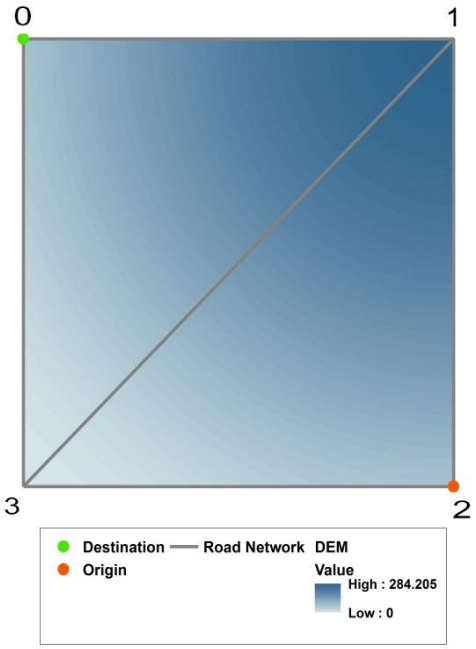

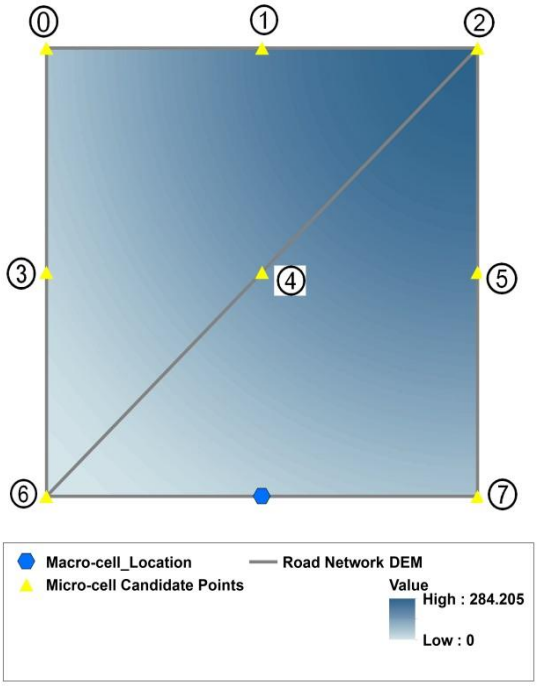

Figure 4-12: road network of small example

Figure 4-13: base-station locations

The candidate locations of Macro-cell station and Micro-cell station as input of TELP are displayed in Figure 4-13. These represent the possible locations for each station type, with eight total potential locations for this small-scale example. Micro-cell station locations are determined using the TELP model (recall that micro-cells assist agents in sending and receiving messages during the evacuation process as they travel from origin node to destination node. Information received by an agent may result in route change, destination change, or both).

In this example, we place 10 agents at the origin and assume that individual agent speed is uniformly distributed within a range of 4.16 and 6.667 (Unit: meter/step). Each agent has their own fuzzy cognitive decision map which dictates whether and when the agent speeds up, slows down, changes to an alternate route or stays on the current route. We assume that decisions to change route/destination are only made at road network intersections (i.e., once an agent starts to travel down the road, they will not be able to turn around or change their routing decisions until the next intersection is reached).

IV.5.2.2 Run ABME

We consider 40 simulation iterations as one time slot. Following the steps listed above, we first pre-run ABME for one time unit under the assumption that no micro-cells have been located use this initial run to export agent locations, travel speeds, and current routes in order to predict agent locations for the first 8 time unit run of TELP. Table 4-4 shows the agent predicted locations after performing this step. Once we have predicted agent locations for the first eight time units, TELP is solved to obtain micro-cell locations and any associated micro-cell routing (recall that located micro-cells can be 'shut down' and moved to new locations by traveling along the road network) for first 8 time slots (320 simulation iterations). Table 4-5 gives the micro-cell travel matrix. Table 4-6 shows important parameters in TELP: Radius of Macro-cell and Micro-cell; Pole capacity of Macro-cell and Micro-cell.

By importing the optimal micro-cell locations and routing from TELP (locations shown in Table 4-7), we can motivate the re-run of the ABME model for these initial

eight time units. Figure 4-14 illustrates the evacuation through these eight time units with TELP locations and routing in place.

Table 4-8: Predicted agent locations for time unit 1-8

	Agent Location T1		Agent Location T2		Agent Location T3		Agent Location T4			
Agent ID	X Coordinate	Y Coordinate	X Coordinate	Y Coordinate	X Coordinate	Y Coordinate	X Coordinate	Y Coordinate	Speed	Current Route
0	976631.358	242134	976463.6568	242134	976295.9556	242134	976128.2544	242134	4.19253	2--3--0
1	976589.0076	242134	976375.17	242134	976161.3324	242134	975947.4948	242134	5.345941	2--3--0
2	976712.347	242134	976545.6804	242134	976379.0137	242134	976212.347	242134	4.166667	2--3--0
3	976646.5603	242134	976436.8953	242134	976227.2303	242134	976017.5653	242134	5.241625	2--3--0
4	976562.0833	242134	976340.4648	242134	976118.8462	242134	975897.2276	242134	5.540464	2--3--0
5	976695.6111	242134	976573.8318	242134	976452.0525	242134	976330.2731	242134	3.044483	2--3--0
6	976711.2892	242134	976577.9559	242134	976444.6225	242134	976311.2892	242134	3.333333	2--3--0
7	976589.4509	242134	976374.0247	242134	976158.5986	242134	975943.1724	242134	5.385654	2--3--0
8	976657.4286	242134	976448.9971	242134	976240.5656	242134	976032.1341	242134	5.210787	2--3--0
9	976679.9423	242134	976502.1879	242134	976324.4336	242134	976146.6793	242134	4.443858	2--3--0
	Agent Location T5		Agent Location T6		Agent Location T7		Agent Location T8			
Agent ID	X Coordinate	Y Coordinate	X Coordinate	Y Coordinate	X Coordinate	Y Coordinate	X Coordinate	Y Coordinate	Speed	Current Route
0	975960.5532	242134	975792.852	242134	975625.1508	242134	975520	242196.5504	4.19253	2--3--0
1	975733.6571	242134	975520	242134.1805	975520	242348.0181	975520	242561.8557	5.345941	2--3--0
2	976045.6804	242134	975879.0137	242134	975712.347	242134	975545.6804	242134	4.166667	2--3--0
3	975807.9003	242134	975598.2353	242134	975520	242265.4297	975520	242475.0947	5.241625	2--3--0
4	975675.6091	242134	975453.9905	242134	975520	242421.6281	975520	242643.2466	5.540464	2--3--0
5	976208.4938	242134	976086.7145	242134	975964.9351	242134	975843.1558	242134	3.044483	2--3--0
6	976177.9559	242134	976044.6225	242134	975911.2892	242134	975777.9559	242134	3.333333	2--3--0
7	975727.7462	242134	975520	242141.6799	975520	242357.1061	975520	242572.5323	5.385654	2--3--0
8	975823.7026	242134	975615.2711	242134	975520	242247.1603	975520	242455.5918	5.210787	2--3--0
9	975968.9249	242134	975791.1706	242134	975613.4163	242134	975520	242218.3381	4.443858	2--3--0

Table 4-9: Micro-cell candidate points travel matrix (unit: simulation time)

	Point 0	Point 1	Point 2	Point 3	Point 4	Point 5	Point 6	Point 7
Point 0	0	40	80	40	80	120	80	160
Point 1	40	0	40	80	40	80	120	120
Point 2	80	40	0	120	80	40	160	80
Point 3	40	80	120	0	40	80	40	120
Point 4	80	40	80	40	0	40	80	80
Point 5	120	80	40	80	40	0	120	40
Point 6	80	120	160	40	80	120	0	80
Point 7	160	120	80	120	80	40	80	0

	Point Location	
Point ID	**X Coordinate**	**Y Coordinate**
0	975520	243334
1	976120	243334
2	976720	243334
3	975520	242734
4	976120	242734
5	976720	242734
6	975520	242134
7	976720	242134

Table 4-10: Parameter settings for a small example

Parameter	Notation	Value
Coverage Radius of Macro-cell Station	Rm	650 Meter
Coverage Radius of Micro-cell Station	Rj	350 Meter
Pole Capacity of Macro-cell Station	Km	8
Pole Capacity of Micro-cell Station	Kj	5
Total number of Micro-cell Station	P	2

Table 4-11: Solution output of TELP for time unit 1-8

Time Unit	**Micro-cell Candidate Point ID**
T1	*7*
T2	*7*
T3	*7*
T4	
T5	*6*
T6	
T7	*6*
T8	*6, 3*

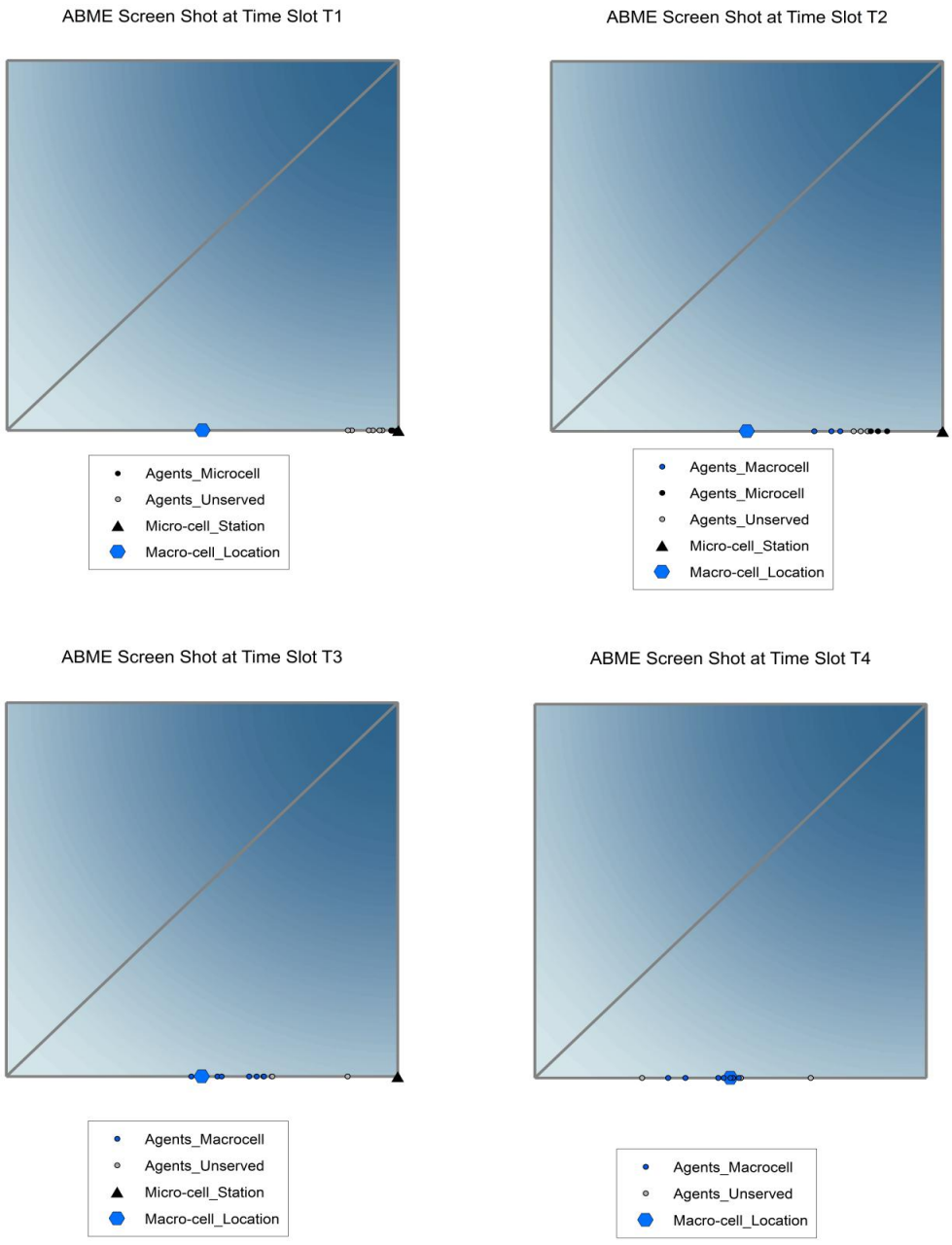

Figure 4-14: ABME illustration example agent locations time slot T1-T8

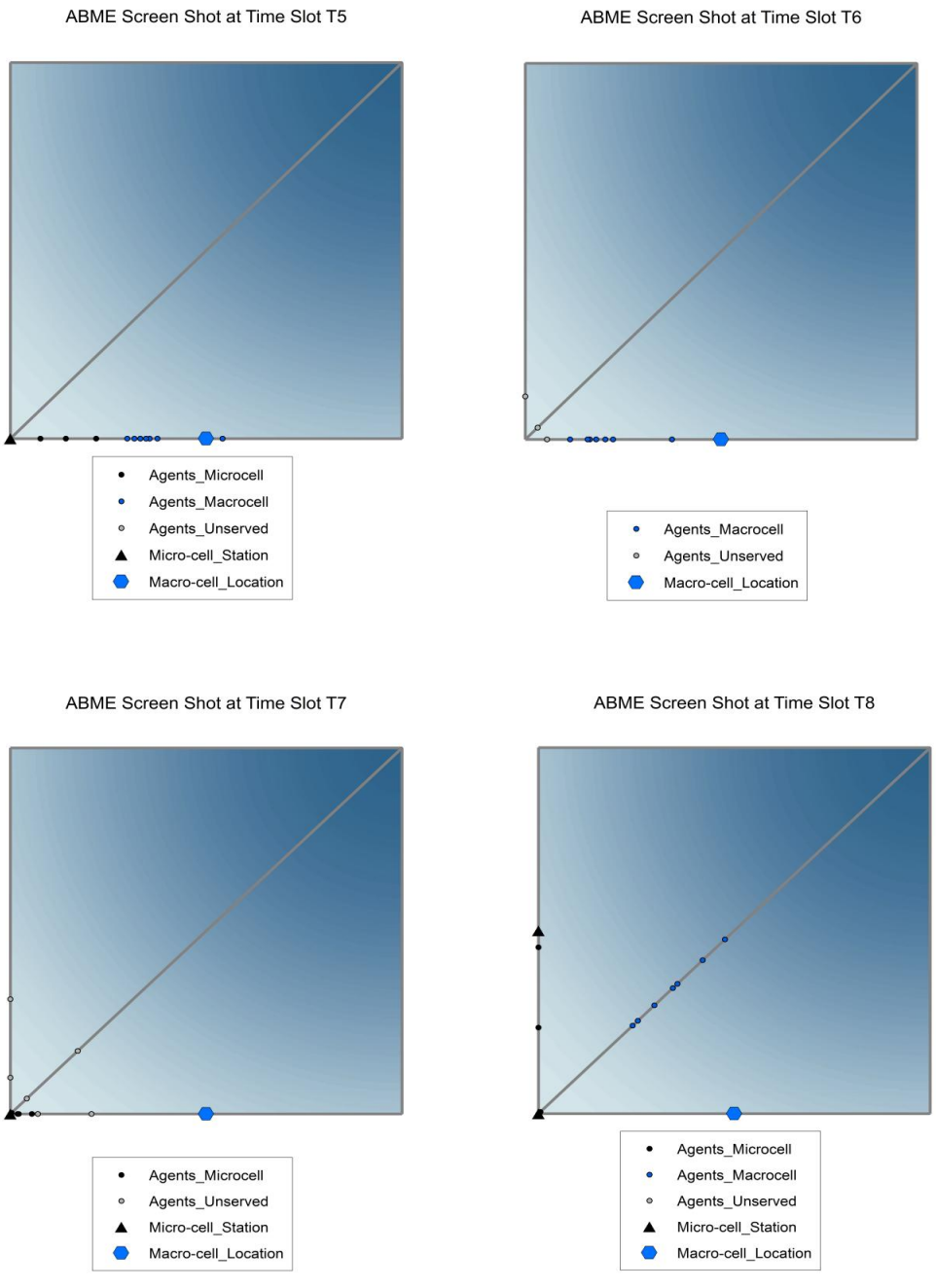

Figure 4-14 continued

To this point, we finish the first ABME → TELP → ABME iteration and begin the second. At the end of 8th time unit, we export agent locations, current routes and corresponding speeds to generate a prediction for time units 9-16 which will be used to facilitate solving the TELP (predictions provided in Table 4-8). Solve TELP for time unit 9-16. Micro-cell locations for each time unit can be found in Table 4-9.

Table 4-12: Predicted agent locations of time unit 9-16

	Agent Location T9		Agent Location T10		Agent Location T11		Agent Location T12			
Agent ID	X Coordinate	Y Coordinate	X Coordinate	Y Coordinate	X Coordinate	Y Coordinate	X Coordinate	Y Coordinate	Speed	Current Route
0	975740.5516	242354.5516	975896.3207	242510.3207	976052.0898	242666.0898	976207.8589	242821.8589	5.50727	3--1--0
1	975520	242782.3533	975520	243031.72	975520	243281.0866	975520	243334	6.234166	3--0
2	976009.9468	242623.9468	976195.0157	242809.0157	976380.0846	242994.0846	976565.1535	243179.1535	6.543173	3--1--0
3	975520	242273.4711	975520	242472.8367	975520	242672.2023	975520	242871.5679	4.98414	3--0
4	975663.1299	242277.1299	975806.3454	242420.3454	975949.5609	242563.5609	976092.7763	242706.7763	5.063432	3--1--0
5	975549.4071	242163.4071	975680.2997	242294.2997	975811.1924	242425.1924	975942.0851	242556.0851	4.627755	3--1--0
6	975595.6322	242209.6322	975716.6436	242330.6436	975837.655	242451.655	975958.6665	242572.6665	4.278401	3--1--0
7	975744.366	242358.366	975894.0975	242508.0975	976043.829	242657.829	976193.5605	242807.5605	5.293809	3--1--0
8	975757.6445	242371.6445	975916.2533	242530.2533	976074.8621	242688.8621	976233.4709	242847.4709	5.607668	3--1--0
9	975979.09	242593.09	976151.2691	242765.2691	976323.4483	242937.4483	976495.6275	243109.6275	6.087453	3--1--0
	Agent Location T13		Agent Location T14		Agent Location T15		Agent Location T16			
Agent ID	X Coordinate	Y Coordinate	X Coordinate	Y Coordinate	X Coordinate	Y Coordinate	X Coordinate	Y Coordinate	Speed	Current Route
0	976363.628	242977.628	976519.3971	243133.3971	976675.1663	243289.1663	976563.1137	243334	5.50727	3--1--0
1	975520	243334	975520	243334	975520	243334	975520	243334	6.234166	3--0
2	976750.2223	243364.2223	976550.3144	243334	976288.5875	243334	976026.8605	243334	6.543173	3--1--0
3	975520	243070.9334	975520	243270.299	975520	243334	975520	243334	4.98414	3--0
4	976235.9918	242849.9918	976379.2073	242993.2073	976522.4228	243136.4228	976665.6383	243279.6383	5.063432	3--1--0
5	976072.9777	242686.9777	976203.8704	242817.8704	976334.7631	242948.7631	976465.6558	243079.6558	4.627755	3--1--0
6	976079.6779	242693.6779	976200.6894	242814.6894	976321.7008	242935.7008	976442.7123	243056.7123	4.278401	3--1--0
7	976343.2921	242957.2921	976493.0236	243107.0236	976642.7551	243256.7551	976617.4884	243334	5.293809	3--1--0
8	976392.0797	243006.0797	976550.6885	243164.6885	976709.2973	243323.2973	976510.8291	243334	5.607668	3--1--0
9	976667.8067	243281.8067	976550.3144	243334	976306.8163	243334	976063.3181	243334	6.087453	3--1--0

Table 4-13: Solution output of TELP for time unit 9-16

Time Unit	Micro-cell Candidate Point ID
T9	
T10	*4*
T11	*4,2*
T12	*4,2*
T13	*2*
T14	*2*
T15	*0,2*
T16	*0,2*

Continue running ABME with updated micro-cell station locations and routing for time unit 9-16. The screen shots of ABME for each time unit are shown in Figure 4-15. At the end of time unit 16, all agents are on an arc which connects directly to the destination. Given that no changes in agent decision making can be made from this point onward (as per the FCM logic discussed previously), we conclude this example. Outputs from the ABME to assess evacuation performance and policy will be discussed in the next section.

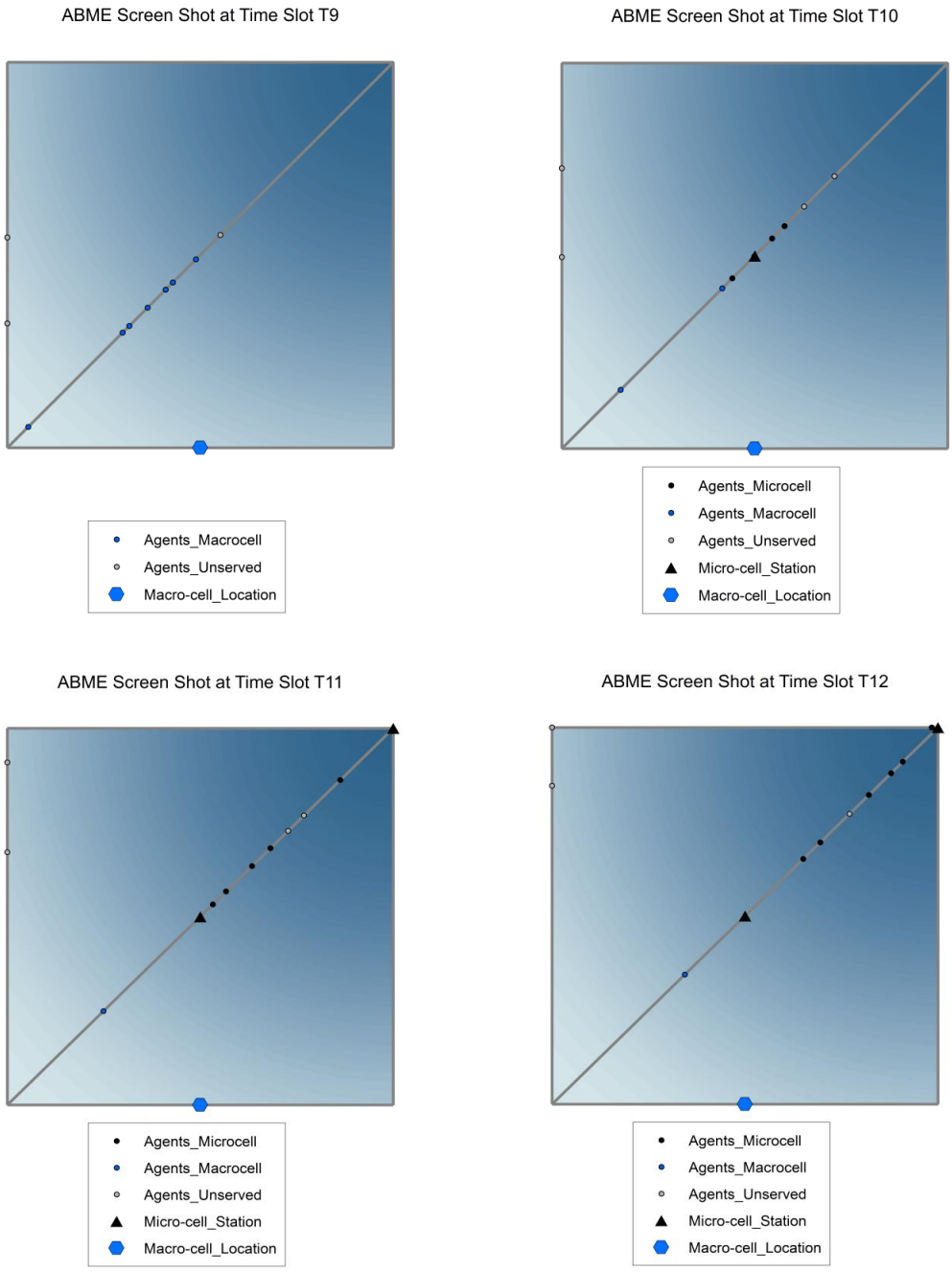

Figure 4-14: ABME illustration example agent locations time slot T9-T16

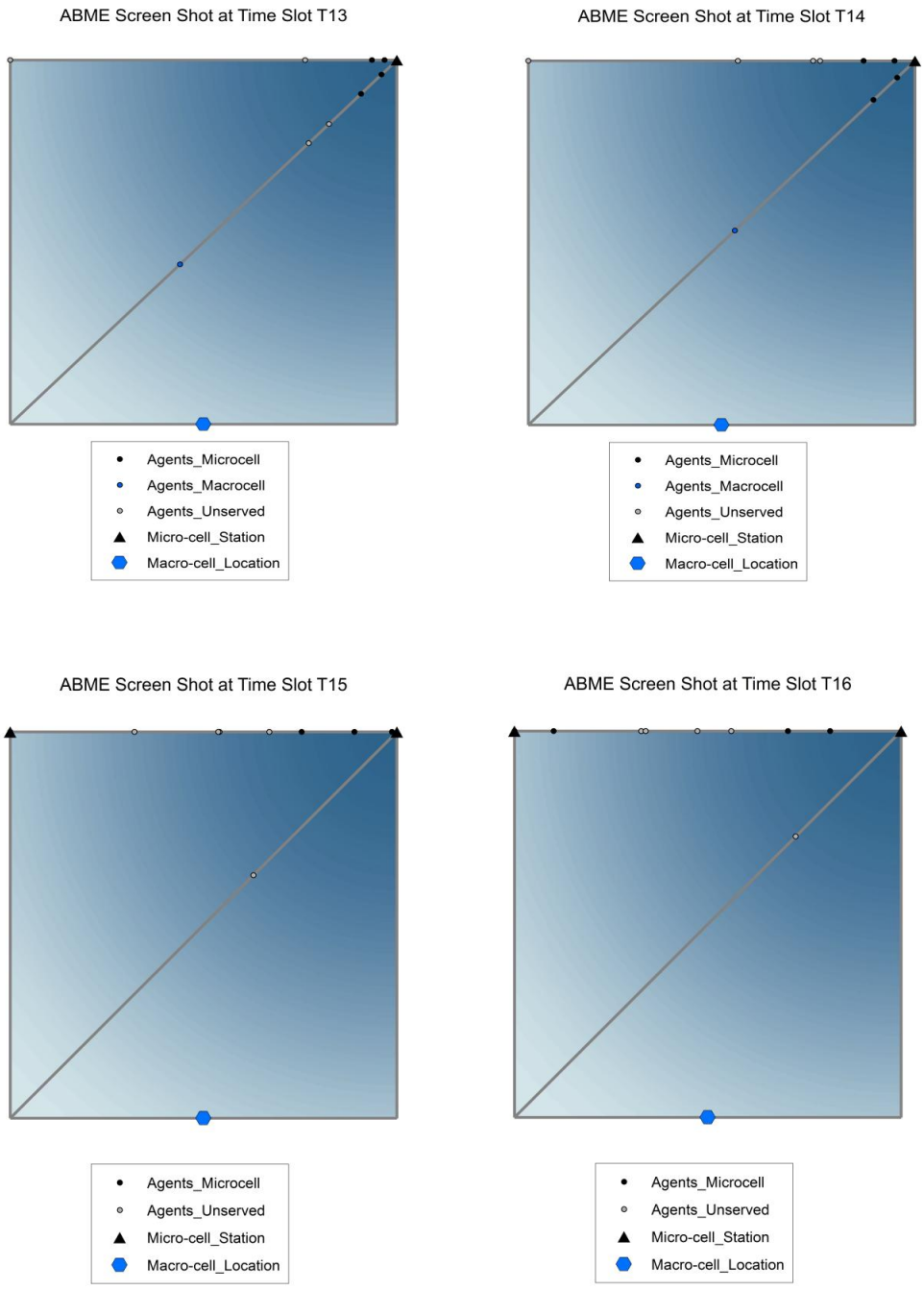

Figure 4-14: Continued**.**

IV.5.3 Output Data

We track and output ABME data at every simulation step level. The output data can be measured into 3 catalogues: system performance, individual performance and road segment performance. System performance data capture general information for all the agents; individual performance data capture detail information for each agent; road segments performance data provides the traffic load information. Specifically, we collect following data for system performance and individual performance: agent's travel data (such as speed, lane change and route change), telecommunication service data (such as number of agents served by macro-cell, number of agents served by micro-cell and number of unserved agents), and evacuation process data (such as total evacuation time). The complete list of output data is presented in Table 4-10.

Table 4-14: Output data from ABME

System Performance	Individual Performance
average speed total # of agents reach desire speed total # of change lane total # of routes change total # of destination change	speed reach desire speed or not # of lane change # of routes change # of destination change
total # of agents unserved by Telecom total # of agents sending out message total # of agents need to send out message total # of agents served by Micro-cell total # of agents served by Macro-cell	agent is served by Telecom or not # of receiving message # of message that impact on agent's *destination* decision # of message that impact on agent's *route* decision
total evacuation time time that destination capacity is fulfilled	evacuation time

IV.6. Summary

We introduce the ABME model for explore travel behavior in emergency evacuation. Each component of ABME, and variables and parameters from both environment and individual agent are presented in detail. We develop the FCMs for agent decision-making on travel behaviors such as speedup, slowdown, route change and destination change. We illustrate the logic of FCMs and how it can develop adaptive knowledge for each agent. Finally, we show how TELP can be integrated in ABME to provide dynamic and accurate mobile telecommunication station location solutions.

CHAPTER V

APPLICATIONS AND RESULTS

In this chapter, we use the cities of Boston and San Francisco as study areas to show the implementation of our ABME model for a large-scale evacuation scenario. We examine how social networks impact the evacuation process in terms of evacuation time and travel behavior from the system and agent perspectives. Meanwhile, we explore how mobile Micro-Stations assist existing cellular networks to satisfy the surging user demand during the evacuation process.

V.1. Working Environment

We performed simulations in MASON, a fast, easily extensible, multi-agent simulation toolkit in Java (Luke et al., 2004) and its extension package GeoMASON (Sullivan et al., 2010). Among other simulation tools, we choose MASON because the system's flexibility allows us to build up the novel, FCM decision-making model. Besides, GeoMASON integrates into the GIS, which can support spatial data (both raster and vector data) very well. In our ABM, agents interact with the environment that consists of a road network, which is in vector format, and the Digital Elevation Model (DEM), which is in raster format. Because of the embedded GIS feature, our ABM agents can make decisions based on updated geographic information, which makes our ABM more realistic. Our TELP model can benefit from this feature as well by having accurate user locations exported from ABM as input. Moreover, the visualization in

MASON can help us observe the aggregated agents' travel behavior while running the simulations.

V.2. Data Preparation

In this section, we describe the data used for the simulation tests. It includes the road network, DEM, the fixed simulation parameters, and the assumptions associated with each component.

V.2.1 Road Network and DEM

The road networks imported to ABME are from the US Census website. The Boston main road network consists of 297 main roads projected in the NAD_1983_StatePlane coordinate system. The San Francisco main road network consists of 484 main roads projected in NAD_1983_UTM_Zone_10N. The visualization of these main roads can be found in Figures 5-1 and 5-2, respectively.

In MASON, a road network is represented as nodes and arcs. Nodes represent intersections where agents can take actions of route changes and destination changes. Arcs represent road segments where agents perform behaviors, such as speed up, slow down, change lanes, and make decisions on route changes or destination changes.

Figures 5-1 and 5-2 also display the corresponding DEM layers. The DEM file of Boston is from the Massachusetts state government. The cell size of this DEM file is 5 meters by 5 meters. The DEM file of San Francisco is obtained from California's Department of Water Resources, and the raster cell is 10 meters by 10 meters. The value

of each cell, in meters, represents its elevation above (positive value) or below (negative value) sea level.

We assume the same speed limitation for each road segment; each road segment has four lanes, with two lanes for each direction. In our simulations, we do not use traffic lights. When agents reach intersections, the FCM-slowDown model can adjust their speed spontaneously by detecting the speed and distance of the vehicles in front.

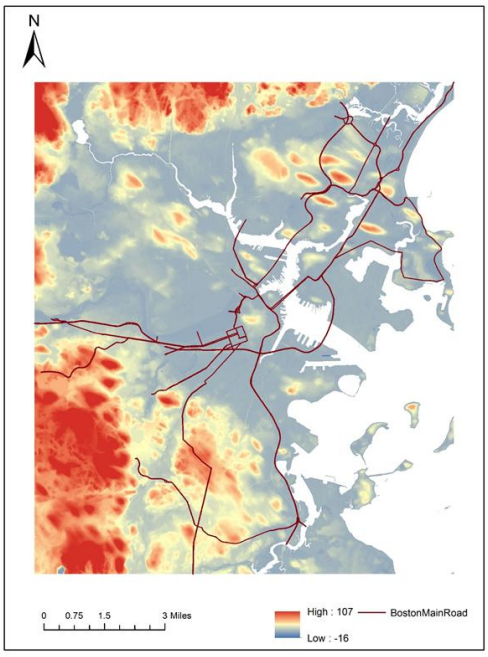

Figure 5-1: Boston main roads & DEM

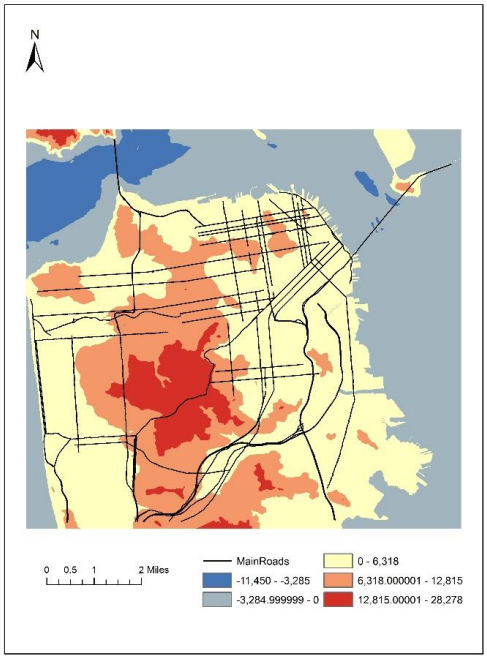

Figure 5-2: San Francisco main roads & DEM

V.2.2 Simulation Settings

At the initial step, all agents were randomly located in a set of origin nodes. All agents took evacuation actions within a short time window. Hence, we could consider that they made evacuation decisions almost simultaneously. For the specific experiments we performed, the agents left their points of origin during the first 30 units of the simulation time (one unit is equivalent to 4 seconds of real time in our tests). Then the agents traveled toward their selected destination nodes. We tested our model under the single-destination and multiple-destination scenarios. For the multiple-destination case, we had the following assumptions: 1. The capacity of each destination would be set at the same value. 2. At the initial time, the majority of the agents would decide to go to the closest destination, and a small number of agents (seed agents) would be informed to go to a specific destination (Note that this would just be the initial setting, and all agents could make destination changes during the evacuation process, according to their FCMs). 3. Within a short time period, each agent would be allowed to make a limited number of destination change decisions. We also assumed that initially, each agent would choose the shortest path to one's destination.

Concerning the computational time for solving TELP inside ABME, we used the Lagrangian relaxation heuristic approach to solve TELP for the two study cases. The TELP model was executed in our ABM model after all agents left their points of origin. For specific experiments, the TELP model starts at 40 units of the simulation time. Why did we not trigger the TELP model at the initial time? It would take time for the agents to leave their congested points of origin and accelerate to the normal speed that would be

used for predicting their future locations. Since the TELP model uses the predicted agent locations as the input, using their normal travel speed and current locations could provide better predicted agent locations. We set the multiple time period parameter $|\mathcal{T}|$ to 8 in the TELP model, with each time period consisting of 40 units of the simulation time.

Finally, the top travel speed for each agent was randomly selected from a range of 40–70 mph. An agent could not exceed its top travel speed while taking the speed-up action.

V.3. Examining Social Media's Impact on Evacuation

We conducted 36 experiments for both the Boston and San Francisco cases to explore how social media would impact the evacuation efficiency for the entire population and the individual's travel behavior. We aimed to answer the following research questions: 1. In terms of evacuation efficiency, is it beneficial to utilize social networks during evacuation? 2. To what extent do social networks influence evacuation travel behavior?

V.3.1 Agents and Simulated Social Networks

Three population sizes were tested: 100, 200, and 300 agents. Then the social networks were constructed among the generated population.

We considered two types of simulated social networks: scale-free network (SF-NW) and random network (RND-NW). The SF-NW has degree distributions following the power law, and it reflects real-world social network properties, such as the small-

world phenomenon. In the RND-NW, each agent is randomly connected to *n* other agents. The random network is easily built and has been widely adopted in laboratory tests.

For each population size, we constructed an SF-NW, an RND-NW with 5 degrees for each agent (RND-NW5), and an RND-NW with 20 degrees for each agent (RND-NW20). To fairly compare SF-NWs and RND-NWs, we chose the SF-NWs with the same total number of connections as those of RND-NW5. Together with the no social connectivity scenario, we had a total of 4 levels of social connectivity for each population level. All simulated social networks were generated beforehand and kept the same connection structure for the corresponding population sizes.

V.3.2 Origins and Destinations

For each study area, two sets of origin-destination (O-D) pairs were generated for single-destination and multiple-destination tests. Figures 5-3 and 5-4 show the locations of O-D1 and O-D2 for the two study areas. The two O-D sets share the same origins. Recall that for the multiple-destination case, a small number of agents (called "seed agents") were informed to go to a specific destination, which might not be the closest one. We tested different numbers of "seed agents," measured by the percentage of the population, to determine whether it would be helpful to notify more agents to save on the evacuation time. We set the "seed agents" to 10% of the population and 16% in the multiple-destination case.

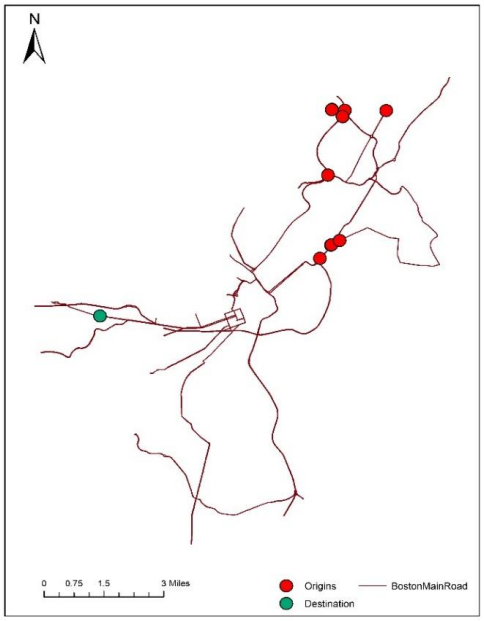

Figure 5-3-1: Boston O-D1

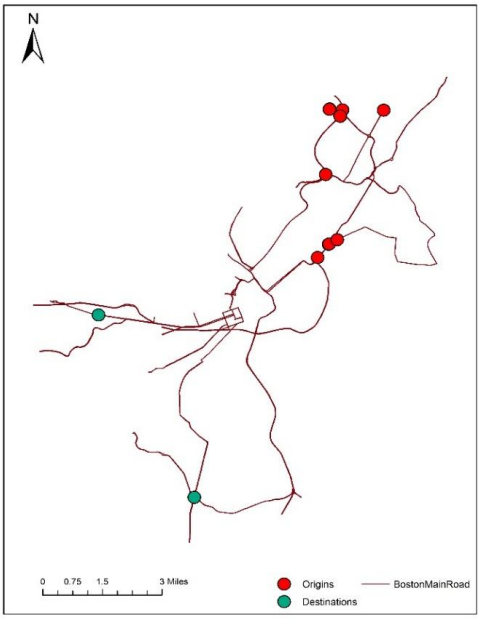

Figure 5-3-2: Boston O-D2

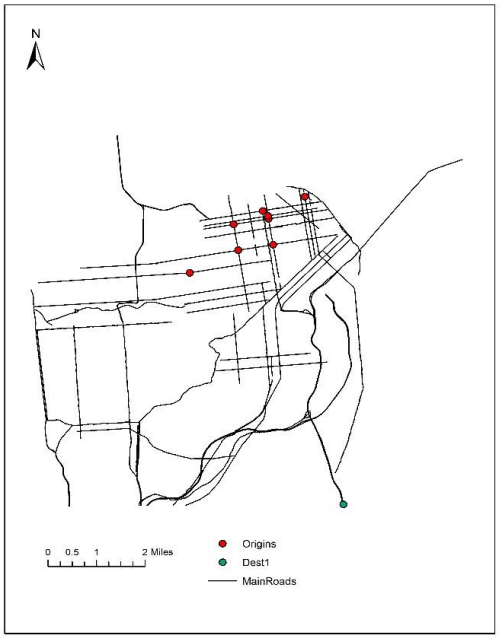

Figure 5-4-1: San Francisco O-D1

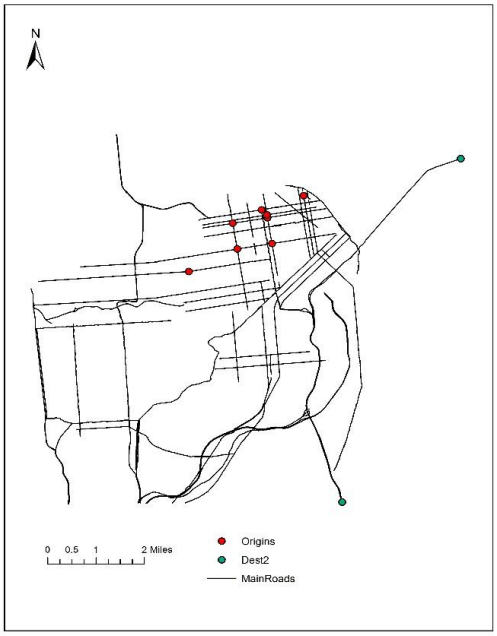

Figure 5-4-2: San Francisco O-D2

V.3.3 Fixed Factors

Social media could play a role in affecting agents' behavior only when the information could be shared among the social networks. To observe the influence of social media, we had to ensure that relatively sufficient telecommunication power was available to support information sharing. Hence, we set the parameters related to cellular power at a high level.

For the experiments described below, the number and locations of the Macro-Stations were artificially assigned. We set up 10 Macro-Stations for the Boston experiments and 13 for the San Francisco experiments. Both cases had 15 micro-station facilities available for installation. The capacity of each macro-station and micro-station was fixed at different levels, based on the population size. Moreover, 70 candidate micro-station locations were identified for both cases. Figure 5-5 shows the locations of the macro-stations and the candidate micro-station locations.

Table 5-1 presents the complete list of experiments and corresponding parameters. For each experiment, we set up 10 replications. The simulation stopped at the time when all agents reached their destinations.

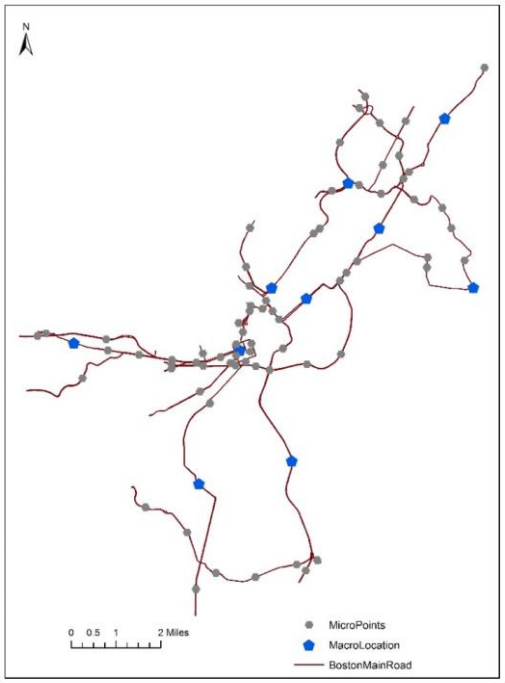

Figure 5-5-1: Boston Macro locations & CML

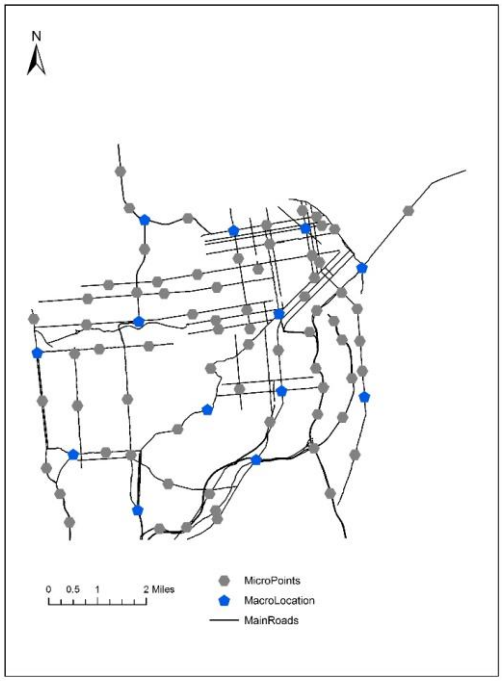

Figure 5-5-2: SF Macro locations & CML

Table 5-1: Experiments for examining social media impact

O-D1					O-D2									
					10%-seed-agent					16%-seed-agent				
set	#Agents	SocialNetwork	Km	Kj	set	#Agents	SocialNetwork	Km	Kj	set	#Agents	SocialNetwork	Km	Kj
1	100	K0	16	10	13	100	K0	16	10	25	100	K0	16	10
2	100	SF-NW	16	10	14	100	SF-NW	16	10	26	100	SF-NW	16	10
3	100	RND-NW5	16	10	15	100	RND-NW5	16	10	27	100	RND-NW5	16	10
4	100	RND-NW20	16	10	16	100	RND-NW20	16	10	28	100	RND-NW20	16	10
5	200	K0	32	20	17	200	K0	32	20	29	200	K0	32	20
6	200	SF-NW	32	20	18	200	SF-NW	32	20	30	200	SF-NW	32	20
7	200	RND-NW5	32	20	19	200	RND-NW5	32	20	31	200	RND-NW5	32	20
8	200	RND-NW20	32	20	20	200	RND-NW20	32	20	32	200	RND-NW20	32	20
9	300	K0	56	35	21	300	K0	56	35	33	300	K0	56	35
10	300	SF-NW	56	35	22	300	SF-NW	56	35	34	300	SF-NW	56	35
11	300	RND-NW5	56	35	23	300	RND-NW5	56	35	35	300	RND-NW5	56	35
12	300	RND-NW20	56	35	24	300	RND-NW20	56	35	36	300	RND-NW20	56	35

V.3.4 Results and Analysis

V.3.4.1 Single Destination Case

We start our discussion with the single-destination case, where the agents could make route change decisions but not destination changes.

Evacuation Efficiency

Table 5-2 presents the output details of the Boston case for evacuation efficiency from the entire population perspective. In Table 5-2, "clear time" means the duration from the time the first agent leaves its point of origin till the last agent reaches its destination. This concept represents the overall evacuation time. While it is important to use "clear time" to measure the evacuation efficiency, it is also essential to know the time when the majority of the population reach the shelters. In Table 5-2, "95 reach time" and "90 reach time" refer to the times when 95% and 90% of the population, respectively, arrive at their destinations. To observe the pattern of how agents reach their destinations, we use the average and standard deviation of the time it takes them to do so.

We use "total traffic over time" to measure the degree of congestion on the road network. It counts the number of agents whose travel speed is less than 25 mph over the evacuation "clear time." Figure 5-6 demonstrates this measurement. The blue area in the figure is calculated as the "total traffic over time." By dividing "total traffic over time" by "clear time," we can obtain the average number of agents in traffic. The same measurements are examined for the San Francisco case in Table 5-3.

Table 5-2: Boston: social media impact output of single destination – evacuation efficiency

Set	Experiment	Avg Spd	Avg preferred Spd	Clear Time	95 Reach Time	90 Reach Time	Avg Reach Time	Std Reach Time	Total inTraff over time	Avg Num inTraff	inTraff Compare
1	100Agents_Kj10_Km16_OD1_K0	39.92	54.47	485.90	472.00	458.90	358.02	76.23	6520.8	14.2	1
2	100Agents_Kj10_Km16_OD1_SF-NW	40.49	54.82	494.10	476.00	461.60	355.65	79.11	6219.7	13.5	-4.62%
3	100Agents_Kj10_Km16_OD1_RND-NW5	39.92	54.60	490.20	479.60	465.30	357.50	78.51	6599.4	14.2	1.21%
4	100Agents_Kj10_Km16_OD1_RND-NW20	39.50	54.42	501.20	489.70	476.20	364.31	82.61	7057.30	14.8	8.23%
5	200Agents_Kj20_Km32_OD1_K0	30.69	54.60	702.67	679.33	655.89	471.06	136.29	39687.8	60.5	1
6	200Agents_Kj20_Km32_OD1_SF-NW	30.73	54.37	718.70	689.40	661.10	470.47	137.92	39148.9	59.2	-1.36%
7	200Agents_Kj20_Km32_OD1_RND-NW5	30.89	54.80	716.40	685.50	660.50	472.28	136.85	39224.9	59.4	-1.17%
8	200Agents_Kj20_Km32_OD1_RND-NW20	30.83	54.47	720.90	691.80	664.00	474.22	140.21	39282.3	59.2	-1.02%
9	300Agents_Kj35_Km56_OD1_K0	25.76	54.88	934.00	898.80	861.50	587.21	200.50	94651.40	109.9	1
10	300Agents_Kj35_Km56_OD1_SF-NW	26.12	54.87	943.20	899.20	857.00	578.70	197.79	92616.20	108.1	-2.15%
11	300Agents_Kj35_Km56_OD1_RND-NW5	26.53	54.59	930.30	886.50	846.60	574.38	195.68	90814.30	107.3	-4.05%
12	300Agents_Kj35_Km56_OD1_RND-NW20	26.14	54.64	937.10	894.80	854.10	578.39	197.34	91705.90	107.4	-3.11%

Notes: Clear Time: duration from the time first agent leaves his or her point of origin until last agent reaches his or her destination
95 Reach Time: time when 95% of population reach their destinations
90 Reach Time: time when 90% of population reach their destinations
Avg Reach Time: average time agents take to reach their destinations
Std Reach Time: standard deviation in agents' time to reach their destinations
Dest Duration: time window from when first agent enters the destination to the time the destination is filled/last agent reaches it
Total inTraff over time: cumulative number of agents in traffic over the whole evacuation time
Avg Num inTraff: Total inTraff over time/Clear Time
inTraff Compare: comparison of total inTraff over time

Table 5-3: San Francisco: social media impact output of single destination – evacuation efficiency

Set	Experiment	Avg Spd	Avg preferred Spd	Clear Time	95 Reach Time	90 Reach Time	Avg Reach Time	Std Reach Time	Total inTraff over time	Avg Num inTraff	inTraff Compare
1	100Agents_Kj10_Km16_OD1_K0	33.12	54.56	476.00	465.00	451.63	353.70	75.32	7062.0	15.6	1
2	100Agents_Kj10_Km16_OD1_SF-NW	33.75	54.74	483.67	462.11	449.22	349.71	74.80	6338.333	14.1	-10.25%
3	100Agents_Kj10_Km16_OD1_RND-NW5	33.94	55.19	510.40	474.60	459.90	352.76	79.96	6669.6	14.5	-5.56%
4	100Agents_Kj10_Km16_OD1_RND-NW20	33.39	54.72	498.80	480.70	466.50	356.54	81.35	7181.70	15.4	1.69%
5	200Agents_Kj20_Km32_OD1_K0	25.88	54.96	693.38	667.38	642.88	462.37	131.52	35082.6	54.6	1
6	200Agents_Kj20_Km32_OD1_SF-NW	26.20	54.63	709.86	677.57	653.14	462.81	135.70	34604.1	53.0	-1.36%
7	200Agents_Kj20_Km32_OD1_RND-NW5	25.94	54.52	725.10	691.10	661.10	468.64	138.79	35557.3	53.8	1.35%
8	200Agents_Kj20_Km32_OD1_RND-NW20	25.92	54.52	714.50	690.00	664.50	470.46	141.11	35924.6	54.1	2.40%
9	300Agents_Kj35_Km56_OD1_K0	21.98	55.21	901.17	868.00	831.17	566.44	192.12	84070.67	101.1	1
10	300Agents_Kj35_Km56_OD1_SF-NW	21.94	54.69	917.50	885.17	850.00	571.65	197.81	83714.67	98.5	-0.42%
11	300Agents_Kj35_Km56_OD1_RND-NW5	22.09	54.84	929.88	893.25	857.13	573.45	201.90	84768.75	98.9	0.83%
12	300Agents_Kj35_Km56_OD1_RND-NW20	21.67	54.72	932.40	893.50	857.70	579.83	199.82	86825.80	101.2	3.28%

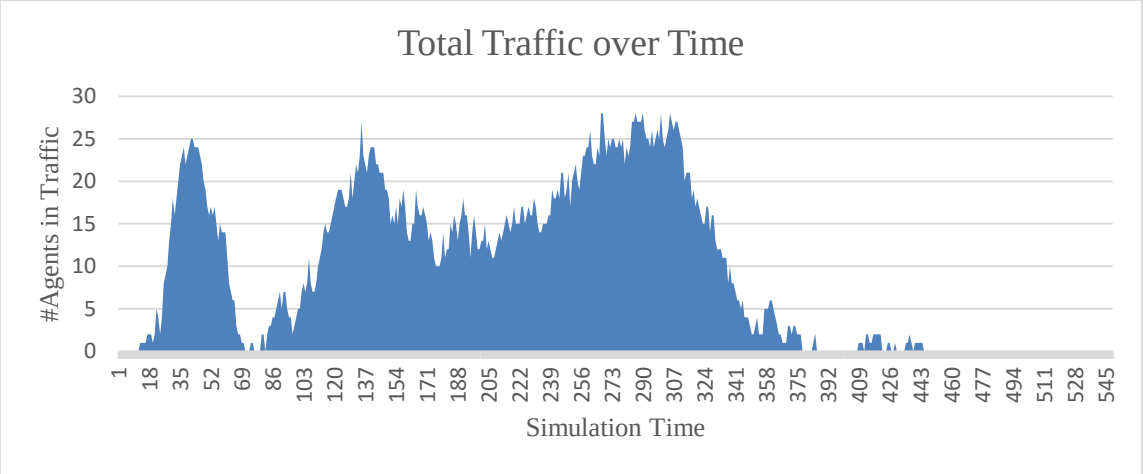

Figure 5-6: Measuring total traffic over time

To answer the first research question (Is it beneficial to use social media for evacuation?), we first performed hypothesis tests on whether or not there would be a significant difference in terms of evacuation time between the absence and the presence of social media usage. We compared "no social media usage" and "having social media" on the SF-NW (K0 vs SF-NW) for the following factors: clear time, 90 reach time, 95 reach time, average reach time, and standard deviation of reach time.

We tested the following hypotheses:

H_0: No social media usage and having social media on the scale-free network have equal means.

H_1: The mean of no social media usage is not equal to the mean of having social media on the scale-free network.

The calculated p-values are given in Tables 5-4 and 5-5. The α value of the hypothesis test is set at 0.05, and the p-value smaller than 0.05 is highlighted, indicating

that the corresponding factors are significantly different, and we can reject H_0 with 95% confidence.

Table 5-4: Boston: P-values of K0 vs SF-NW – Single-destination

	100Agents	200Agents	300Agents
Clear Time	0.037024142	0.009405932	0.02121405
90 Reach Time	0.457186381	0.268238839	0.28833885
95 Reach Time	0.327050583	0.067572775	0.92586371
Avg. Reach Time	0.336883442	0.87546527	0.00019301
Std. Reach Time	0.034107865	0.204093952	0.01666112

Table 5-5: San Francisco: P-values of K0 vs SF-NW – Single-destination

	100Agents	200Agents	300Agents
Clear Time	0.350479676	0.093703372	0.006154589
90 Reach Time	0.641821059	0.069801825	0.001368944
95 Reach Time	0.609300346	0.06673333	0.008938625
Avg. Reach Time	0.371638519	0.886547902	0.105060932
Std. Reach Time	0.648759864	0.118293148	0.012051658

For the Boston case, “clear time” was significantly different for all population sizes. In the “no social media” scenario, “clear time” was shorter than that of “having social media”. Although in the San Francisco case, the small p-value of “clear time” was only found in 300 agents, we could observe the same trend that “clear time” under the “no social media” scenario was shorter than that of “having social media” for all population sizes. During the simulations, we observed that some agents changed their routes although they were very close to the destination. This behavior was probably caused by social media; those agents tried to follow others’ routes instead of traveling on

their shortest routes. A longer "clear time" might also be caused by changing routes. "Having social media" would increase the number of route changes, as shown in Tables 5-6 and 5-7. Because the initial routes were the shortest ones, changing routes would increase the travel distance, making it possible to take a longer travel time.

However, we observed that the majority of the population arrived at the destination almost at the same time for "no social media" and "having social media" in the single-destination case for both study areas. The "average reach (destination) time" was very close between "no social media" and "having social media" in most instances, except for 300-agent instances. There seemed to be little difference between "no social media" and "having social media" in terms of the time the agents reached the destination in the single-destination case.

We used the "total traffic over time" measurement to determine the congestion level of the road segments. Considering "K0" as the baseline, we found that "having social media" on the SF-NW could help reduce congestion a little for both study areas although the decrease did not seem very significant. Notice that the social media on the RND-NW could bring more traffic in some instances. This could be an example showing that the RND-NW would be unsuitable for exploring social network activities

. Although more agents traveled on alternative routes to avoid traffic because of the information they received through social media, alternative routes shared a lot of the same road segments with the shortest routes in the single-destination case. If the road segments in alternative routes were very different from those of the shortest routes, then the congestion level might drop significantly. Hence, we would expect to observe a more

significant reduction of congestion for "having social media" under the multiple-destination scenario.

Individual Travel Behavior

Tables 5-6 and 5-7 show the output details of individual travel behavior for a similar set of experiments as those presented in Tables 5-2 and 5-3. For travel behavior, we consider the agent's travel speed, lane changes, and route changes. If an agent can travel at his or her preferred speed most of the time and does not spend too much time on congested roads, then the agent's travel experience is considered good. To measure this travel experience, we use "agent inTraff time" (T_{aj}) and "preferred speed time" (T_{dp}), and T_{aji} represents the total time that an agent i is in traffic during his or her evacuation process. Then $\overline{T_{aJ}} = \frac{\sum_i T_{aji}}{total\ number\ of\ agents}$ can represent the average time that an individual would be in traffic during evacuation. Similarly, T_{dpi} represents the total time that an agent i travels at his or her preferred speed. Then $\overline{T_{dp}} = \frac{\sum_i T_{dpi}}{total\ number\ of\ agents}$ represents the average time that an individual would drive at his or her preferred speed.

Generally, when the population size increases, an individual's travel speed drops, and more traffic happens. More lane changes and route changes occur in a larger population size. When social connectivity increases, more route changes can be observed. This phenomenon seems intuitive because when an agent is able to connect to more agents, he or she can collect more information, which may lead to decision changes.

Table 5-6: Boston: social media impact output of single destination – travel behavior

Set	Experiment	Avg Spd	Avg preferred Spd	Clear Time	Avg. Agent inTraff Time	Avg. preferred Speed Time	Avg. Lane Change	Avg. Route Change	Agent inTraff Compare	Preferred Speed Time Compare
1	100Agents_Kj10_Km16_OD1_K0	39.92	54.47	485.90	60.05	125.44	9.89	0.00	1.000	1.000
2	100Agents_Kj10_Km16_OD1_SF-NW	40.49	54.82	494.10	56.81	128.44	10.03	2.56	-0.054	0.024
3	100Agents_Kj10_Km16_OD1_RND-NW5	39.92	54.60	490.20	59.61	128.82	10.21	3.56	-0.007	0.027
4	100Agents_Kj10_Km16_OD1_RND-NW20	39.50	54.42	501.20	65.07	130.00	10.01	6.73	0.084	0.036
5	200Agents_Kj20_Km32_OD1_K0	30.69	54.60	702.67	193.05	92.89	10.76	0.00	1.000	1.000
6	200Agents_Kj20_Km32_OD1_SF-NW	30.73	54.37	718.70	190.99	96.85	10.80	4.44	-0.011	0.043
7	200Agents_Kj20_Km32_OD1_RND-NW5	30.89	54.80	716.40	190.86	94.19	10.92	5.95	-0.011	0.014
8	200Agents_Kj20_Km32_OD1_RND-NW20	30.83	54.47	720.90	192.54	96.62	10.75	11.05	-0.003	0.040
9	300Agents_Kj35_Km56_OD1_K0	25.76	54.88	934.00	310.95	85.80	11.48	0.00	1.000	1.000
10	300Agents_Kj35_Km56_OD1_SF-NW	26.12	54.87	943.20	304.06	84.45	11.49	4.55	-0.022	-0.016
11	300Agents_Kj35_Km56_OD1_RND-NW5	26.53	54.59	930.30	297.54	86.53	11.45	7.13	-0.043	0.009
12	300Agents_Kj35_Km56_OD1_RND-NW20	26.14	54.64	937.10	301.21	83.31	11.42	11.37	-0.031	-0.029

Table 5-7: San Francisco: social media impact output of single destination – travel behavior

Set	Experiment	Avg Spd	Avg preferred Spd	Clear Time	Avg. Agent inTraff Time	Avg. preferred Speed Time	Avg. Lane Change	Avg. Route Change	Agent inTraff Compare	Preferred Speed Time Compare
1	100Agents_Kj10_Km16_OD1_K0	33.12	54.56	476.00	84.84	76.37	9.23	0.00	1	1
2	100Agents_Kj10_Km16_OD1_SF-NW	33.75	54.74	483.67	77.71	78.37	9.26	2.09	-8.40%	2.63%
3	100Agents_Kj10_Km16_OD1_RND-NW5	33.94	55.19	510.40	80.80	80.32	9.47	3.26	-4.76%	5.18%
4	100Agents_Kj10_Km16_OD1_RND-NW20	33.39	54.72	498.80	85.44	79.66	9.54	5.73	0.71%	4.32%
5	200Agents_Kj20_Km32_OD1_K0	25.88	54.96	693.38	199.50	58.29	9.92	0.00	1	1
6	200Agents_Kj20_Km32_OD1_SF-NW	26.20	54.63	709.86	197.49	61.93	10.23	3.24	-1.01%	6.26%
7	200Agents_Kj20_Km32_OD1_RND-NW5	25.94	54.52	725.10	204.48	63.50	10.40	5.18	2.50%	8.95%
8	200Agents_Kj20_Km32_OD1_RND-NW20	25.92	54.52	714.50	206.43	62.37	10.43	8.11	3.47%	7.00%
9	300Agents_Kj35_Km56_OD1_K0	21.98	55.21	901.17	308.77	51.52	10.75	0.00	1	1
10	300Agents_Kj35_Km56_OD1_SF-NW	21.94	54.69	917.50	311.14	53.11	10.92	4.12	0.77%	0.77%
11	300Agents_Kj35_Km56_OD1_RND-NW5	22.09	54.84	929.88	315.25	54.35	11.15	6.24	2.10%	2.10%
12	300Agents_Kj35_Km56_OD1_RND-NW20	21.67	54.72	932.40	321.64	54.12	11.16	9.61	4.17%	4.17%

Compared to “no social media” instances, agents spend less time on congested roads for most SF-NW instances. Meanwhile, the SF-NW also increases the time allowed for an individual to drive at his or her preferred speed. The results of agent travel behavior presented in Tables 5-6 and 5-7 are consistent with those in Tables 5-2 and 5-3. For the

same reason, the improvement in using social media from an individual's point of view is insignificant under the single-destination scenario.

V.3.4.2 Multiple-Destination Case

Although we can observe a certain degree of dissimilarity between different social network structures from single-destination instances, the overlap of routes caused by having the same destination makes it difficult to identify the differences. Therefore, we would expect to find more significant variations in the multiple-destination case due to more destination and route options.

Evacuation Efficiency

Tables 5-8 and 5-9 show the outputs of evacuation efficiency for 10% and 16% seed agents, respectively, for the Boston area. The results from San Francisco are given in Tables 5-10 and 5-11.

Again, we conducted the hypothesis tests to compare "no social media use" and "having social media" on the SF-NW (K0 vs SF-NW), considering the following factors: clear time, 90 reach time, 95 reach time, average reach time, and standard deviation of reach time. Tables 5-12, 5-13, 5-14, and 5-15 show the calculated p-values of 10% and 16% seed agents for Boston and San Francisco, highlighting the values smaller than 0.05 (α = 0.05). From these four tables, we found that "90 reach time" and "standard deviation of reach time" were significantly different between K0 and SF-NW for all test instances. There were 10 SF-NW instances out of 12 that reduced "90 reach time" by at least 10%, and it could be reduced by as much as 26% for some specific instances. This shows that social media usage can assist the majority of evacuees in reaching their

destinations faster although the overall clear time is relatively longer compared to not using social media.

For most instances, the SF-NW results in a longer "clear time," which is consistent with the outcome in the single-destination case, especially for a larger population size. From the above observations, we can conclude that most evacuees benefit from social media since they can reach their destinations earlier. The disadvantage of adopting social media only occurs for a few agents. Influenced by other socially connected agents, certain agents tend to frequently change their destinations and routes, resulting in longer travel distance and time to arrive at their destinations.

Observing these phenomena, governmental agencies can utilize the power of social media to reassign the traffic flow that results from evacuees' spontaneous decision-making while traveling toward their destinations. At the later evacuation stage, governmental agencies can use their own resources, focusing on the minority who are behind. By doing so, the entire population can be evacuated quickly. Moreover, governmental agencies can use their resources more effectively, which is crucial when considering the high demand for resources during extreme events.

Table 5-8: Boston: social media impact output of multiple destinations with 10%-seed-agent – evacuation efficiency

Set	Experiment	Avg Spd	Avg Preferred Spd	Clear Time	95 Reach Time	90 Reach Time	Avg Reach Time	Std Reach Time	Total inTraff over time	Avg Num inTraff	inTraff Compare	90 Reach Time Compare
13	100Agents_Kj10_Km16_10%OD2_K0	42.75	54.77	728.00	703.20	687.80	438.27	176.59	6321.10	9.19	1.0000	1.0000
14	100Agents_Kj10_Km16_10%OD2_SF-NW	40.86	54.38	792.90	647.30	572.30	445.11	100.28	4522.30	7.90	-0.2846	-0.1679
15	100Agents_Kj10_Km16_10%OD2_RND-NW5	43.40	54.64	726.30	655.50	554.90	391.30	107.74	4708.90	8.49	-0.2551	-0.1932
16	100Agents_Kj10_Km16_10%OD2_RND-NW20	42.92	54.85	748.67	653.67	599.00	400.55	113.91	5200.78	8.68	-0.1772	-0.1291
17	200Agents_Kj20_Km32_10%OD2_K0	34.79	54.54	880.20	853.00	823.10	518.04	205.82	35146.00	41.20	1.0000	1.0000
18	200Agents_Kj20_Km32_10%OD2_SF-NW	36.19	54.65	881.40	754.80	684.30	478.74	146.49	29585.10	39.20	-0.1582	-0.1686
19	200Agents_Kj20_Km32_10%OD2_RND-NW5	35.79	54.79	907.70	758.50	728.10	505.98	165.51	31796.40	41.92	-0.0953	-0.1154
20	200Agents_Kj20_Km32_10%OD2_RND-NW20	34.95	54.44	1034.20	866.50	832.40	511.73	192.91	34233.80	39.51	-0.0260	0.0113
21	300Agents_Kj35_Km56_10%OD2_K0	30.39	54.56	1031.80	987.70	954.70	588.88	244.15	80451.00	81.45	1.0000	1.0000
22	300Agents_Kj35_Km56_10%OD2_SF-NW	32.09	54.64	1129.40	886.90	826.80	556.05	191.64	68489.60	77.22	-0.1487	-0.1340
23	300Agents_Kj35_Km56_10%OD2_RND-NW5	31.49	54.88	1146.20	857.90	811.00	570.61	186.27	72609.90	84.64	-0.0975	-0.1505
24	300Agents_Kj35_Km56_10%OD2_RND-NW20	30.88	54.55	1209.10	881.20	832.50	580.53	197.17	76718.20	87.06	-0.0464	-0.1280

Table 5-9: Boston: social media impact output of multiple destinations with 16%-seed-agent – evacuation efficiency

Set	Experiment	Avg Spd	Avg Preferred Spd	Clear Time	95 Reach Time	90 Reach Time	Avg Reach Time	Std Reach Time	Total inTraff over time	Avg Num inTraff	inTraff Compare	90 Reach Time Compare
25	100Agents_Kj10_Km16_16%OD2_K0	43.09	55.04	709.90	685.70	667.20	419.57	165.74	5757.70	8.63	1.0000	1.0000
26	100Agents_Kj10_Km16_16%OD2_SF-NW	43.67	54.25	714.30	569.30	491.20	382.74	89.53	4033.90	8.21	-0.2994	-0.2638
27	100Agents_Kj10_Km16_16%OD2_RND-NW5	44.09	54.91	718.30	620.40	503.30	386.01	98.82	4051.40	8.05	-0.2964	-0.2457
28	100Agents_Kj10_Km16_16%OD2_RND-NW20	43.31	54.10	751.50	625.50	562.80	388.04	100.98	4314.50	7.67	-0.2507	-0.2457
29	200Agents_Kj20_Km32_16%OD2_K0	35.76	54.64	876.80	844.20	811.10	504.54	203.09	32101.80	39.58	1.0000	1.0000
30	200Agents_Kj20_Km32_16%OD2_SF-NW	36.41	54.70	928.90	728.30	681.20	472.23	144.60	28101.20	41.25	-0.1246	-0.1602
31	200Agents_Kj20_Km32_16%OD2_RND-NW5	36.66	54.80	952.60	769.80	693.60	484.06	159.13	28382.40	40.92	-0.1159	-0.1449
32	200Agents_Kj20_Km32_16%OD2_RND-NW20	35.95	54.51	1025.50	814.60	739.30	506.12	180.75	31825.60	43.05	-0.0086	-0.0885
33	300Agents_Kj35_Km56_16%OD2_K0	30.86	54.95	1024.30	986.20	949.10	579.82	241.99	77944.70	82.12	1.0000	1.0000
34	300Agents_Kj35_Km56_16%OD2_SF-NW	32.24	54.88	1107.20	827.50	775.90	544.86	179.56	66612.90	85.85	-0.1454	-0.1825
35	300Agents_Kj35_Km56_16%OD2_RND-NW5	31.60	54.79	1158.80	883.40	816.60	566.16	198.73	72638.20	88.95	-0.0681	-0.1396
36	300Agents_Kj35_Km56_16%OD2_RND-NW20	31.24	54.75	1185.80	876.60	840.30	574.70	199.83	75327.20	89.64	-0.0336	-0.1146

Table 5-10: SF: social media impact output of multiple destinations with 10%-seed-agent – evacuation efficiency

Set	Experiment	Avg Spd	Avg preferred Spd	Clear Time	95 Reach Time	90 Reach Time	Avg Reach Time	Std Reach Time	Total inTraff over time	Avg Num inTraff	inTraff Compare	90 Reach Time Compare
13	100Agents_Kj10_Km16_10%OD2_K0	35.91	54.68	697.80	677.60	657.30	372.21	177.40	6627.80	9.5	1	1
14	100Agents_Kj10_Km16_10%OD2_SF-NW	35.87	54.60	656.90	587.20	543.00	367.87	112.86	6412.90	9.8	-3.24%	-17.39%
15	100Agents_Kj10_Km16_10%OD2_RND-NW5	36.07	55.21	728.30	642.90	581.90	390.33	122.75	6905.5	9.5	4.19%	-11.47%
16	100Agents_Kj10_Km16_10%OD2_RND-NW20	35.89	54.62	761.40	665.90	626.30	409.96	132.66	6373.40	8.4	-3.84%	-4.72%
17	200Agents_Kj20_Km32_10%OD2_K0	28.50	54.53	809.78	774.44	746.44	443.12	198.05	32337.8	39.9	1	1
18	200Agents_Kj20_Km32_10%OD2_SF-NW	29.12	54.73	889.00	755.50	672.00	452.13	158.24	31406.6	35.3	-2.88%	-9.97%
19	200Agents_Kj20_Km32_10%OD2_RND-NW5	28.63	54.64	885.50	739.90	665.00	473.47	147.67	31779.2	35.9	-1.73%	-10.91%
20	200Agents_Kj20_Km32_10%OD2_RND-NW20	28.32	55.09	846.40	705.40	673.10	483.59	146.17	32880.7	38.8	1.68%	-9.83%
21	300Agents_Kj35_Km56_10%OD2_K0	23.99	54.69	974.10	937.70	903.20	527.79	248.00	77262.20	79.3	1	1
22	300Agents_Kj35_Km56_10%OD2_SF-NW	25.03	54.80	1024.10	937.20	862.20	550.51	205.10	74199.50	72.5	-3.96%	-4.54%
23	300Agents_Kj35_Km56_10%OD2_RND-NW5	24.88	54.80	1136.20	1021.30	845.80	577.99	213.70	77122.50	67.9	-0.18%	-6.36%
24	300Agents_Kj35_Km56_10%OD2_RND-NW20	24.58	54.66	1076.22	961.89	898.00	580.40	198.63	76391.11	71.0	-1.13%	-0.58%

Table 5-11: SF: social media impact output of multiple destinations with 16%-seed-agent – evacuation efficiency

Set	Experiment	Avg Spd	Avg preferred Spd	Clear Time	95 Reach Time	90 Reach Time	Avg Reach Time	Std Reach Time	Total inTraff over time	Avg Num inTraff	inTraff Compare	90 Reach Time Compare
25	100Agents_Kj10_Km16_16%OD2_K0	35.87	54.75	685.00	652.75	628.00	354.87	156.86	6618.88	9.7	1	1
26	100Agents_Kj10_Km16_16%OD2_SF-NW	35.78	54.96	636.00	575.00	503.89	363.77	102.47	6457.22	10.2	-2.44%	-19.76%
27	100Agents_Kj10_Km16_16%OD2_RND-NW5	35.84	54.55	665.60	593.30	560.20	382.72	112.62	6459.3	9.7	-2.41%	-10.80%
28	100Agents_Kj10_Km16_16%OD2_RND-NW20	36.26	55.17	727.50	669.80	625.80	413.71	135.41	6396.30	8.8	-3.36%	-0.35%
29	200Agents_Kj20_Km32_16%OD2_K0	28.72	54.75	811.86	769.29	742.43	437.89	195.87	32250.4	39.7	1	1
30	200Agents_Kj20_Km32_16%OD2_SF-NW	29.19	55.09	878.43	716.14	630.43	448.42	145.64	29986.3	34.1	-7.02%	-15.09%
31	200Agents_Kj20_Km32_16%OD2_RND-NW5	28.45	54.70	872.00	717.20	656.80	473.03	144.76	32039.3	36.7	-0.65%	-11.53%
32	200Agents_Kj20_Km32_16%OD2_RND-NW20	28.64	54.81	858.40	724.40	666.60	471.37	143.21	30428.2	35.4	-5.65%	-10.21%
33	300Agents_Kj35_Km56_16%OD2_K0	24.23	55.00	963.50	929.40	893.50	520.63	244.47	76525.30	79.4	1	1
34	300Agents_Kj35_Km56_16%OD2_SF-NW	24.94	54.57	1007.44	908.33	840.00	541.95	197.21	74394.89	73.8	-2.78%	-5.99%
35	300Agents_Kj35_Km56_16%OD2_RND-NW5	24.63	54.29	998.50	879.70	808.10	558.58	178.64	72797.10	72.9	-4.87%	-9.56%
36	300Agents_Kj35_Km56_16%OD2_RND-NW20	24.86	54.84	1127.50	1024.80	887.90	583.89	217.21	75443.70	66.9	-1.41%	-0.63%

Table 5-12: Boston: P-values of K0 vs SF-NW – multiple destinations 10%-seed-agent

	100Agents	200Agents	300Agents
Clear Time	0.048650	0.963034	0.019895
90 Reach Time	0.000187	0.000002	0.000250
95 Reach Time	0.127776	0.003431	0.002295
Avg. Reach Time	0.211907	0.000074	0.000852
Std. Reach Time	0.000002	0.000001	0.000001

Table 5-13: Boston: P-values of K0 vs SF-NW – multiple destinations 16%-seed-agent

	100Agents	200Agents	300Agents
Clear Time	0.879034552	0.0719332	0.016488278
90 Reach Time	6.87904E-08	2.0747E-05	3.73293E-14
95 Reach Time	0.001133665	0.0002426	2.37105E-12
Avg. Reach Time	4.11702E-06	6.168E-07	1.02978E-06
Std. Reach Time	2.19047E-10	8.9248E-11	4.2195E-12

Table 5-14: SF: P-values of K0 vs SF-NW – multiple destinations 10%-seed-agent

	100Agents	200Agents	300Agents
Clear Time	0.283526641	0.060292234	0.035353739
90 Reach Time	0.00394143	0.048703959	0.036113881
95 Reach Time	0.023457693	0.653669843	0.972252644
Avg. Reach Time	0.516508989	0.294218745	0.001890463
Std. Reach Time	2.9824E-05	0.000916376	2.42001E-07

Table 5-15: SF: P-values of K0 vs SF-NW – multiple destinations 16%-seed-agent

	100Agents	200Agents	300Agents
Clear Time	0.175011879	0.161996265	0.03321079
90 Reach Time	4.03071E-05	4.63937E-08	0.003361667
95 Reach Time	0.026258001	0.137232711	0.244531998
Avg. Reach Time	0.312784162	0.026090488	0.007271158
Std. Reach Time	5.71171E-06	1.0456E-05	3.62929E-08

Next, we examine the time it takes to reach the destination, based on the "average reach time" and "standard deviation of reach time." As stated before, the "standard deviation of reach time" is significantly different between K0 and SF-NW for all test instances. Compared to K0, SF-NW results in a significantly smaller standard deviation in the arrival time at the destination for every instance pair. The "average reach time" is very close for most K0 and SF-NW instances. In the Boston case, most SF-NW instances have a slightly shorter "average reach time" than those of K0; on the other hand, in the San Francisco case, most K0 instances have a shorter "average reach time." Hence, not enough evidence shows that "having social media" can help reduce the "average reach time." However, the two measurements together show that "having social media" on the SF-NW can shorten the duration window of destination arrivals although the "average reach time" is close compared to "no social media usage." Reducing the duration window of reaching destinations can further assist governmental agencies in improving logistics and resource planning at the shelters.

Note that it is not always beneficial to increase the social connectivity degrees. When an individual's connectivity degree increases from 5 to 20, the clear time, 95 reach time, and 90 reach time increase in most instances. In other words, a strongly connected RND-NW does not help the entire population evacuate fast, not even for the majority of the population, which indicates that sharing too much information may result in the same evacuation efficiency as no information sharing.

The last measurement factor we compare for different social network structures is "total traffic over time." For the Boston case, we can observe the dramatic traffic

reduction by “having social media” for a smaller population size, whereas the improvement is less significant for a larger population size due to the population overload on the evacuation routes. However, for the San Francisco case, the improvement is below 5% for most instances. It requires further research to determine whether or not the congestions on road segments that are related to other factors, such as the road network structure, methods for generating alternative routes.

The next question is: Does the entire population take advantage of having more agents informed to go to a specific destination? We find that increasing the percentage of seed agents from 10% to 16% reduces the evacuation time in almost all instances. Tables 5-16 and 5-17 show the percentage of time reduced in the 16%-seed agent case compared to the 10%-seed agent case for Boston and San Francisco, respectively. Moreover, the evacuation time reduced is amplified in the SF-NW structure compared to “no social media” in most instances.

Table 5-16: Boston: evacuation time reduce in 16%-seed-agent case

	Clear Time	95 Reach Time	90 Reach Time	Avg. Reach Time	Std. Reach Time
100Agents_K0	-2.49%	-2.49%	-3.00%	-4.27%	-6.15%
100Agents_SF-NW	-9.91%	-12.05%	-14.17%	-14.01%	-10.72%
200Agents_K0	-0.39%	-1.03%	-1.46%	-2.61%	-1.33%
200Agents_SF-NW	5.39%	-3.51%	-0.45%	-1.36%	-1.29%
300Agents_K0	-0.73%	-0.15%	-0.59%	-1.54%	-0.89%
300Agents_SF-NW	-1.97%	-6.70%	-6.16%	-2.01%	-6.30%

Table 5- 17: SF: evacuation time reduce in 16%-seed-agent case

	Clear Time	95 Reach Time	90 Reach Time	Avg. Reach Time	Std. Reach Time
100Agents_K0	-1.83%	-3.67%	-4.46%	-4.66%	-11.58%
100Agents_SF-NW	-3.18%	-2.08%	-7.20%	-1.11%	-9.21%
200Agents_K0	0.26%	-0.67%	-0.54%	-1.18%	-1.10%
200Agents_SF-NW	-1.19%	-5.21%	-6.19%	-0.82%	-7.97%
300Agents_K0	-1.09%	-0.89%	-1.07%	-1.36%	-1.42%
300Agents_SF-NW	-1.63%	-3.08%	-2.57%	-1.55%	-3.85%

This insight can be very helpful for evacuation managers; by utilizing social media, the entire population can complete the evacuation faster when emergency managers make the same effort in notifying individuals as no social media usage. This is another advantage taken from the small-world character of the SF-NW. Note that the seed agents were randomly picked in our experiments. If we can smartly select the core agents with dominant social connections as the seed agents, we can expect less notifying efforts and better improvement in the evacuation time.

Individual Travel Behavior

Tables 5-18 and 5-19 provide the detailed outputs of individual travel behavior in experiment sets 13–36 for the Boston case, while Tables 5-20 and 5-21 give the corresponding information for the San Francisco case. Similarly, we calculate the average agent in traffic time ($\overline{T_{aJ}}$), average preferred speed time ($\overline{T_{dp}}$), average number of lane changes, average number of route changes, and average number of destination changes. Consistent with the results of the evacuation efficiency analysis, the traffic on the routes requires further examination. For most instances, having social media can reduce the time spent by an individual on congested road segments. However, the improvement in San Francisco is insignificant, and social media may bring more traffic in some instances.

Table 5-18: Boston: social media impact output of multiple destinations with 10%-seed-agent – travel behavior

Set	Experiment	Avg Reach Time	Std Reach Time	Avg. Agent inTraff Time	Avg. preferred Speed Time	Avg. Lane Change	Avg. Route Change	Avg. Dest Change	Wavg Route Change Time	Wavg Dest Change Time	DestInfo DisSat	Agent inTraff Compare	Preferred Speed Time Compare	DestInfo DisSat Compare
13	100Agents_Kj10_Km16_10%OD2_K0	438.27	176.59	57.42	193.65	11.45	1.00	1.00	363.51	363.51	1518.30	1	1	1
14	100Agents_Kj10_Km16_10%OD2_SF-NW	445.11	100.28	70.41	209.82	9.90	2.90	1.59	200.29	200.61	187.40	22.63%	8.35%	-87.66%
15	100Agents_Kj10_Km16_10%OD2_RND-NW5	391.30	107.74	41.60	194.06	10.10	4.07	1.87	197.36	191.20	188.50	-27.56%	0.21%	-87.58%
16	100Agents_Kj10_Km16_10%OD2_RND-NW20	400.55	113.91	46.40	193.22	10.19	7.20	1.94	203.03	196.04	271.89	-19.18%	-0.22%	-82.09%
17	200Agents_Kj20_Km32_10%OD2_K0	518.04	205.82	170.81	149.77	11.70	0.97	0.97	450.29	450.29	4228.80	1	1	1
18	200Agents_Kj20_Km32_10%OD2_SF-NW	478.74	146.49	143.14	162.10	10.99	4.60	1.83	268.26	264.28	550.40	-16.20%	8.23%	-86.98%
19	200Agents_Kj20_Km32_10%OD2_RND-NW5	505.98	165.51	154.29	162.76	11.36	3.24	1.30	283.03	305.64	2837.10	-9.67%	8.67%	-32.91%
20	200Agents_Kj20_Km32_10%OD2_RND-NW20	511.73	192.91	166.08	160.66	11.45	10.86	2.28	273.12	255.48	398.50	-2.77%	7.27%	-90.58%
21	300Agents_Kj35_Km56_10%OD2_K0	588.88	244.15	263.01	130.96	11.76	1.05	1.05	498.37	498.37	6541.70	1	1	1
22	300Agents_Kj35_Km56_10%OD2_SF-NW	556.05	191.64	223.46	149.69	11.54	5.28	2.03	312.52	321.22	1831.30	-15.04%	14.30%	-72.01%
23	300Agents_Kj35_Km56_10%OD2_RND-NW5	570.61	186.27	237.63	148.44	11.89	7.23	2.39	325.33	319.10	867.70	-9.65%	13.34%	-86.74%
24	300Agents_Kj35_Km56_10%OD2_RND-NW20	580.53	197.17	250.97	148.07	11.92	12.43	2.49	326.40	314.55	886.60	-4.58%	13.06%	-86.45%

Table 5-19: Boston: social media impact output of multiple destinations with 16%-seed-agent – travel behavior

Set	Experiment	Avg Reach Time	Std Reach Time	Avg. Agent inTraff Time	Avg. preferred Speed Time	Avg. Lane Change	Avg. Route Change	Avg. Dest Change	Wavg Route Change Time	Wavg Dest Change Time	DestInfo DisSat	Agent inTraff Compare	Preferred Speed Time Compare	DestInfo DisSat Compare
25	100Agents_Kj10_Km16_16%OD2_K0	419.57	165.74	52.42	188.36	11.01	0.98	0.98	331.96	331.96	1281.20	1	1	1
26	100Agents_Kj10_Km16_16%OD2_SF-NW	382.74	89.53	35.25	193.40	9.67	2.88	1.61	192.88	183.27	106.50	-32.75%	2.68%	-91.69%
27	100Agents_Kj10_Km16_16%OD2_RND-NW5	386.01	98.82	35.11	192.55	9.72	3.62	1.85	189.98	174.66	122.30	-33.02%	2.22%	-90.45%
28	100Agents_Kj10_Km16_16%OD2_RND-NW20	388.04	100.98	37.76	192.88	9.89	6.54	1.87	197.06	187.13	139.00	-27.97%	2.40%	-89.15%
29	200Agents_Kj20_Km32_16%OD2_K0	504.54	203.09	155.98	151.75	11.46	1.01	1.01	420.37	420.37	3891.00	1	1	1
30	200Agents_Kj20_Km32_16%OD2_SF-NW	472.23	144.60	135.49	160.54	10.52	4.41	1.82	253.04	252.77	518.00	-13.13%	5.79%	-86.69%
31	200Agents_Kj20_Km32_16%OD2_RND-NW5	484.06	159.13	137.16	164.45	10.75	6.20	2.17	262.43	249.68	439.70	-12.07%	8.37%	-88.70%
32	200Agents_Kj20_Km32_16%OD2_RND-NW20	506.12	180.75	154.15	167.97	11.26	10.86	2.34	275.22	258.32	552.40	-1.17%	10.69%	-85.80%
33	300Agents_Kj35_Km56_16%OD2_K0	579.82	241.99	255.11	129.86	11.64	1.08	1.08	476.04	476.04	6196.30	1	1	1
34	300Agents_Kj35_Km56_16%OD2_SF-NW	544.86	179.56	216.92	146.78	11.37	5.31	2.08	306.55	303.43	872.70	-14.97%	13.03%	-85.92%
35	300Agents_Kj35_Km56_16%OD2_RND-NW5	566.16	198.73	237.55	144.62	11.87	8.41	2.54	319.42	302.77	969.80	-6.89%	11.37%	-84.35%
36	300Agents_Kj35_Km56_16%OD2_RND-NW20	574.70	199.83	246.24	143.16	11.80	12.31	2.51	324.94	306.70	830.30	-3.48%	10.24%	-86.60%

Table 5-20: SF: social media impact output of multiple destinations with 10%-seed-agent – travel behavior

Set	Experiment	Avg Reach Time	Std Reach Time	Avg. Agent inTraff Time	Avg. preferred Speed Time	Avg. Lane Change	Avg. Route Change	Avg. Dest Change	Wavg Route Change Time	Wavg Dest Change Time	DestInfo DisSat	Agent inTraff Compare	Preferred Speed Time Compare	DestInfo DisSat Compare
13	100Agents_Kj10_Km16_10%OD2_K0	372.21	177.40	76.16	121.38	9.42	0.85	0.85	352.81	352.81	1703.50	1	1	1
14	100Agents_Kj10_Km16_10%OD2_SF-NW	367.87	112.86	74.42	129.94	9.26	2.65	1.56	165.43	179.26	167.90	-2.28%	7.05%	-90.14%
15	100Agents_Kj10_Km16_10%OD2_RND-NW5	390.33	122.75	79.65	139.64	9.75	3.05	1.79	187.85	202.42	153.80	4.58%	15.04%	-90.97%
16	100Agents_Kj10_Km16_10%OD2_RND-NW20	409.96	132.66	75.29	140.75	10.19	4.50	1.99	180.01	201.03	227.00	-1.14%	15.96%	-86.67%
17	200Agents_Kj20_Km32_10%OD2_K0	443.12	198.05	179.75	93.48	9.75	0.81	0.81	420.45	420.45	3348.78	1	1	1
18	200Agents_Kj20_Km32_10%OD2_SF-NW	452.13	158.24	174.95	113.99	9.93	2.59	1.59	235.87	259.18	764.50	-2.67%	21.93%	-77.17%
19	200Agents_Kj20_Km32_10%OD2_RND-NW5	473.47	147.67	178.56	109.52	10.28	4.25	1.97	230.77	246.72	594.60	-0.66%	17.16%	-82.24%
20	200Agents_Kj20_Km32_10%OD2_RND-NW20	483.59	146.17	184.98	104.71	10.44	5.92	2.06	256.04	245.36	438.50	2.91%	12.01%	-86.91%
21	300Agents_Kj35_Km56_10%OD2_K0	527.79	248.00	277.99	79.49	9.93	0.88	0.88	515.36	515.36	7149.20	1	1	1
22	300Agents_Kj35_Km56_10%OD2_SF-NW	550.51	205.10	268.45	105.66	10.43	3.59	1.94	298.52	335.87	2712.50	-3.43%	32.92%	-62.06%
23	300Agents_Kj35_Km56_10%OD2_RND-NW5	577.99	213.70	278.54	111.89	10.85	4.94	2.29	294.90	340.69	3349.30	0.20%	40.76%	-53.15%
24	300Agents_Kj35_Km56_10%OD2_RND-NW20	580.40	198.63	277.07	104.82	10.84	7.44	2.40	297.02	322.95	2572.44	-0.33%	31.87%	-64.02%

Table 5-21: SF: social media impact output of multiple destinations with 16%-seed-agent – travel behavior

Set	Experiment	Avg Reach Time	Std Reach Time	Avg. Agent inTraff Time	Avg. preferred Speed Time	Avg. Lane Change	Avg. Route Change	Avg. Dest Change	Wavg Route Change Time	Wavg Dest Change Time	DestInfo DisSat	Agent inTraff Compare	Preferred Speed Time Compare	DestInfo DisSat Compare
25	100Agents_Kj10_Km16_16%OD2_K0	354.87	156.86	75.84	122.07	8.99	0.80	0.80	309.18	309.18	1288.75	1	1	1
26	100Agents_Kj10_Km16_16%OD2_SF-NW	363.77	102.47	74.90	123.79	9.37	2.63	1.54	159.26	164.60	81.67	-1.24%	1.41%	-93.66%
27	100Agents_Kj10_Km16_16%OD2_RND-NW5	382.72	112.62	75.73	133.29	9.67	3.05	1.73	167.32	176.38	114.00	-0.15%	9.19%	-91.15%
28	100Agents_Kj10_Km16_16%OD2_RND-NW20	413.71	135.41	75.27	138.93	10.43	5.49	1.99	177.30	198.66	189.70	-0.76%	13.82%	-85.28%
29	200Agents_Kj20_Km32_16%OD2_K0	437.89	195.87	178.07	95.78	9.59	0.84	0.84	403.37	403.37	3180.00	1	1	1
30	200Agents_Kj20_Km32_16%OD2_SF-NW	448.42	145.64	167.72	108.12	9.93	3.28	1.76	224.99	231.31	464.86	-5.81%	12.89%	-85.38%
31	200Agents_Kj20_Km32_16%OD2_RND-NW5	473.03	144.76	179.63	107.93	10.31	4.03	2.00	236.82	238.65	471.80	0.88%	12.69%	-85.16%
32	200Agents_Kj20_Km32_16%OD2_RND-NW20	471.37	143.21	172.97	102.56	10.40	6.50	2.07	244.76	229.53	505.40	-2.86%	7.08%	-84.11%
33	300Agents_Kj35_Km56_16%OD2_K0	520.63	244.47	274.90	80.52	9.98	0.89	0.89	485.91	485.91	6444.80	1	1	1
34	300Agents_Kj35_Km56_16%OD2_SF-NW	541.95	197.21	268.05	104.37	10.35	3.26	1.85	294.81	311.84	2258.33	-2.49%	29.62%	-64.96%
35	300Agents_Kj35_Km56_16%OD2_RND-NW5	558.58	178.64	265.82	99.42	10.74	5.08	2.22	280.58	289.84	1732.90	-3.30%	23.47%	-73.11%
36	300Agents_Kj35_Km56_16%OD2_RND-NW20	583.89	217.21	274.64	104.15	11.15	7.59	2.48	313.65	319.78	2418.50	-0.09%	29.35%	-62.47%

The “preferred speed time compare” column in these tables shows that having social media can increase the time that individuals can travel at their desired speed. Information sharing on social networks makes individuals perform more route and destination changes. As individuals travel on the alternative, less congested routes, they can drive at their desired speed.

In multiple-destination cases, route and destination changes become more dynamic. As we track the individual’s decision-making time on the route and destination changes, we find different patterns between “no social media use” and “having social media.” Figure 5-7 shows a typical pattern of route and destination decision-making time under the no social media, 200-agent scenario.

The x-axis represents the simulation time, and the y-axis indicates the number of agents who have made route/destination change decisions. In this figure, we can see a lot of destination change decisions made at a later stage (after 400 units of simulation time). What happened during 400-450 unit simulation time? For this specific run, one destination/shelter is overloaded around the 430^{th} unit of simulation time. Afterwards, agents who are still going to that shelter will be notified by emergency managers if these agents have telecommunication service. Once the agents receive this message, they will make a decision on the destination change. Figure 5-8 shows the number of agents who need to be notified and the number of agents who receive the messages when one shelter is exceeding its capacity.

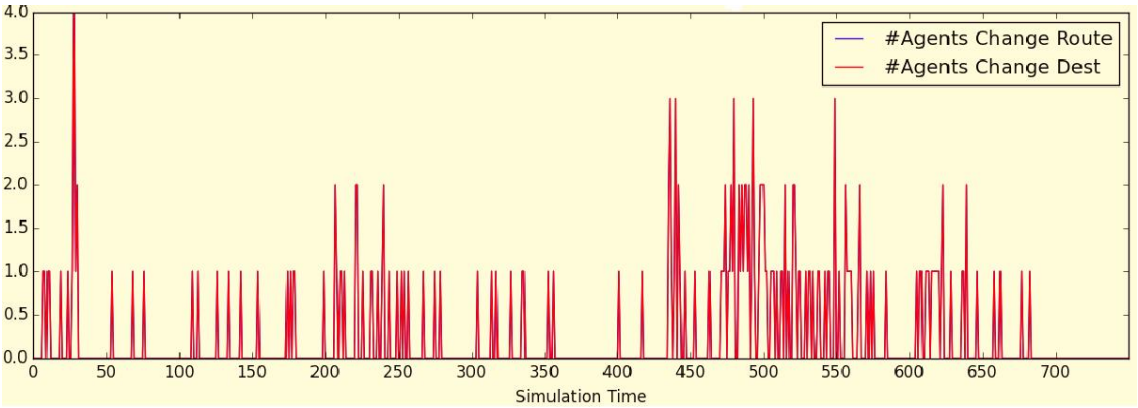

Figure 5-7: Route/destination change pattern – no social media

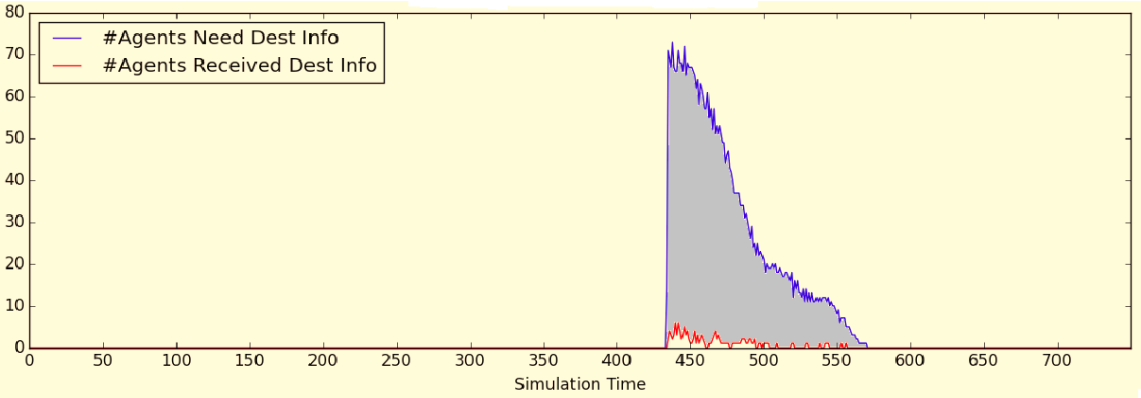

Figure 5-8: Overloaded destination notification – no social media

In contrast, under the "having social media" scenario, individuals tend to make route/destination changes at an earlier stage. A typical route/destination decision change pattern for a 200-agent scenario is displayed in Figure 5-9. The corresponding destination notification record is shown in Figure 5-10. Compared to the "no social media" scenario, we have the following observations for "having social media": (1) The time when one shelter is overloaded happens later. (2) A fewer number of individuals

need to be notified. (3) The time duration for sending out a message till all agents turn to the other shelter is shorter.

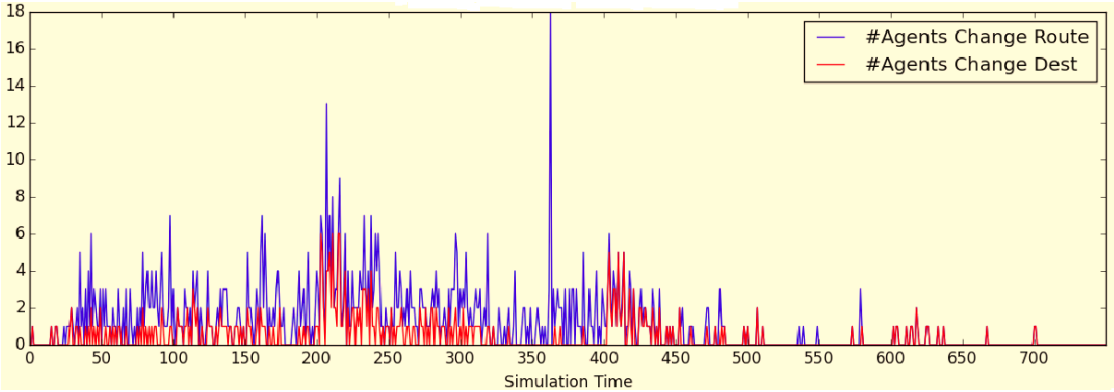

Figure 5-9: Route/destination change pattern – having social media

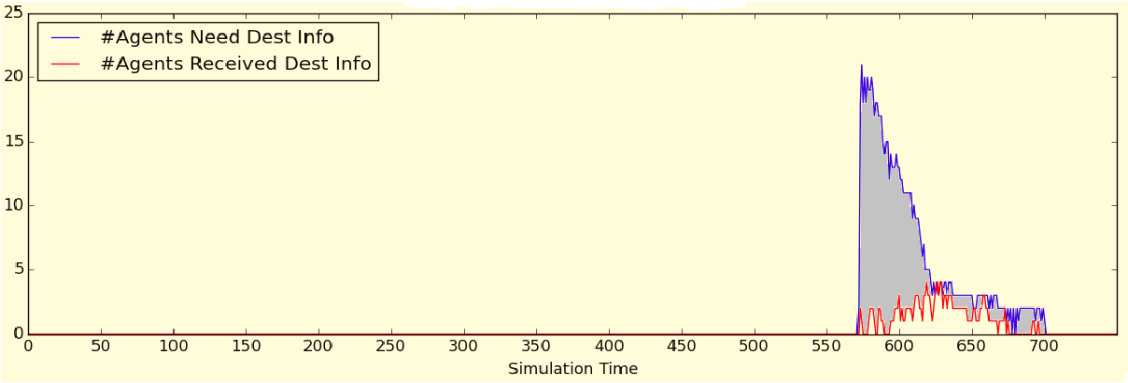

Figure 5-10: Overloaded destination notification – having social media

To capture the route and destination change pattern, we use the "weighted route change time" (T_{wr}) and "weighted destination change time" (T_{wd}), where $T_{wr} = \frac{\sum_t N_{rt}*t}{\sum_t N_{rt}}$, $T_{wd} = \frac{\sum_t N_{dt}*t}{\sum_t N_{dt}}$, and N_{rt} refers to the number of agents who make route change decisions

at time t. Similarly, N_{dt} indicates the number of agents who make destination change decisions at time t. T_{wr} represents the most likely time that an agent makes a route change decision, and T_{wd} represents the most likely time that an agent makes a destination change decision.

From the travel behavior tables (Tables 5-18 to 5-21), by comparing T_{wr} and T_{wd} with the "average reach time" and "standard deviation reach time," different route/destination change behaviors can be observed between "no social media" and "having social media." Agents from the "no social media" scenario tend to change routes/destinations at a later stage when certain agents have already reached the destination. On the contrary, agents from the "having social media" scenario tend to have route/destination changes at an earlier stage, before any agent arrives at the destination. This different travel behavior can be considered a different evacuation experience. In the "no social media" scenario, the destination change decisions are not made from the agents' own will but from the fact that no other option is available. This "no other choice" situation only happens to a few agents in the "having social media" scenario.

Although we set up relatively sufficient telecommunication power, a number of agents still cannot receive the destination information because they lack telecommunication service. The grey regions in Figures 5-8 and 5-10 represent the unsatisfied teleservice demand over the time it was requested. The grey areas can measure the number of agents who need to receive the destination information and the

time duration of sending out the destination information. We list this value in the "DestInfoDisSat" column in the behavior tables.

"Having social media" can reduce destination information dissatisfaction by 80%-90% compared to the "no social media" scenario for almost all instances of both study areas. This dramatic improvement from social media can relieve the burden of the telecommunication system. By integrating TELP into ABME, we are able to find this significant teleservice improvement resulting from social media usage. To our best knowledge, this is the first time that the usage of social media is examined through the usage of facilities and the service quality for an extreme-event evacuation. Because of the power of social media, agents select their destinations according to their own preferences, resulting in a balanced traffic flow to multiple destinations and further reducing the telecommunication demands. At this point, we realize that the important role played by social media does not only involve the evacuation time but also the performance of micro-station facilities.

V.4. Examining the Usage of Micro-Stations in Evacuation

In this section, we examine how different telecommunication infrastructures influence the service quality and evacuation efficiency. Concerning the limited budget, we intend to find out how the usage of micro-stations impacts service satisfaction. Given the simulated social networks, a set of candidate micro-station locations, and a set of fixed macro-stations, we test different numbers of micro-stations on three population levels and two O-D sets. The social network structure used for this section is the SF-

NW. The locations of existing macro-stations and candidate micro-stations are the same as those in experiment set 1-36 and shown in Figure 5-5. The two O-D sets are displayed in Figures 5-3 and 5-4. The complete list of experiments for testing micro-station usage can be found in Table 5-22.

Table 5-22: Experiments for examining Micro-Station usage

O-D1					O-D2				
set	#Agents	#Micro-Stations	Km	Kj	set	#Agents	#Micro-Stations	Km	Kj
37	100	0	16	10	49	100	0	16	10
38	100	5	16	10	50	100	5	16	10
39	100	10	16	10	51	100	10	16	10
40	100	15	16	10	52	100	15	16	10
41	200	0	32	20	53	200	0	32	20
42	200	5	32	20	54	200	5	32	20
43	200	10	32	20	55	200	10	32	20
44	200	15	32	20	56	200	15	32	20
45	300	0	56	35	57	300	0	56	35
46	300	5	56	35	58	300	5	56	35
47	300	10	56	35	59	300	10	56	35
48	300	15	56	35	60	300	15	56	35

V.4.1 Telecommunication Service Analysis

The detailed outputs of micro-station usage in the single-destination and multiple-destination cases for Boston are presented in Tables 5-23 and 5-24, respectively. The outputs for San Francisco are given in Tables 5-25 and 5-26. The number of individuals served by macro-stations or micro-stations is collected at every simulation time unit. This accumulated number on the service request time gives us the

total number of users served by macro-stations/micro-stations. The corresponding total number of dissatisfied users can be calculated as well.

Table 5-23: Boston: Micro-Station usage output of single destination – TeleService

Set	Experiment	Total Macro Serve	Total Micro Serve	Total UnServe	Avg. UnServe	TraffInfo DisSat	unServe compare	TraffInfo DisSat compare
37	100Agents_Kj10_Km16_OD1_P0	21180.90	0.00	18559.70	39.86	3233.00	1	1
38	100Agents_Kj10_Km16_OD1_P5	18393.80	6973.00	13391.20	28.87	2717.50	-27.85%	-15.94%
39	100Agents_Kj10_Km16_OD1_P10	15615.10	8861.00	13939.40	29.98	2766.60	-24.89%	-14.43%
40	100Agents_Kj10_Km16_OD1_P15	13717.20	12314.90	12394.40	26.85	2533.90	-33.22%	-21.62%
41	200Agents_Kj20_Km32_OD1_P0	62126.60	0.00	45897.80	69.49	17159.60	1	1
42	200Agents_Kj20_Km32_OD1_P5	49800.30	21967.00	34695.80	51.74	14988.30	-24.41%	-12.65%
43	200Agents_Kj20_Km32_OD1_P10	35784.50	38676.10	28020.00	42.50	12755.90	-38.95%	-25.66%
44	200Agents_Kj20_Km32_OD1_P15	31747.33	47736.67	23206.67	35.07	11030.22	-49.44%	-35.72%
45	300Agents_Kj35_Km56_OD1_P0	139942.90	0.00	71990.40	82.55	35851.70	1	1
46	300Agents_Kj35_Km56_OD1_P5	97037.90	47220.10	50712.00	59.51	31107.00	-29.56%	-13.23%
47	300Agents_Kj35_Km56_OD1_P10	80124.10	71390.60	44761.90	52.47	25864.70	-37.82%	-27.86%
48	300Agents_Kj35_Km56_OD1_P15	68523.70	84561.90	43235.00	50.45	25957.20	-39.94%	-27.60%

Table 5-24: Boston: Micro-Station usage output of multiple destinations – TeleService

Set	Experiment	Total Macro Serve	Total Micro Serve	Total UnServe	Avg. UnServe	TraffInfo DisSat	DestInfo DisSat	unServe compare	TraffInfo DisSat compare	DestInfo DisSat compare
49	100Agents_Kj10_Km16_OD2_P0	31158.40	0.00	16195.80	35.47	2015.60	134.30	1	1	1
50	100Agents_Kj10_Km16_OD2_P5	22004.10	11416.40	12949.10	28.03	1474.40	109.20	-20.05%	-26.85%	-18.69%
51	100Agents_Kj10_Km16_OD2_P10	20783.57	14394.86	11784.43	23.70	1714.43	132.57	-27.24%	-14.94%	-1.29%
52	100Agents_Kj10_Km16_OD2_P15	19264.10	15435.50	11542.30	23.50	1621.10	106.50	-28.73%	-19.57%	-20.70%
53	200Agents_Kj20_Km32_OD2_P0	82375.80	0.00	37028.90	54.62	11381.40	806.00	1	1	1
54	200Agents_Kj20_Km32_OD2_P5	63786.50	26760.50	31029.70	45.70	9429.40	576.40	-16.20%	-17.15%	-28.49%
55	200Agents_Kj20_Km32_OD2_P10	48209.30	42833.60	27085.30	40.28	9973.30	425.70	-26.85%	-12.37%	-47.18%
56	200Agents_Kj20_Km32_OD2_P15	44444.00	51681.80	22756.60	33.41	9203.40	518.00	-38.54%	-19.14%	-35.73%
57	300Agents_Kj35_Km56_OD2_P0	174259.90	0.00	51412.70	64.63	20830.60	1685.70	1	1	1
58	300Agents_Kj35_Km56_OD2_P5	127011.40	47361.00	44900.60	56.06	20504.20	1518.50	-12.67%	-1.57%	-9.92%
59	300Agents_Kj35_Km56_OD2_P10	114526.80	67941.60	36553.70	44.54	17176.90	1683.70	-28.90%	-17.54%	-0.12%
60	300Agents_Kj35_Km56_OD2_P15	85743.70	99032.20	32398.80	41.76	14884.90	872.70	-36.98%	-28.54%	-48.23%

Table 5-25: SF: Micro-Station usage output of single destination – TeleService

Set	Experiment	Total Macro Serve	Total Micro Serve	Total UnServe	Avg. UnServe	TraffInfo DisSat	unServe compare	TraffInfo DisSat compare
37	100Agents_Kj10_Km16_OD1_P0	15005.80	0.00	20085.50	44.62	4332.10	1	1
38	100Agents_Kj10_Km16_OD1_P5	14980.90	2778.20	16819.40	37.61	2888.40	-16.26%	-33.33%
39	100Agents_Kj10_Km16_OD1_P10	12420.10	7811.40	14976.00	33.13	3159.40	-25.44%	-27.07%
40	100Agents_Kj10_Km16_OD1_P15	14164.50	9522.40	13098.60	24.12	2848.50	-34.79%	-34.25%
41	200Agents_Kj20_Km32_OD1_P0	43623.30	0.00	49130.50	75.99	17853.00	1	1
42	200Agents_Kj20_Km32_OD1_P5	38514.00	20428.60	34574.80	52.76	13584.90	-29.63%	-23.91%
43	200Agents_Kj20_Km32_OD1_P10	32446.80	30814.30	30374.10	46.13	11954.10	-38.18%	-33.04%
44	200Agents_Kj20_Km32_OD1_P15	32985.20	24777.50	35431.40	54.05	13699.70	-27.88%	-23.26%
45	300Agents_Kj35_Km56_OD1_P0	83530.30	0.00	87454.50	104.16	41780.50	1	1
46	300Agents_Kj35_Km56_OD1_P5	88208.50	2472.70	80751.50	96.64	34548.50	-7.66%	-17.31%
47	300Agents_Kj35_Km56_OD1_P10	85845.60	6299.40	78576.00	94.37	35381.30	-10.15%	-15.32%
48	300Agents_Kj35_Km56_OD1_P15	49128.10	70688.00	53016.00	62.21	26736.60	-39.38%	-36.01%

Table 5-26: SF: Micro-Station usage output of multiple destinations – TeleService

Set	Experiment	Total Macro Serve	Total Micro Serve	Total UnServe	Avg. UnServe	TraffInfo DisSat	unServe compare	TraffInfo DisSat compare
49	100Agents_Kj10_Km16_OD2_P0	17497.90	0.00	18355.30	35.92	164.60	1	1
50	100Agents_Kj10_Km16_OD2_P5	16231.10	4912.20	15898.30	30.59	84.60	-13.39%	-48.60%
51	100Agents_Kj10_Km16_OD2_P10	14867.00	6769.78	14164.00	27.44	140.44	-22.83%	-14.68%
52	100Agents_Kj10_Km16_OD2_P15	13980.50	8631.20	13907.10	27.42	101.60	-24.23%	-38.27%
53	200Agents_Kj20_Km32_OD2_P0	40261.00	0.00	48685.00	76.46	645.57	1	1
54	200Agents_Kj20_Km32_OD2_P5	41116.38	9242.13	40540.38	62.65	536.88	-16.73%	-16.84%
55	200Agents_Kj20_Km32_OD2_P10	36126.80	12323.80	39923.00	65.53	616.60	-18.00%	-4.49%
56	200Agents_Kj20_Km32_OD2_P15	30745.67	24282.00	35029.22	55.57	438.00	-28.05%	-32.15%
57	300Agents_Kj35_Km56_OD2_P0	78537.33	0.00	83486.67	101.76	2193.56	1	1
58	300Agents_Kj35_Km56_OD2_P5	84776.30	3102.40	72902.20	90.35	1832.80	-12.68%	-16.45%
59	300Agents_Kj35_Km56_OD2_P10	85013.40	3018.20	72400.20	89.47	2049.20	-13.28%	-6.58%
60	300Agents_Kj35_Km56_OD2_P15	61161.33	35688.89	66142.89	78.59	2160.78	-20.77%	-1.49%

Besides the total service number, we are also interested in examining the users' dissatisfaction with service at a critical time, such as when an individual tries to send out information about a congested road and when an individual needs information about an overloaded destination. We use "traffic info dissatisfaction" to capture the number and time duration of service requests for information about congested roads. The grey region in Figure 5-11 illustrates this concept. Similarly, for the multiple-destination case, we use "destination info dissatisfaction" to represent the number and time duration of teleservice requests for information about overloaded destinations.

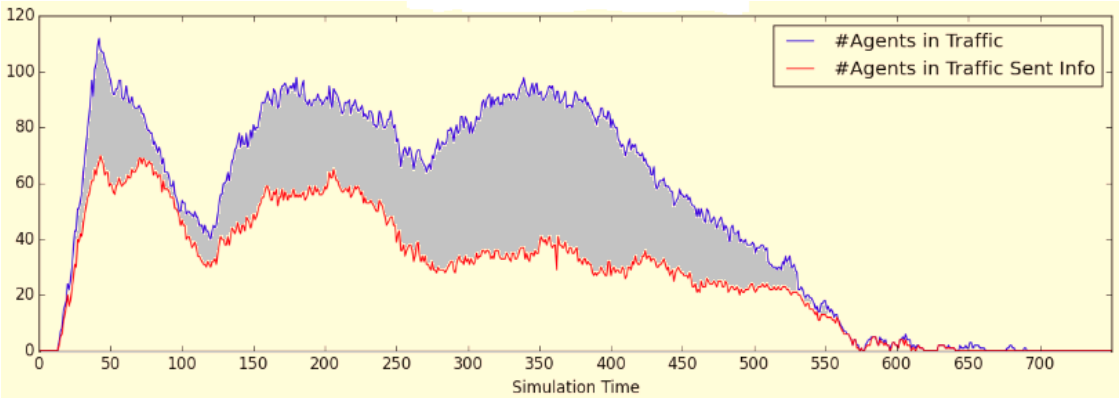

Figure 5-11: Illustration of Traffic Info Dissatisfaction

For both the single-destination and multiple-destination cases, adding more Micro-Stations relieves the burden on Macro-Stations and reduces the total number of unserved agents. However, the improvement is not linear when we linearly increase the number of micro-station facilities. One possible reason is the nonlinear signal-interference constraints. Adding more micro-stations within a nearby region results in interference noise to macro-stations and other micro-stations, which limits the increase

in the number of served users. In the multiple-destination case, with a small number of micro-stations, the increased number of served users is not as significant as in the single-destination case, especially for a larger population size. Therefore, adding a larger number of micro-stations may not result in significant improvement compared to a relatively small number of micro-stations. This is important information for governmental agencies to consider when they have limited budgets.

V.4.2 Evacuation Efficiency Analysis

With the knowledge that more agents can be served with additional micro-station facilities during an evacuation, the next question is whether or not the improved teleservice helps evacuation efficiency. The outputs of "evacuation reach time" are given in Tables 5-27 and 5-28 for the Boston and San Francisco areas, respectively.

For each set of experiments, we barely observe differences in clear time, destination reach time, and total traffic over time. For example, in the no micro-station experiment set 41, about 35% of evacuees lack teleservice, but the evacuation time is very close to that of experiment set 44 with 15 micro-stations, with only 17% of evacuees not having teleservice.

Does this mean that telecommunication service has no impact on the evacuation time? Note that all these experiments are conducted on an SF-NW. Although certain agents cannot send or receive route/destination information because they lack teleservice at some point in time, they can avail of information sharing on social networks once they travel to a region where they are able to connect to a cell station. Moreover, the small-world property of social networks makes the information reach every agent quickly,

which helps guarantee that all agents can receive the information even when they cannot have telecommunication service all the time. This is another proof that having social media can improve the agent evacuation experience.

Table 5-27: Boston: Micro-Station usage output of single destination – evacuation efficiency

Set	Experiment	Avg. Spd	Avg. UnServe	Clear Time	95 Reach Time	90 Reach Time	Avg Reach Time	Std Reach Time	Total inTraff over time
37	100Agents_Kj10_Km16_OD1_P0	40.26	39.86	489.90	478.70	465.60	359.13	79.48	6445.30
38	100Agents_Kj10_Km16_OD1_P5	40.04	28.87	490.70	474.80	463.90	358.13	77.91	6445.60
39	100Agents_Kj10_Km16_OD1_P10	40.66	29.98	491.60	479.10	464.90	357.98	79.94	6215.60
40	100Agents_Kj10_Km16_OD1_P15	40.49	26.85	494.10	476.00	461.60	355.65	79.11	6219.70
41	200Agents_Kj20_Km32_OD1_P0	31.16	69.49	716.50	690.10	660.50	469.28	139.39	38340.80
42	200Agents_Kj20_Km32_OD1_P5	30.55	51.74	730.10	701.00	670.60	475.83	141.37	40223.70
43	200Agents_Kj20_Km32_OD1_P10	31.31	42.50	713.70	686.50	659.30	469.12	138.56	38623.10
44	200Agents_Kj20_Km32_OD1_P15	30.72	35.07	719.56	689.78	661.78	470.65	138.20	39126.22
45	300Agents_Kj35_Km56_OD1_P0	25.73	82.55	962.30	913.80	872.10	584.94	202.94	94907.70
46	300Agents_Kj35_Km56_OD1_P5	26.00	59.51	942.30	896.50	852.20	578.22	198.33	92816.30
47	300Agents_Kj35_Km56_OD1_P10	26.09	52.47	939.30	892.30	853.10	577.47	196.50	92313.90
48	300Agents_Kj35_Km56_OD1_P15	26.12	50.45	943.20	899.20	857.00	578.70	197.79	92615.70
49	100Agents_Kj10_Km16_OD2_P0	43.81	35.47	709.00	539.60	456.60	373.35	84.48	4203.50
50	100Agents_Kj10_Km16_OD2_P5	43.73	28.03	744.90	554.90	461.90	375.64	91.29	3941.70
51	100Agents_Kj10_Km16_OD2_P10	43.66	23.70	744.43	582.14	497.14	383.35	93.62	4280.14
52	100Agents_Kj10_Km16_OD2_P15	43.67	23.50	714.30	569.30	491.20	382.74	89.53	4033.90
53	200Agents_Kj20_Km32_OD2_P0	36.80	54.62	872.20	748.20	677.90	464.86	140.51	27318.00
54	200Agents_Kj20_Km32_OD2_P5	36.63	45.70	976.80	755.20	679.00	472.14	148.48	27776.70
55	200Agents_Kj20_Km32_OD2_P10	36.28	40.28	887.50	730.70	672.40	477.49	142.41	28705.80
56	200Agents_Kj20_Km32_OD2_P15	36.41	33.41	928.90	728.30	681.20	472.23	144.60	28101.20
57	300Agents_Kj35_Km56_OD2_P0	32.11	64.63	1036.70	890.80	795.50	539.25	181.96	66404.80
58	300Agents_Kj35_Km56_OD2_P5	32.10	56.06	1073.40	897.50	800.90	541.66	186.48	66701.20
59	300Agents_Kj35_Km56_OD2_P10	32.17	44.54	1060.10	893.60	820.70	546.49	189.75	66919.40
60	300Agents_Kj35_Km56_OD2_P15	32.24	41.76	1107.20	827.50	775.90	544.86	179.56	66612.90

Table 5-28: SF: Micro-Station usage output of single destination – evacuation efficiency

Set	Experiment	Avg. Spd	Avg. UnServe	Clear Time	95 Reach Time	90 Reach Time	Avg Reach Time	Std Reach Time	Total inTraff over time
37	100Agents_Kj10_Km16_OD1_P0	33.35	44.62	477.30	462.10	450.10	350.92	75.19	6820.00
38	100Agents_Kj10_Km16_OD1_P5	34.18	37.61	473.10	460.90	447.20	345.80	76.53	6161.90
39	100Agents_Kj10_Km16_OD1_P10	33.47	33.13	485.50	465.50	452.10	352.09	75.63	6695.30
40	100Agents_Kj10_Km16_OD1_P15	33.75	24.12	483.67	462.11	449.22	349.71	74.80	6338.33
41	200Agents_Kj20_Km32_OD1_P0	25.90	75.99	710.80	670.60	646.50	463.77	132.88	34932.20
42	200Agents_Kj20_Km32_OD1_P5	26.00	52.76	707.20	682.70	655.30	467.59	137.30	35345.30
43	200Agents_Kj20_Km32_OD1_P10	25.92	46.13	720.40	685.10	658.50	468.18	137.91	35451.70
44	200Agents_Kj20_Km32_OD1_P15	26.20	54.05	709.86	677.57	653.14	462.81	135.70	34604.14
45	300Agents_Kj35_Km56_OD1_P0	21.81	104.16	916.60	874.60	839.60	569.95	192.41	84197.60
46	300Agents_Kj35_Km56_OD1_P5	21.79	96.64	913.20	872.50	835.60	571.45	193.09	84424.00
47	300Agents_Kj35_Km56_OD1_P10	21.89	94.37	906.80	867.10	832.60	569.07	191.42	84032.10
48	300Agents_Kj35_Km56_OD1_P15	21.94	62.21	917.50	885.17	850.00	571.65	197.81	83714.67
49	100Agents_Kj10_Km16_OD2_P0	35.20	35.92	659.60	562.30	511.00	358.54	99.29	6689.90
50	100Agents_Kj10_Km16_OD2_P5	36.75	30.59	635.20	561.50	519.80	370.43	102.77	5842.10
51	100Agents_Kj10_Km16_OD2_P10	35.66	27.44	638.00	569.11	516.22	358.02	98.05	6332.56
52	100Agents_Kj10_Km16_OD2_P15	35.78	27.42	636.00	575.00	503.89	363.77	102.47	6457.22
53	200Agents_Kj20_Km32_OD2_P0	29.71	76.46	843.57	695.57	636.71	444.74	144.75	29154.14
54	200Agents_Kj20_Km32_OD2_P5	28.60	62.65	843.13	716.63	647.13	454.50	144.41	31709.50
55	200Agents_Kj20_Km32_OD2_P10	29.40	65.53	909.60	694.00	609.20	441.87	142.05	29719.00
56	200Agents_Kj20_Km32_OD2_P15	29.19	55.57	878.43	716.14	630.43	448.42	145.64	29986.29
57	300Agents_Kj35_Km56_OD2_P0	25.38	101.76	1052.89	878.22	820.44	540.08	197.26	72078.56
58	300Agents_Kj35_Km56_OD2_P5	25.18	90.35	1060.30	867.50	806.90	535.94	192.07	72028.50
59	300Agents_Kj35_Km56_OD2_P10	25.45	89.47	1065.20	911.80	809.20	534.78	196.32	71338.10
60	300Agents_Kj35_Km56_OD2_P15	24.94	78.59	1007.44	908.33	840.00	541.95	197.21	74394.89

V.5. Summary and Conclusion

To sum up, in this chapter we have identified the importance of utilizing social media for an emergency evacuation by examining the simulation outputs of the Boston and San Francisco city areas. We have answered our research question—having social media can improve evacuation efficiency. Specifically, having social media can save on evacuation time for the majority of the population, and it can shorten the time duration

of agents' arrival at their destinations. It can also increase the time allowed for individuals to travel at their desired speed by using alternative routes. Moreover, information sharing on social networks can help balance the traffic flow and reduce teleservice requests at a critical time. In other words, using social media not only influences individual and group behaviors but also affects the system facility usage.

CHAPTER VI

CONCLUSIONS AND FUTURE WORKS

VI.1. Conclusions

In this research, we have studied the mobile telecommunication facilities' location problem to generate a planning strategy for them during a regional evacuation to ensure maximum connectivity and resilience of the communication systems. In our TELP model, besides considering the traditional coverage problem, we have also included the signal interference requirement, which is a necessary condition in cellular systems. The user teleservice demand is time-dependent, and its geographic distribution has been considered. These two characteristics reflect real-world situations and are important to consider, especially for evacuation scenarios in which user demands change spatially at different time stages. The routing constraints are integrated to utilize the mobile feature of telecommunication facilities, reuse these facilities, and fulfill more teleservice demands even with a limited budget.

Even for the small-sized problems, it is very hard to find optimal solutions by using an optimization solver for the linearization model. Furthermore, the optimization solver cannot provide solutions for medium-sized problems within several hours. To obtain good solutions with less computation effort for this NP-hard problem, we propose two heuristic approaches: the greedy randomized adaptive search procedure (GRASP) and Lagrangean heuristics. Both heuristic approaches can solve test problems quickly compared to solving the linearization model. The GRASP can yield very competitive

solutions but needs more computational effort. In contrast, the Lagrangian relaxation heuristics can obtain solutions very quickly but sacrifices the solution quality.

A spatial, behavioral evacuation, agent-based simulation model is proposed as well. Our ABM uses novel FCMs as the agent decision logic that integrates the physical environment, interpersonal communication, and historical empirical data when determining agent decisions. This is the first time that FCMs have been applied and implemented in the domain of travel behavior under the complicated scenario of an extreme-event evacuation. The FCMs are suitable for representing more realistic behavior models; with the help of FCMs, evacuees are able to make dynamic and adaptive decisions based on real-time and updated information. By integrating the TELP model with ABM, we are able to explore the use of mobile telecommunication facilities and evacuees' behaviors simultaneously.

We have utilized our ABM to examine whether or not the adoption of social media can improve evacuation efficiency. How mobile micro-stations assist existing cellular networks to satisfy the surging user demand during an evacuation process has been investigated as well. The experiments were conducted on two citywide regions: Boston and San Francisco. We have found that social media can help the majority of the population reach their destinations faster although it may take longer to have the entire population evacuated. Meanwhile, using social media can also shorten the time duration of individual arrivals at the destinations. Moreover, we have shown that using social media can improve the usage of mobile micro-stations and fulfill more teleservice demands. Emphasizing the importance of social media use during facility planning can

help emergency managers or commercial agencies improve facility use, enhance service quality, and reduce expenses.

VI.2. Future Works

Although many interesting insights have been revealed in this research, it can be further extended and improved in multiple directions.

Considering the TELP model, the proposed heuristic approaches can be improved in terms of computational time. Different Lagrangian heuristics can be developed by using different structures or solutions from other heuristics as a starting point. More efficient preprocessing techniques can be developed to replace the numeration in examining the signal-interference constraints in our heuristics. To extend the TELP model for a more general and large problem, the demand aggregation is needed and the probability associated with demand points may be introduced.

For the ABME model, computational effort is necessary for simulating a large-sized realistic problem. For a more realistic and accurate model, the population distribution can be generated at the level of the census block. A further study on using FCMs to represent travel behavior will be beneficial for this research. The travel behavior for different groups can be explored by using different structures of FCMs to represent different groups of evacuees.

To gain further understanding of social media usage during evacuation, the social network structure needs to be revisited. More attention should be paid to the correlation of geographic parameters and social connectivity. Further research is needed to show the

impact of social media on the road congestion level, considering different road network structures.

The ABME model developed in this research can be used for the study of different evacuation strategies and individual evacuation decisions (when to evacuate). It can also be generalized for travel behavior studies, information dissemination, and so on.

REFERENCES

Acampora, G., and Loia, V., 2009, "A dynamical cognitive multi-agent system for enhancing ambient intelligence scenarios," *in Proc. IEEE Int. Conf. Fuzzy Syst., pp. 770–777*.

Aguilar, J., 2005, "A survey about fuzzy cognitive maps papers (Invited paper)," *Int. J. Comput. Cogn., vol. 3, no. 2, pp. 27–33*.

Akella, M. R., Batta, R., Delmelle, E. M., Rogerson, P. A., Blatt, A., Wilson, G., 2005. Base station location and channel allocation in a cellular network with emergency coverage requirements. *Eur. J. Oper. Res. 164(2) 301–323*.

Alsnih, R., Stopher, P.R., 2004. Review of procedures associated with devising emergency evacuation plans. *Transportation Research Record (1865), 89–97.*

Amaldi, E., Capone, A., Malucelli, F., Signori, F., 2003. Optimizing base station location and con figuration in UMTS networks. *In: Proceedings of INOC 2003, pp 13–18*

Amaldi, E., Capone, A., Malucelli, F., 2003. Planning UMTS Base Station Location: Optimization Models with Power Control and Algorithms. *IEEE Transactions on Wireless Communications, 2(5), 939–952.*

Amaldi, E., Capone, A., Malucelli, F., 2003. A Mathematical Programming Approach for W-CDMA Radio Planning with Uplink and Downlink Constraints. *In: Proceedings of IEEE VTC Fall 2003, Vol. 2, 806–810.*

Arentze, T. and Timmermans, H. 2008. Social networks, social interactions, and activity-travel behavior: a framework for microsimulation. *Environment and Planning B: Planning and Design pp1012 – 1027*

Bertolini, M., and Bevilacqua, M., 2010, "Fuzzy cognitive maps for human reliability analysis in production systems," Prod. Eng. Manage. Under Fuzziness Stud. Fuzziness Soft Comput., vol. 252/2010, pp. 381–415.

Billionnet, A., Elloumi, S., Lambert, 2008, A.: Linear reformulations of integer quadratic programs. In: Le Thi, H.A., Bouvry, P., Tao, P.D. (eds.) Modelling, Computation and Optimization in Information Systems and Management Sciences, Second International Conference.

Bo, Y., Yong-gang, W., Cheng, W. 2009. A multi-agent and GIS based simulation for emergency evacuation in park and public square, *in: Int'l Conf. Computational Intelligence and Security, pp. 211–216*.

Bonabeau, E. 2002. Agent-Based Modeling: Methods and Techniques for Simulating Human Systems. *Proceedings of the National Academy of Sciences of the United States of America 99 (suppl.3):7280-7287*

Bose, R. 2001. A smart technique for determining base-station locations in an urban environment. *IEEE Transactions on Vehicular Technology, 50 (1) (2001), pp. 43–47*

Butts, C.T., Acton, R.M., Hipp, J.R., and Nagle, N.N. 2012. Geographical variability and network structure. Social Networks, Vol. 34, pp. 82-100

Cal´egari, P., Guidec, F., Kuonen, P., and Wagner, D., 1997. Genetic Approach to Radio Network Oprimization for Mobile Systems. *In: Proceedings of IEEE VTC 97, pp. 755–759.*

Carvalho, J. P., 2010, "On the semantics and the use of fuzzy cognitive maps in social sciences," in Proc. IEEE World Cong. Comput. Intell., pp. 1–6.

Chen, X. and Zhan, F. B., 2004. Agent-based modeling and simulation of urban evacuation: Relative effectiveness of simultaneous and staged evacuation strategies, Presented at 83rd Annual Meeting of the Transportation Research Board, Washington, D.C., 11–15 January.

Christensen, K., Sasaki, Y., 2008. Agent-based emergency evacuation simulation with individuals with disabilities in the population, *Journal of Artificial Societies and Social Simulation 11 (3) 9–21.*

Coombs, R. and Steele, R., 1999, "Introducing Microcells in Macrocellular Networks- A Case Study," *IEEE Trans. On Comm., Vol.47, No.4.*

Eisenman, D.P., Cordasco, K.M., Asch, S., Golden, J.F., Glik, D. 2007. Disaster planning and risk communication with vulnerable communities: lessons from Hurricane Katrina. Am J Public Health 97(Supplement 1):S109–S115

Fortet, R., 1960, Applications de l'Algebre de Boole en Recherche Operationelle. *Revue Francaise De Recherche Operationelle. 4, 17-25*

Fritzsche H-T (1994). A model for traffic simulation. Traffic Eng Control 35: 317–321. Kishore, S., Greenstein, L., Poor, H., and Schwartz, S., 2003. Uplink user capacity in a CDMA macrocell with a hotspot microcell: exact and approximate analyses. IEEE Trans. Wireless Communication, vol. 2, no. 2, 364–374.

Georgopoulos, V. C., Malandraki, G. A., and Stylios, C. D., 2003, "A fuzzy cognitive map approach to deferential diagnosis of specific language impairment," Artif. Intell. Med., vol. 29, no. 3, pp. 261–278
Gilhousen, K. S., et al, 1991, "On the capacity of a cellular CDMA system," IEEE Transactions on Vehicular Technology, vol. 40, pp. 303–312.

Hackney, J. and Marchal, F. 2009. A Model for Coupling Multi-Agent Social Interactions and Traffic Simulation. Proceedings of the 88th TRB Annual Meeting

Han, Q., Arentze, T.A., Timmermans, H.J.P., Janssens, D., Wets, G., 2007. The effects of social networks on choice set dynamics: results of numerical simulations. Frontiers in Transportation, Social Interactions, Amsterdam.

Han, Q., Arentze, T., Timmermans, H., Janssens, D., Wets, G. 2011. The effects of social networks on choice set dynamics: Results of numerical simulations using an agent-based approach. Transportation Research Part A 45(2011)310-322

Handford, D., and Rogers, A. 2012. An agent-based social forces model for driver evacuation behaviors. Progress in Artificial Intelligence Volume 1, Number 2, 173-181, DOI: 10.1007/s13748-012-0015-9

Hasan, S., Ukkusuri, S.V. 2011. A threshold model of social contagion process for evacuation decision making. Transportation Research Part B Methodology 45(10):1590–1605

Hughes, A., Palen, L., Sutton, J., Liu, S., and Vieweg, S. 2008. "Site-Seeing" in Disaster: An Examination of On-Line Social Convergence. Proceedings of the 5th International ISCRAM Conference

Kishore, S., Greenstein, L., Poor, H., and Schwartz, S., 2003. Uplink user capacity in a CDMA macrocell with a hotspot microcell: exact and approximate analyses. IEEE Trans. Wireless Communication, vol. 2, no. 2, 364–374.

Kosko, B.1986. Fuzzy Cognitive Maps. Int. Journal of Man-Machine Studies, Vol. 24, pp. 65-75

Kosko, B. 1992. A dynamic system approach to machine intelligence, Neural Networks and Fuzzy systems, Prentice Hall, New Jersey.

Kosko B., Dickerson J. 1994. "Fuzzy virtual worlds". AI Expert, pp. 25-31.

Kosko B., 1997, Fuzzy Engineering, Prentice-Hall, New Jersey.

Kosko B., 1998, "Global Stability of Generalized Additive Fuzzy Systems", IEEE

Transactions on Systems, Man and Cybernetics- Part C: Applications and Reviews, Vol. 28, No 3

Lindell, M., Kang, J.E. and Prater, C. 2011, Natural Hazards, Vol. 58, pp. 1093 – 1109

Lee, C.Y. and Kang, H.G, 2000. Cell Planning with Capacity Expansion in Mobile Communications: A Tabu Search Approach. *IEEE Trans. on Vehicular Technology, 49(5), 1678–1690*

Luke, S, Cioffi-Revilla, C et al. 2004. MASON: A Multi-Agent Simulation Environment. Paper presented at the 2004 SwarmFest Workshop, Ann Arbor, MI.

Miao, Y., Miao, C., Tao, X., Shen, Z., and Liu, Z., 2010, "Transformation of cognitive maps," IEEE Trans. Fuzzy Syst., vol. 18, no. 1, pp. 114–124

Mislove, A., Marcon, M., and Gummadi, K. P. 2007. Measurement and Analysis of Online Social Networks. Internet Measurement Conference 2007 (IMC'07). pp. 29-42

Olstam, J.J. and Tapani, A., 2004, Comparison of car-following models. VTI meddelande 960A, Swedish National Road and Transport Research Institute: Link¨oping, Sweden.

Pan, X., Han, C.S., Dauber, K., and Law, K.H., 2007. A multi-agent based framework for the simulation of human and social behaviors during emergency evacuations. AI Soc 22(2): 113–132

Papageorgiou, E. I., Spyridonos, P., Ravazoula, P., Stylios, C. D., Groumpos, P. P., and Nikiforidis, G., 2006, "Advanced soft computing diagnosis method for tumor grading," Artif. Intell. Med., vol. 36, no. 1, pp. 59–70

Papageorgiou, E. I., Stylios, C. D., and Groumpos, P. P., 2006, "Unsupervised learning techniques for fine-tuning FCM causal links," Int. J. Human-Comput. Stud., vol. 64, no. 8, pp. 727–743

Papageorgiou, E. I., Stylios, C. D., and Groumpos, P. P., 2008 "The soft computing technique of fuzzy cognitive maps for decision making in radiotherapy," in Intelligent and Adaptive Systems in Medicine, O. Haas and K. Burnham, Eds. New York: Taylor & Francis.

Pel, A.J., Bliemer, M.C.J., Hoogendoorn, S.P., 2012. A review on travel behaviour modelling in dynamic traffic simulation models for evacuations. Transportation 39 (1), 97–123.

Sherali, H.D., Adams, W.P., 1986, A tight linearization and an algorithm for zero-one quadratic programming problems. Management Science. 32(10), 1274-90

Shklovski, I., Palen, L., and Sutton, J. 2008. Finding Community through Information and Communication Technology during Disaster Events. CSCW'08(CSCW 2008 - Computer Supported Cooperative Work)

Statamatelos and Ephremides, 1996, Spectral efficiency and optimal base placement for indoor wireless networks, *IEEE JSAC, 1 (1996), pp. 434–438*

Stylios, C. D. and Groumpos, P. P., 2004, "Modeling complex systems using fuzzy cognitive maps," IEEE Trans. Syst.,Man Cybern. A, Syst. Humans, vol. 34, no. 1, pp. 155–162.

Sullivan, K., Coletti, M., Luke, S., GeoMason 2010: geospatial support for MASON. Department of Computer Science, George Mason University, Fairfax, VA. Technical Report Series

Sutton, J., Palen, L., and Shklovski, I. 2008. Back-Channels on the Front Lines: Emerging Use of Social Media in the 2007 Southern California Wildfires. Proceedings of the 5th International ISCRAM Conference

Sutton, J., Hansard, B., and Hewett, P. 2011. Changing Channels: Communicating Tsunami Warning Information in Hawaii. Presented at the 3rd International Joint Topical Meeting on Emergency Preparedness and Response, Robotics, and Remote Systems

Tcha et al. 2000. Base station location in a cellular CDMA system. *Telecommunication Systems, 14 (2000), pp. 163–173*

The Federal Response to Hurricane Katerina Lessons Learned, 2006: http://www.disastersrus.org/katrina/White%20House%20Katrina%20report.pdf

Tsai, J., Fridman, N., Bowring, E., Brown, M., Epstein, S., Kaminka, G., Marsella, S., Ogden, A., Rika, I., Sheel, A., Taylor, M.E., Wang, X., Zilka, A., & Tambe, M. 2011. ESCAPES—Evacuation simulation with children, authorities, parents, emotions, and social comparison. In: K., Tumer, P., Yolum, L., Sonenberg, & P., Stone (Eds.), Proceedings of the 10th international conference on autonomous agents and multiagent systems (AAMAS). Valencia: Innovative Applications Track.

Veeravalli, V.V. and Sendonaris, A., 1999. The Coverage-Capacity Tradeoff in Cellular CDMA Systems. IEEE Trans. on Vehicular Technology, 1443–1451.

Wang, X., 2012. *Discrete optimization and agent-based simulation for regional evacuation network design problem.* PhD Thesis, Texas A&M University

Widener, M., Horner, M., Metcalf, S., 2012. Simulating the effects of social networks on a population's hurricane evacuation participation, Journal of geographical systems 1–17.

Yen, J. Y., 1971, Finding the *K* shortest loopless paths in a network. *Management Science*, 17:712–716.

Zhang, B., S. Ukkusuri, and W. K. Chan. 2009. "Agent-Based Modeling for Household Level Hurricane Evacuation." *In Proceedings of the 2009 Winter Simulation Conference (WSC)*